NOVEL MECHANISMS UNDERLYING SMOOTH MUSCLE DIFFERENTIATION AND VASCULAR DISEASES

by

KUN DONG

(Under the Direction of Shi-You Chen)

ABSTRACT

Smooth muscle cell (SMC) differentiation is an important process during vasculogenesis and angiogenesis. However, molecular mechanisms controlling VSMC differentiation are not completely understood. Here, we identified a novel role of Mesenchyme homeobox 1 (Meox1) in SMC differentiation. Transforming growth factor-β (TGF-β) induces Meox1 expression in the initial phase of SMC differentiation of pluripotent C3H10T1/2 cells. Knockdown of Meox1 by specific shRNA suppresses TGF-β-induced expression of SMC early markers in both in vivo and in vitro. Meox1 overexpression increased these markers expression. Mechanistically, Meox1 promoted high level Smad3 nuclear retention during the early stage of TGF-β stimulation, which was achieved by inhibiting phosphorylated Smad2/3 phosphatase, Mg^{2+}/Mn^{2+} dependent 1A (PPM1A) expression through increasing its degradation rate, leading to a sustained level of Smad3 phosphorylation and thus allows Smad3 to precisely regulate SMC marker gene transcription.

SMC is also the main component of the fibrous cap which is participated in plaque stabilization during atherosclerosis progression. Therefore, elucidating mechanisms controlling VSMC function during the development of atherosclerosis is critical for the

understanding of disease formation. Here, by using Smad2-SMC knockout LDLR$^{-/-}$ mouse model, we found SMC Smad2 deficiency caused a larger atherosclerotic plaque area in the whole aorta but not the aortic root and led to an unstable plaque formation due to the increased MMP2/9 expression and activity. Also, SMCs Smad2 was involved in impeding SMC to macrophage-like cells transdifferentiation.

SMC has multiple functions during abdominal aortic aneurysm (AAA) formation. However, the role of SMC Smad2 during AAA development is still unknown. By using a SMC-specific Smad2 disruption animal model undergone elastase induced AAA formation, we found that Smad2 deficiency in SMC increased vessel diameter and AAA incidence as well as increased extracellular matrix degradation and SMCs loss. Additionally, we observed the increased aorta media layer matrix metalloproteinases MMP-2 and MMP-9 expression and a thinner adventitia layer with less fibroblasts proliferation when Smad2 was deleted in SMC. Moreover, we found SMC-derived factors may partially lead to decreased fibroblasts proliferation in Smad2 sm-/- mice AAA model. RNA-seq screening indicated that thrombosponding1 (TSP1) might be a potential secreted factor during this process.

INDEX WORDS: smooth muscle cell, TGF-β, Smad3, Meox1,
smooth muscle cell differentiation, Smad2, atherosclerosis,
abdominal aortic aneurysm

NOVEL MECHANISMS UNDERLYING SMOOTH MUSCLE DIFFERENTIATION AND VASCULAR DISEASES

by

KUN DONG

BS, China Agricultural University, P.R. China, 2011

A Dissertation Submitted to the Graduate Faculty of The University of Georgia in Partial Fulfillment of the Requirements for the Degree

DOCTOR OF PHILOSOPHY

ATHENS, GEORGIA

2017

NOVEL MECHANISMS UNDERLYING SMOOTH MUSCLE DIFFERENTIATION AND VASCULAR DISEASES

by

KUN DONG

Major Professor: Shi-You Chen

Committee: Wan-I Oliver Li

John J. Wagner

Electronic Version Approved:

Suzanne Barbour

Dean of the Graduate School

The University of Georgia

December 2017

ACKNOWLEDGEMENTS

First I would like to express my deep gratitude to my advisor, Dr. Shi-You Chen. I have worked in Dr. Chen's laboratory for six years, and I am honored to have been given the opportunity to work with Dr. Chen. His knowledge and attitude to science have deeply impressed me.

I would also like to give thanks to the members of Dr. Chen's lab, Drs. Weibing Xie, Ning Shi, Jianing Wang, Junming Tang, Jia Fei, Xiaobing Cui, Yongyi Wang, Shaojiang Tian , Zaiyan Xu, Jing Zhang, Xia Guo, Gui Zhang, Chenming Sun, Rui Tang, Li Li and Yung-Chun Wang, Chenxiao Li, Xiaohan Mei and Dunpeng Cai, for their kind help in my dissertation work. I truly enjoyed the teamwork with Mrs Gui Zhang, who have put in great effort in the experiments and analytical work.

Special thanks are given to my committee members, Drs. Wan-i Oliver Li and John Wagner. They have guided me a lot in my projects and dissertation during my 6-year PhD study.

Last but not least, I want to express my deepest gratitude to my family. I want to thank my parents and husband for their strongly support throughout the good days and the bad days.

For those I have failed to mention above, I would like to acknowledge all of their valuable assistance. Without the support and help from my advisor, my committee members, friends, and family, I would not be where I am today.

TABLE OF CONTENTS

Page

LIST OF FIGURES

Page

CHAPTER 1

INTRODUCTION

Problem statement

According to World health organization (WHO) statistics updated in 2017, cardiovascular diseases (CVDs) are the number 1 cause of death, accounting for about 31 % mortality globally. The artery can be divided into three layers: tunica intima, tunica meida and tunica adventitia. Smooth muscle cells (SMCs) are the major cells in the aorta media layer involved in blood vessel contraction, pressure regulation, and blood flow distribution. Additionally, SMCs are essential in maintaining aortic structure and functions through controlling proliferation and by secreting and maintaining a dynamic extracellular matrix (ECM).

Previous studies have suggested that several cardiovascular diseases including atherosclerosis are associated with the diversity of SMCs originating from different sources. The molecular mechanism and function of activated downstream transcription factors that are involved in regulating SMC growth and differentiation remain elusive.

As one of the most important cells in vessel, smooth muscle cells are involved in a variety of cardiovascular diseases including atherosclerosis and aneurysm. Atherosclerosis is a chronic inflammatory disease characterized by narrowing of blood vessels due to the formation of atherosclerotic plaque. SMC is a major component of the fibrous cap, which is critical for plaque stability. Recent studies indicated that SMC participates in necrotic core formation through differentiation to foam cell. Additionally,

phenotypically modulated SMC may contribute to the weakened atherosclerotic plaque. Abdominal aortic aneurysm (AAA) is a localized dilatation of the abdominal aorta. A ruptured AAA is the 15th leading cause of death in the US and the 10th leading cause of death globally. AAA usually develops in the infra-renal segment characterized by increased inflammation, extracellular matrix (ECM) degradation, and media SMC apoptosis. Furthermore, depletion of medial SMC makes an important contribution to this disease by eliminating a cell population capable of directing connective tissue repair. In spite of its importance during cardiovascular diseases development, the mechanism underlying the disease progression regulated by SMC remains largely unknown.

Therefore, the proposed studies investigating the cellular and molecular mechanisms of SMC differentiation and cardiovascular diseases will lead to a better understanding of the disease development and further provide potential drug targets for therapeutic invention.

Objective, hypotheses, and specific aims

Our first aim is to identify the role of a homeobox regulator in TGF-β-induced smooth muscle cell differentiation. SMC differentiation is essential for vascular development as well as vascular remodeling, and TGF-β-Smad signaling plays a critical role in this process. Among transcription factors involved in regulating SMC growth and differentiation, homeobox proteins appear to regulate vascular development in embryogenesis, angiogenesis and adult vascular diseases. Particularly, we have found that mesenchyme homeobox 1 (Meox1) promotes SMC contractile marker expression by maintaining Smad3 nuclear retention after TGF-β treatment. We hypothesize that Meox1 is a novel regulator controlling smooth muscle cell differentiation from mesenchymal

progenitor cells through promoting Smad3 nuclear retention during the early stage of TGF-β stimulation.

The second aim is to establish the role of Smad2 in the development of atherosclerosis. The role of the anti-inflammatory cytokine TGF-β in atherosclerosis has been a subject of considerable debate for a decade. In TGF-β signaling pathways, Smad signaling is the major pathway controlling cell-fate determination, cell-cycle arrest and apoptosis. Our previous studies have shown that Smad2, an important TGF-β signaling transducer, plays a critical role in SMC differentiation from neural crest cells and the blood vessel formation during embryonic development. But it's unknown if Smad2 is involved in adult cardiovascular diseases. According to the data that Smad2 deficiency caused more atherosclerotic plaques and decreased plaque stability. We hypothesize that Smad2 may protect atherosclerosis formation through maintaining its plaque stability.

Our third aim is to elucidate the role of Smad2 in abdominal aortic aneurysm (AAA) formation. Current views on whether TGF-β promotes or inhibits AAA formation remain contradictory. It is unknown whether or not Smad2 is involved in the development of AAA. Our preliminary data have shown that Smad2 SMC deletion leads to an increased artery dilation with a decreased vessel wall thickness, higher incidence of AAA development and enhanced level of proteinases for extracellular matrix (EMC) degradation. We hypothesize that SMC Smad2 deficiency promotes AAA formation through causing more EMC degradation, SMC loss, and less adventitial proliferation.

CHAPTER 2

LITERATURE REVIEW

TGF-B SIGNALING IN AORTIC ANEURYSM FORMATION

Introduction

Aortic aneurysm

Cardiovascular diseases (CVDs) are the leading cause of death in the world. Every year, more than 30% death can be attributed to CVDs. Aortic aneurysm is one of the CVDs. In the United States, aortic aneurysm is the 13th leading cause of death. In 2016, Aortic aneurysms accounted for 9,846 deaths (1,2).

An aortic aneurysm is a focal, balloon or bulge-like dilation of a blood vessel wall (3). Aortic aneurysm development starts when the blood vessel wall weakens. The causes of death of aneurysms mostly are dissection and rupture. During the dissection process, the pulsating force of blood flow can split the layers of the artery to cause blood leaking inside. When the rupture happens, the aneurysm bursts and leads to bleeding inside the body. A localized dilatation of an aortic aneurysm is identified as the diameter of the aneurysm increases by 150%. Along the different location of the aorta, aortic aneurysms can be categorized into thoracic aortic aneurysm (TAA) and abdominal aortic aneurysm (AAA). TAA occurs in the chest and AAA occurs in abdominal aorta where the infrarenal aorta is the most common location.

Thoracic aortic aneurysm (TAA)

Thoracic aortic aneurysm can be categorized into several groups according to the aorta locations, such as ascending aortic aneurysms (40% prevalence of all TAAs), aortic arch aneurysms (10%), descending thoracic aneurysms (35%) and thoracoabdominal aneurysms (15%). Thoracic aortic aneurysms are rare, occurring in approximately 6-10 individuals per every 100,000 people. About 20% of these cases are linked to family history.

Risk factor—TAA

Genetically triggered aneurysm syndromes

Marfan syndrome (MFS) is a connective tissue disorder associated with fibrillin-1 deficiency. This mutation leads to the elastin degeneration in artery wall and dilation. As a result, artery dilation and stiffness occurs(4). Family history is also an important factor for TAA formation. A study shows that TAA was present in 21.5% of non-MFS patients. The predominant inheritance pattern was autosomal dominant (5,6). Up to date, several autosomal-dominant mutation loci have been found including 3p24.2–25(7) and 5q13–14 (8,9).

Aortitis

Noninfectious and infectious aortitis has been increasingly recognized as an important aneurysm risk factor. The main cause is medial degeneration(10). For example, syphilis is the most common cause of infectious aortitis. It can cause an endarteritis of the proximal ascending thoracic aorta and destruction of collagen and elastic tissue. As a result, the dilation occurs in the aorta (11,12).

Abdominal aortic aneurysm (AAA)

AAA is a localized dilatation of the abdominal aorta which is 1.5-fold larger than normal, for patients, the diameters are 3.0 cm or greater (13). AAA is the most common aortic aneurysm (14). The aortic aneurysms occur in the abdominal artery is more than 3 times higher than that in the thoracic artery (1). Every year, 200,000 people in the U.S. are diagnosed with an abdominal aortic aneurysm (AAA). In most these cases, patients are asymptomatic. A ruptured AAA is the 15th leading cause of death in the US, and the 10th leading cause of death in men older than 55.

Risk factors—AAA

Up to date, though the etiology is still unclear, several risk factors have been identified to associate with AAA development such as genetics and familial risk high level of cholesterol and low level of HDL (15-19). Here we mainly focus on introducing several representatives of these risk factors.

Age and Sex

AAA development is associated with both aging and sex. The AAA in women is 4 times less than that of men (20). Also, the number of diagnosed patients is increased along with aging. According to the report from American Heart Association, the prevalence of AAAs with 2.9-4.9 cm diameter in men increases from 1.3% (age 45-54 years old) to 12.5% (age 75-84 years old) (1). In contrast, the prevalence of women increases from 0% (youngest age) to 5.2% (the oldest age) (21,22).

It is reported that estradiol (E2) is associated with inhibition of proinflammatory gene expression and lower MMP2 and MMP9 level in angiotensin II (Ang II) induced AAA model and elastase infusion AAA model respectively (23,24). This finding is also

supported by the study demonstrated that increased estrogen receptor α (ERα) is related to the decreased MMP activity and AAA formation. In the meanwhile, it is also observed a phenomenon that exogenous estrogen inhibits AAA formation in males which implies that estrogen supplementation is likely a further therapy method to prevent AAA formation (25).

Smoking

Several studies have shown that a history of smoking has been associated with a 3 to 5 fold increase in AAA prevalence across all age groups. An infrarenal abdominal aortic aneurysm is the most aneurismal diseases caused by smoking. Especially, the AAA risk is directly associated with the number of years of smoking (21,26,27) as well as the number of years after cessation (28). Female smokers experience a higher risk of AAA than current male smokers (28-30).

The effect of nicotine on AAA development has been well studied. It is reported that nicotine can facilitate or function alone to induce AAA development in both Angiotensin II mouse model and porcine pancreatic elastase (PPE) perfusion model (31). Nicotine has been demonstrated to promote AAA progression by participating in increasing matrix metalloproteinase (MMPs) expression which leads to extracellular matrix degradation and cellular inflammation (32-34).

Hypertension

Hypertension has been identified to promote AAA development in rat elastase infusion AAA model. Both MMPs intercellular adhesion molecule expressions are increased accompanied with elevated nuclear factor κB (NFκB) level in rat with hypertension group (35). Though hypertension has been demonstrated to be positively correlated with AAA

incidence in men (36), the recent analysis of database study including data on 6,619 AAA patients have been screened which indicated that hypertension is not associated with AAA expansion (37).

Animal model

To better study the process of aortic aneurysm and treatment methods, animal models has been developed. An ideal aortic aneurysm animal model would reflect the pathology of the human aortic aneurysm and help better understanding the mechanisms underlying this disease. However, current animal models for aortic aneurysm only share some aspects (biochemical, cellular mechanism) of similarity of the real human aortic aneurysm.

A variety of animal species have been used as aortic aneurysm animal models, such as mouse, rat, canine, swine, rabbit, sheep and turkey. Different animal species have their advantages and disadvantages. For example, the mouse models have low cost and are relatively easy to handle. This model can mimic some facets of aneurysm symptoms including medial degeneration, inflammation, and thrombus formation. However, unlike humans, the mouse usually develops AAA in suprarenal rather than infrarenal (38).

Swine shares similar arterial morphology to humans. However, the cost is high for large experimental numbers (39). In the meanwhile, swine model also forms several different aneurysms to human aneurysms (40). Considering a lot of studies have used the mouse as an arterial aneurysm model species as well as our lab, we only discuss different mouse model used for aneurysm investigation.

TAA model

Genetically determined TAA model

TAA is one of the characteristics of Marfan syndrome. Marfan syndrome model is often used for TAA formation study. Fibrillin-1 deficiency can efficiently induce Marfan syndrome model via connective tissue disorder (41).

Chemical infused TAA model

Angiotensin II (AngII) infusion

Angiotensin II infusion can induce mouse TAA formation (42). Kanematsu et al. demonstrated that C57BL/6J male mice could be induced to form TAA and AAA by co-administration AngII or deoxycorticosterone acetate (DOCA)-salt with beta-aminopropionitrile (BAPN). They combined two factors that are associated with human aortic aneurysm—hypertension, and degeneration of elastic lamina. AngII or DOCA are used for hypertension induction, while BAPN is a lysyl oxidase inhibitor which promotes elastin destruction (43).

Periarterial Calcium Chloride Model

Periarterial calcium chloride model is a unique model of isolated TAA production in the murine species. Application of periarterial calcium chloride to descending aorta is also a common method for TAA model induction. Extracellular matrix degradation occurs in this model (42).

AAA model

Current mouse AAA model includes spontaneously mutated and genetically engineered mice model and chemical-induced AAA model.

Genetically determined AAA model

Several mutated mouse models are developed with engineered deficiency of in extracellular matrix, matrix metalloproteinases and lipoprotein receptors. For example, lysyl oxidase (Lox) deficiency mouse shows highly fragmented elastic fibers and discontinuity in tunica media layer. This model can cause aneurysm formation and may lead to rupture. Another example is the hyperlipidemic mouse, besides being a classic atherosclerosis model, apoE and LDL receptor deficiency mice fed with high-fat diet also frequently develop AAAs. Recent studies demonstrate that chow diet apoE or LDL receptor deficiency mice may also develop AAA automatically. However, in this model, it's very common that the AAAs develop in suprarenal segment rather than infrarenal segment where human AAA usually forms.

Chemical-induced AAA model

Periarterial Calcium Chloride Model

Periarterial calcium chloride model was firstly used in rabbit (44) and introduced into a mouse by a peri-aortic incubation later. A gauze soaked in a calcium chloride solution or concentrated solution is placed on the aorta between renal branches and iliac bifurcation. After 14 days, a significant dilation can be observed in the infrarenal region. In this model, the structure of medial layer is destroyed, and inflammation process occurs.

Elastase infusion model

The process to develop elastase infusion model is to introduce a catheter at the iliac bifurcation and isolate the segment of abdominal aorta by a distal suture. Porcine pancreatic elastase (PPE) is then introduced into the lumen and incubates for 5 minutes before restoring the blood flow. After 14 days, dilation and inflammation can be found in the location where PPE was incubated. In this model, destruction of elastin lamellae and adventitia lead to inflammatory cell infiltration. Elastase infusion model well mimics human AAA where aneurysm forms in infrarenal. However, because real blood vessel doesn't contain as high concentration of PPE as that in this model, this model still has its own restriction in AAA mechanism study. Recently, periarterial PPE model is also introduced as an AAA model (45). In this model, PPE is peri-aortic incubated for 5 minutes in the infrarenal segment.

Angiotensin II (AngII) infusion model

Infusion of AngII into apoE or LDL receptor deficiency mice is a well established AAA model. AngII solution is infused into the body at 1000ng/kg per minute via osmotic mini-pump which is subcutaneously implanted in the mouse. After 28-day infusion, apoE or LDL receptor deficiency mice can form AAA in the suprarenal segment. In this model, elastin lamellae are destroyed and inflammatory response is activated. In this model, male mice develop AAA approximately twice more than female mice. Also, study shows that AngII infusion in AAA model wouldn't cause hypertension in these hyperlipidemic mice. Recently, an article reported that C57BL/6J mouse also could be used in AngII infusion model when co-administration AngII or deoxycorticosterone acetate (DOCA) with beta-aminopropionitrile (43).

TGF-β signaling in aortic aneurysm

The transforming growth factor-β (TGF-β) superfamily is mainly composed of 4 groups, including activins/inhibins family, glial cell line-derived neurotrophic factor family, bone morphogenetic proteins/growth differentiation factors family and TGF-β family. In TGF-β family, three TGF-β isoforms (TGF-β1, TGF-β2, TGF-β3) have been identified in mammals (46,47). TGF-β functions through its signaling pathways. In TGF-β signaling pathways, the Smad pathways are the major pathway which controls cell-fate determination, cell-cycle arrest, apoptosis and extracellular matrix synthesis (48). Upon TGF beta ligand inducement, the type II receptor transphosphorylates and activates the type I receptor, which subsequently propagates the signal by phosphorylating receptor-regulated (R-) SMAD2 and 3. On activation, R-SMADs form heteromeric complexes with a related partner molecule, the Co-SMAD (SMAD4 in mammals), and import together into the nucleus where they participate in gene transcription such as connective tissue growth factor (CTGF), plasminogen activator inhibitor-1 (PAI-1) and multiple collagens (49).

Many diseases have been proved to be associated with TGF-β signaling. For example, researchers have demonstrated that the role of TGF-β in cancer is paradoxical. On the one hand, TGF-β can act as a tumor suppressor in healthy epithelial cells and early stage of tumor progression. On the other hand, during tumor progression, TGF-β becomes an oncogenic factor inducing proliferation, angiogenesis, invasion, and metastasis (50,51).

Because TGF-β signaling has multiple functions in smooth muscle cell as well as endothelial cell, TGF-β signaling is very active in artery diseases. In recent years, more and more studies start to focus on the function of TGF-β signaling in the aortic aneurysm.

Some of the results are even controversial. Here, we summarized different opinions on the role of TGF-β during aortic aneurysm development.

TGF-β activity and TAA progression

A lot of studies have been conducted to elucidate the role of TGF-β during TAA development, however, the conclusions are different.

Marfan syndrome--Marfan syndrome is an inherited connective tissue disorder due to the mutation of the fibrillin-1 gene (*FBN1*) which is the main component of microfibrils that form the scaffold for elastin assembly within the extracellular matrix (ECM) (52). TGF-β is secreted as a large latent complex (LLC) and remains inactive in ECM. Abnormalities in FBN-1 function may lead to impaired sequestration of latent TGF-β complexes by leading to LLC disassociation, thereby making more available for activation, and potentially leading to enhanced TGF-β signaling (53). The increased plasma TGF-β in MFS patients also supports this result (54). It is reported that aortic aneurysm in a mouse model of MFS is associated with increased TGF-beta signaling. In 2006, Habashi et al. found TGF-beta antagonists such as TGF-β-neutralizing antibody or the angiotensin II type 1 receptor (AT1) blocker, losartan may effectively prevent TAA formation in Marfan syndrome (55). Also, increased activity of TGF-β has been demonstrated from the increased presence of phosphorylated SMAD2 (pSmad2) (56).

Besides the Marfan syndrome which is due to the pathogenesis of FBN1 mutation, the Marfan syndrome type 2 is a result from TGF-β-receptor 2 (TGFBR2) gene defects (57). Interestingly, in Marfan syndrome type 2, the loss of TGF-β signaling appeared to be linked to aneurysm formation.

Loeys-Dietz Syndrome--Leys-Dietz syndrome (LDS) is an autosomal dominant disorder characterized by hypertelorism, bifid uvula, and/or cleft palate, and aggressive arteriopathy causing vascular aneurysms and dissections. In LDS, an aggressive syndrome progression developed when TGF-β signaling was blocked by TGFBR1 or TGFBR2 mutation (58) likely suggesting that the loss of TGF-β signaling may be the underlying cause of LDS. Specifically, TGFBR2 mutation patients are at a high risk of aortic dissections at relatively small aortic diameters, with reported dissections occurring with minimal enlargements. But interestingly, tissues derived from affected individuals showed increased expression of both collagen and connective tissue growth factor, as well as nuclear enrichment of p-Smad2 indicating that there was an enhancement, not a repression, of TGF-β signaling in these aortic specimens (59).

Ehlers–Danlos syndrome type IV--Ehlers–Danlos syndrome type IV primarily affects the skin and large arteries and can lead to medial degenerative disease of the aorta resulting in acute dissection. The original cause was linked to a 3.3 kb DNA deletion in one allele of the type III procollagen gene (COL3A1), which results in a truncated procollagen monomer that has decreased thermal stability, cannot be proteolytically processed, and cannot be efficiently secreted. Study on patients with vascular EDS indicates that circulating TGF-β1 and TGF-β2 levels were increased as well as vascular inflammatory markers (60).

Familial thoracic aortic aneurysms and dissections (FTAAD)--Approximately 20% of patients with TAAD have a family history of TAAD. The age of patients with FTAAD are usually younger and present more rapidly enlarging aneurysms than patients without a family history of aortic diseases suggesting the familial disease is more clinically more

aggressive than the sporadic disease. Genetic heterogeneity of FTAAD is established, and four genes were causing the disease have been identified: *TGFBR1*, *TGFBR2*, *MYH11*, and *ACTA2*. In 2005, Pannu *et al.*found that TGFBR2 mutations in 4 unrelated families with familial TAAD but not Marfan syndrome suggesting TGFBR2 can lead to FTAAD (61).

Mechanism of TGF-β activity during TAA progression

Thoracic aortic aneurysm shows elastic lamellae disruption, accumulation of glycosaminoglycans, and vascular smooth muscle cell (VSMC) apoptosis with minimal inflammatory response. During past 20 years, a large amount of research has demonstrated that TGF-β signaling pathway as a key culprit in the pathogenesis of TAA. In Marfan syndrome, decreased TGF-β signaling significantly promoted artery dilation, thoracic aneurysm formation. Gomez *et al.* found that TGF-β, p-Smad2 as well as Latent TGF-β Binding Protein 1 (LTBP-1) are up-regulated in syndromic and non-syndromic aneurysms of the ascending aorta (56). This result is also supported by the research of another group that overexpression of TGF-β in Marfan syndrome associated with factors that limited tissue repair and promote aneurysm progression (62). In MFS cultured VSMCs and adventitial fibroblasts, they found an increased TGF-beta level and apoptosis, impaired progenitor cell recruitment, and abnormal directional migration. TGF-β can stimulate extracellular signal-regulated kinase (ERK) 1 and 2 and Smad2 in mouse Marfan syndrome, and both of them are decreased by either TGF-β antibody or losartan TAA therapy. In the meanwhile, N-terminal kinase–1 (JNK1) activity was up-regulated

in Smad4-deficient Marfan syndrome mice and the JNK antagonist impeded aortic growth in this mouse model (63).

In the meanwhile, some studies show that TGF-β deficiency promotes the progression of TAA. Different from the study that neutralizing antibody of TGF-β and losartan effectively prevent TAA development in Marfan syndrome, in 2016, Chen *et al.* found that TGF-β neutralization enhances AngII-induced aortic rupture and aneurysm in both thoracic and abdominal regions. Supportively, a study has demonstrated augmented aortic root aneurysms in both TGF-β2 heterozygous deficient and FBN-1 haploinsufficient mice (64). This result is also confirmed in Leys-Dietz syndrome in which aggressive syndrome progression developed when TGF-β signaling was blocked by TGFBR1 or TGFBR2 mutation (58). Recently, mutation of Smad3 which is a key player in the TGF-β pathway has been identified to cause TAA and dissection formation with early-onset osteoarthritis (65). This finding may provide clues for pharmacological targets for the development of TAA treatment.

Compared with AAA, TAA doesn't induce too much severe inflammatory activity. Matrix metalloproteinases (MMPs) and the tissue inhibitors of metalloproteinases (TIMPs) have been implicated in the pathogenesis of TAA through functions in the loss of smooth muscle cells in the aortic media and the destruction of extracellular matrix (ECM). For example, a study of ascending thoracic aortic aneurysm of Marfan syndrome patient showed increased proteolytic activity in elastin degradation by increased MMP-12. Macrophage MMP-12 has been demonstrated to participate in the pathogenesis of thoracic aneurysm by binding tightly to residual elastin fiber fragments (66). A Recent study also indicates that MMP-2 and MMP-9 may also play a role in thoracic aortic

disease. In human ascending thoracic aortic aneurysm, both MMP-2 and MMP-9 were upregulated when the associated aortic valve was congenitally bicuspid (67). Besides the role TGF-β in matrix deposition such as collagen synthesis, a recent study has investigated how altered TGF-beta is involved in ECM degradation in the thoracic aneurysm. The previous study showed that p38MAPK activation results in the elevated level of both MMP-2 and MMP-9 in breast cancer cells (68). TGF-β can regulate MMP transcription level through TGF-β inhibitory element (TIE) because it is reported that MMP-1, MMP-7, MMP-9 and MMP-13 contain TIE binding sites in their promoters. Also, the MMP-13 level may also partly be regulated by TGF-β by Smad signaling when Smad3 interacts with JunB and Runx-2 (69).

TGF-β activity and AAA progression

Different from TAAs which occur in the ascending aorta, arch, and/or descending thoracic aorta, AAA usually develops in the infra-renal segment. Also, the embryonic origin of thoracic artery media vascular smooth muscle cells (VSMCs) is from somite and neural crest while abdominal artery SMCs are given rise from somite. Different progenitor origin of SMC from different location has distinct response upon TGF-β stimulation (70). AAA is usually characterized with vascular extracellular matrix (ECM) changes, accompanied by transmural inflammation, destructive remodeling of the elastic media, and depletion of medial smooth muscle cells.

In 2010, Mallat et al. demonstrated that TGF-β activity protects against inflammatory aortic aneurysm progression. In this study, they neutralized TGF-β activity in C57BL/6 mice which are induced with AngII to form AAAs. They found that these mice displayed

fissuration, double channel formation and even rupture. Besides, TGF-β neutralization increased matrix metalloproteinase-12 (MMP-12) activity and promoted aneurysm rupture(71). In 2009, King et al. indicated that neutralization of TGF-β diminished AngII-induced AAA dilation in $Apoe^{-/-}$ $Cxcl10^{-/-}$ mice. This result demonstrated that TGF-β activity could promote AAA progression. This result conflicts with Mallat et al.'s result(72). Mallat et al indicated that King et al. group didn't show sufficient data to support the efficiency of their TGF-β neutralization (71). That TGF-β is protective in AAA progression is indirectly demonstrated by that Smad3 deficiency promoted artery remodeling, inflammatory cell infiltration and AAA development (73). In this study, they also observed that NF-κB and ERK1/2 signaling as well as the expression of nuclear Smad2, Smad4, and TGF-β1 increased in the vessel wall of smad3 deficiency mice. However, in 2015, Gao et al. provided a conflicting result from *Li et al.* and confirmed King *et. al.* conclusion. They used smooth muscle cell-specific TGFBR2 disruption mice to induce AAA by elastase infusion method. As a result, elastin degradation, medial smooth muscle loss, and inflammatory cell infiltration were observed. This study demonstrated that TGF-β signaling pathway in smooth muscle cell plays an important role in AAA development and disruption can diminish the aneurysm progression (74).

Mechanism of TGF-β activity during AAA progression

Since AAA is characterized by increased inflammation, ECM degradation, and media SMC apoptosis, we'll introduce the mechanism of TGF-β separately in these three aspects.

TGF-β and inflammation

Compared with its role to induce noninflammatory excessive accumulation of SMCs and lead to ECM remodeling in TAA, TGF-β plays a distinct role in inflammatory AAA progression. TGF-β plays an important role in the control of inflammation, treatment of TGF-β significantly reduced the capacity of IFN-γ, IL-1β, and TNF-α suggesting TGF-β as an immune suppressive factor (75). Another group also reported that TGF-β inhibits the migration of neutrophils through endothelial monolayers activated by TNF-α and impedes leukocyte adhesiveness to the endothelium at least in part by inhibiting the expression of E-selectin (76). Also, TGF-β is involved in suppression of macrophages activation via competition for essential coactivators such as p300 with Smad3 (77).

TGF-β and ECM degradation

AAA is characterized by increased ECM degradation. MMPs and cysteine proteases majorly function in collagen and elastin degradation and leading to artery wall destruction. Studies have shown that tissue samples from AAA exhibited increased levels of (MMPs). For example,elevated MMP-12 participates in ECM degradation and promotes AAA progression (71). Wang et al. demonstrated that neutralizing TGF-β activity promoted AAA rupture in angiotensin II-induced AAA model through eliminating the blockade of MMP-12 activity.

TGF-β and media SMC apoptosis

In 2014, Shi. *et al.* demonstrated that elevation of both TGF-β and Smad3 leads to SMC secretion of VEGF-A that functions as an autocrine inhibitor of SMC apoptosis (78) suggesting loss function of TGF-β/Smad3 signaling pathway may cause SMC apoptosis

and lead to AAA formation. In both rat elastase-infusion model and mouse calcium chloride model, induced TGF-β1 preserved medial and adventitia layer SMC content (79).

Management

Risk factor reduction

Smoking has been demonstrated to be a common risk factor in aortic aneurysm formation. The study has indicated that aneurysm development is associated with numbers of smoking years as well as the numbers of years after cessation. Cessation of smoking would reduce the risk of aortic aneurysm formation and the rate of aneurysm growth (80).

Hypertension and hyperlipidemia have been reported as risk factors for the aortic aneurysm. Medications for hypertension and hyperlipidemia treatment have been recommended to patients with AAA. For example, statins are used for decreasing lipid level in blood. It may also share a therapeutic benefit with AAA patients to slow AAA growth(81).

Surgical treatment

The goal of aneurysm treatment is to prevent rupture and death. It is very important to decide the right time for elective surgery to prevent rupture. For example, surgical intervention can be done when the size of descending aorta is larger than 6cm in patients with degenerative thoracic aneurysm. Some methods have been introduced to avoid surgical damage including regional hypothermic protection of the spinal cord by epidural cooling during surgery and maintenance of distal aortic perfusion during surgery with the

use of atriofemoral (left heart) bypass to the distal aorta (82). The surgical repair for AAA includes transabdominal route and the retroperitoneal route.

Endovascular stent graft repair is a less invasive and less expensive alternative compared to open surgical. Endovascular repair involves insertion of an endograft into the lumen that effectively excludes an aneurysm from blood flow, minimizing the risk of rupture (83,84).

Medical treatment

Medical management can slow the progression of an aneurysm and reduces the risks of dissection or rupture. In 2005 ACC/AHA guideline recommended TGF-β blocker therapy in patients with AAAs who did not undergo surgery (85). The study has shown that propranolol (β-blocker) is effective in slowing the rate of aortic dilatation and reducing the development of aortic complications in some patients with Marfan's syndrome (86). However, it's still unknown if this β-blocker can be used for other aneurysm condition.

Another study has demonstrated that Marfan syndrome is associated with TGF-β disruption. Angiotensin II is important in TGF-β signaling, and blocking TGB-β, using a neutralizing antibody or the angiotensin II type 1 receptor blocker losartan, can prevent or attenuate aneurysm formation in Marfan syndrome (55).

Conclusion

Aortic aneurysm is an asymptomatic disease. It can be induced by many different risk factors including smoking, sex, age, hypertension, and hyperlipidemia. Aortic aneurysm can be categorized into TAA and AAA according to their locations. TAA formation is mostly related to the genetics and familial mutation, while AAA development is most

commonly associated with inflammation. In recent years, a large amount of research have been focusing on the role of TGF-β in aortic aneurysm progression. For TAA study, most of the studies demonstrate that TGF-β protects against aneurysm development. However, for AAA study, the role of TGF-β remains elusive. Understanding of the role of TGF-β during aneurysm development may provide clues for therapeutic targeting.

Reference

1. Writing Group, M., Mozaffarian, D., Benjamin, E. J., Go, A. S., Arnett, D. K., Blaha, M. J., Cushman, M., Das, S. R., de Ferranti, S., Despres, J. P., Fullerton, H. J., Howard, V. J., Huffman, M. D., Isasi, C. R., Jimenez, M. C., Judd, S. E., Kissela, B. M., Lichtman, J. H., Lisabeth, L. D., Liu, S., Mackey, R. H., Magid, D. J., McGuire, D. K., Mohler, E. R., 3rd, Moy, C. S., Muntner, P., Mussolino, M. E., Nasir, K., Neumar, R. W., Nichol, G., Palaniappan, L., Pandey, D. K., Reeves, M. J., Rodriguez, C. J., Rosamond, W., Sorlie, P. D., Stein, J., Towfighi, A., Turan, T. N., Virani, S. S., Woo, D., Yeh, R. W., Turner, M. B., American Heart Association Statistics, C., and Stroke Statistics, S. (2016) Heart Disease and Stroke Statistics-2016 Update: A Report From the American Heart Association. *Circulation* **133**, e38-360
2. Writing Group, M., Mozaffarian, D., Benjamin, E. J., Go, A. S., Arnett, D. K., Blaha, M. J., Cushman, M., Das, S. R., de Ferranti, S., Despres, J. P., Fullerton, H. J., Howard, V. J., Huffman, M. D., Isasi, C. R., Jimenez, M. C., Judd, S. E., Kissela, B. M., Lichtman, J. H., Lisabeth, L. D., Liu, S., Mackey, R. H., Magid, D.

J., McGuire, D. K., Mohler, E. R., 3rd, Moy, C. S., Muntner, P., Mussolino, M. E., Nasir, K., Neumar, R. W., Nichol, G., Palaniappan, L., Pandey, D. K., Reeves, M. J., Rodriguez, C. J., Rosamond, W., Sorlie, P. D., Stein, J., Towfighi, A., Turan, T. N., Virani, S. S., Woo, D., Yeh, R. W., Turner, M. B., American Heart Association Statistics, C., and Stroke Statistics, S. (2016) Executive Summary: Heart Disease and Stroke Statistics--2016 Update: A Report From the American Heart Association. *Circulation* **133**, 447-454

3. Kontopodis, N., Lioudaki, S., Pantidis, D., Papadopoulos, G., Georgakarakos, E., and Ioannou, C. V. (2016) Advances in determining abdominal aortic aneurysm size and growth. *World J Radiol* **8**, 148-158

4. Thakur, V., Rankin, K. N., Hartling, L., and Mackie, A. S. (2013) A systematic review of the pharmacological management of aortic root dilation in Marfan syndrome. *Cardiol Young* **23**, 568-581

5. Albornoz, G., Coady, M. A., Roberts, M., Davies, R. R., Tranquilli, M., Rizzo, J. A., and Elefteriades, J. A. (2006) Familial thoracic aortic aneurysms and dissections--incidence, modes of inheritance, and phenotypic patterns. *Ann Thorac Surg* **82**, 1400-1405

6. Coady, M. A., Davies, R. R., Roberts, M., Goldstein, L. J., Rogalski, M. J., Rizzo, J. A., Hammond, G. L., Kopf, G. S., and Elefteriades, J. A. (1999) Familial patterns of thoracic aortic aneurysms. *Arch Surg* **134**, 361-367

7. Milewicz, D. M., Chen, H., Park, E. S., Petty, E. M., Zaghi, H., Shashidhar, G., Willing, M., and Patel, V. (1998) Reduced penetrance and variable expressivity of familial thoracic aortic aneurysms/dissections. *Am J Cardiol* **82**, 474-479

8. Guo, D., Hasham, S., Kuang, S. Q., Vaughan, C. J., Boerwinkle, E., Chen, H., Abuelo, D., Dietz, H. C., Basson, C. T., Shete, S. S., and Milewicz, D. M. (2001) Familial thoracic aortic aneurysms and dissections: genetic heterogeneity with a major locus mapping to 5q13-14. *Circulation* **103**, 2461-2468

9. Hasham, S. N., Willing, M. C., Guo, D. C., Muilenburg, A., He, R., Tran, V. T., Scherer, S. E., Shete, S. S., and Milewicz, D. M. (2003) Mapping a locus for familial thoracic aortic aneurysms and dissections (TAAD2) to 3p24-25. *Circulation* **107**, 3184-3190

10. Burke, A. P., Tavora, F., Narula, N., Tomaszewski, J. E., and Virmani, R. (2008) Aortitis and ascending aortic aneurysm: description of 52 cases and proposal of a histologic classification. *Hum Pathol* **39**, 514-526

11. Roberts, W. C., Barbin, C. M., Weissenborn, M. R., Ko, J. M., and Henry, A. C. (2015) Syphilis as a Cause of Thoracic Aortic Aneurysm. *Am J Cardiol* **116**, 1298-1303

12. Vasudevan, B., Verma, R., Pragasam, V., and Nema, S. (2014) A rare case of tertiary syphilis complicated with aortic aneurysm in this era of early use of highly effective antibiotics. *Indian J Sex Transm Dis* **35**, 46-48

13. Legg, J. S., and Legg, L. M. (2016) Abdominal Aortic Aneurysms. *Radiol Technol* **88**, 145-163

14. Aggarwal, S., Qamar, A., Sharma, V., and Sharma, A. (2011) Abdominal aortic aneurysm: A comprehensive review. *Exp Clin Cardiol* **16**, 11-15

15. Kuivaniemi, H., Shibamura, H., Arthur, C., Berguer, R., Cole, C. W., Juvonen, T., Kline, R. A., Limet, R., Mackean, G., Norrgard, O., Pals, G., Powell, J. T., Rainio,

P., Sakalihasan, N., van Vlijmen-van Keulen, C., Verloes, A., and Tromp, G. (2003) Familial abdominal aortic aneurysms: collection of 233 multiplex families. *J Vasc Surg* **37**, 340-345

16. Sandford, R. M., Bown, M. J., London, N. J., and Sayers, R. D. (2007) The genetic basis of abdominal aortic aneurysms: a review. *Eur J Vasc Endovasc Surg* **33**, 381-390
17. van Vlijmen-van Keulen, C. J., Pals, G., and Rauwerda, J. A. (2002) Familial abdominal aortic aneurysm: a systematic review of a genetic background. *Eur J Vasc Endovasc Surg* **24**, 105-116
18. Mikolajczyk-Stecyna, J., Korcz, A., Gabriel, M., Pawlaczyk, K., Oszkinis, G., and Slomski, R. (2013) Risk factors in abdominal aortic aneurysm and in Polish population aortoiliac occlusive disease and differences between them [corrected]. *Sci Rep* **3**, 3528
19. Yoshida, S., Fuster, J. J., and Walsh, K. (2014) Adiponectin attenuates abdominal aortic aneurysm formation in hyperlipidemic mice. *Atherosclerosis* **235**, 339-346
20. Hannawa, K. K., Eliason, J. L., and Upchurch, G. R., Jr. (2009) Gender differences in abdominal aortic aneurysms. *Vascular* **17 Suppl 1**, S30-39
21. Singh, K., Bonaa, K. H., Jacobsen, B. K., Bjork, L., and Solberg, S. (2001) Prevalence of and risk factors for abdominal aortic aneurysms in a population-based study : The Tromso Study. *Am J Epidemiol* **154**, 236-244
22. Jaakkola, P. (1997) [Abdominal aortic aneurysm: an illness increasing in the aging population]. *Duodecim* **113**, 2054-2064
23. Martin-McNulty, B., Tham, D. M., da Cunha, V., Ho, J. J., Wilson, D. W.,

Rutledge, J. C., Deng, G. G., Vergona, R., Sullivan, M. E., and Wang, Y. X. (2003) 17 Beta-estradiol attenuates development of angiotensin II-induced aortic abdominal aneurysm in apolipoprotein E-deficient mice. *Arterioscler Thromb Vasc Biol* **23**, 1627-1632

24. Wu, X. F., Zhang, J., Paskauskas, S., Xin, S. J., and Duan, Z. Q. (2009) The role of estrogen in the formation of experimental abdominal aortic aneurysm. *Am J Surg* **197**, 49-54

25. Laser, A., Ghosh, A., Roelofs, K., Sadiq, O., McEvoy, B., DiMusto, P., Eliason, J., and Upchurch, G. R., Jr. (2014) Increased estrogen receptor alpha in experimental aortic aneurysms in females compared with males. *J Surg Res* **186**, 467-474

26. Vardulaki, K. A., Walker, N. M., Day, N. E., Duffy, S. W., Ashton, H. A., and Scott, R. A. (2000) Quantifying the risks of hypertension, age, sex and smoking in patients with abdominal aortic aneurysm. *Br J Surg* **87**, 195-200

27. Norman, P. E., and Curci, J. A. (2013) Understanding the effects of tobacco smoke on the pathogenesis of aortic aneurysm. *Arterioscler Thromb Vasc Biol* **33**, 1473-1477

28. Kent, K. C., Zwolak, R. M., Egorova, N. N., Riles, T. S., Manganaro, A., Moskowitz, A. J., Gelijns, A. C., and Greco, G. (2010) Analysis of risk factors for abdominal aortic aneurysm in a cohort of more than 3 million individuals. *J Vasc Surg* **52**, 539-548

29. Jahangir, E., Lipworth, L., Edwards, T. L., Kabagambe, E. K., Mumma, M. T., Mensah, G. A., Fazio, S., Blot, W. J., and Sampson, U. K. (2015) Smoking, sex, risk factors and abdominal aortic aneurysms: a prospective study of 18 782

persons aged above 65 years in the Southern Community Cohort Study. *J Epidemiol Community Health* **69**, 481-488

30. Nordon, I. M., Hinchliffe, R. J., Loftus, I. M., and Thompson, M. M. (2011) Pathophysiology and epidemiology of abdominal aortic aneurysms. *Nat Rev Cardiol* **8**, 92-102

31. Maegdefessel, L., Azuma, J., Toh, R., Deng, A., Merk, D. R., Raiesdana, A., Leeper, N. J., Raaz, U., Schoelmerich, A. M., McConnell, M. V., Dalman, R. L., Spin, J. M., and Tsao, P. S. (2012) MicroRNA-21 blocks abdominal aortic aneurysm development and nicotine-augmented expansion. *Sci Transl Med* **4**, 122ra122

32. Jacob-Ferreira, A. L., Palei, A. C., Cau, S. B., Moreno, H., Jr., Martinez, M. L., Izidoro-Toledo, T. C., Gerlach, R. F., and Tanus-Santos, J. E. (2010) Evidence for the involvement of matrix metalloproteinases in the cardiovascular effects produced by nicotine. *Eur J Pharmacol* **627**, 216-222

33. Nordskog, B. K., Blixt, A. D., Morgan, W. T., Fields, W. R., and Hellmann, G. M. (2003) Matrix-degrading and pro-inflammatory changes in human vascular endothelial cells exposed to cigarette smoke condensate. *Cardiovasc Toxicol* **3**, 101-117

34. Reeps, C., Pelisek, J., Seidl, S., Schuster, T., Zimmermann, A., Kuehnl, A., and Eckstein, H. H. (2009) Inflammatory infiltrates and neovessels are relevant sources of MMPs in abdominal aortic aneurysm wall. *Pathobiology* **76**, 243-252

35. Shiraya, S., Miwa, K., Aoki, M., Miyake, T., Oishi, M., Kataoka, K., Ohgi, S., Ogihara, T., Kaneda, Y., and Morishita, R. (2006) Hypertension accelerated

experimental abdominal aortic aneurysm through upregulation of nuclear factor kappaB and Ets. *Hypertension* **48**, 628-636

36. Wong, D. R., Willett, W. C., and Rimm, E. B. (2007) Smoking, hypertension, alcohol consumption, and risk of abdominal aortic aneurysm in men. *Am J Epidemiol* **165**, 838-845

37. Takagi, H., Umemoto, T., and Group, A. (2017) Association of Hypertension with Abdominal Aortic Aneurysm Expansion. *Ann Vasc Surg* **39**, 74-89

38. Daugherty, A., and Cassis, L. A. (2004) Mouse models of abdominal aortic aneurysms. *Arterioscler Thromb Vasc Biol* **24**, 429-434

39. Marinov, G. R., Marois, Y., Paris, E., Roby, P., Formichi, M., Douville, Y., and Guidoin, R. (1997) Can the infusion of elastase in the abdominal aorta of the Yucatan miniature swine consistently produce experimental aneurysms? *J Invest Surg* **10**, 129-150

40. Gertz, S. D., Mintz, Y., Beeri, R., Rubinstein, C., Gilon, D., Gavish, L., Berlatzky, Y., Appelbaum, L., and Gavish, L. (2013) Lessons from Animal Models of Arterial Aneurysm. *Aorta (Stamford)* **1**, 244-254

41. Lima, B. L., Santos, E. J., Fernandes, G. R., Merkel, C., Mello, M. R., Gomes, J. P., Soukoyan, M., Kerkis, A., Massironi, S. M., Visintin, J. A., and Pereira, L. V. (2010) A new mouse model for marfan syndrome presents phenotypic variability associated with the genetic background and overall levels of Fbn1 expression. *PLoS One* **5**, e14136

42. Wang, C., Qian, X., Sun, X., and Chang, Q. (2015) Angiotensin II increases matrix metalloproteinase 2 expression in human aortic smooth muscle cells via

AT1R and ERK1/2. *Exp Biol Med (Maywood)* **240**, 1564-1571

43. Kanematsu, Y., Kanematsu, M., Kurihara, C., Tsou, T. L., Nuki, Y., Liang, E. I., Makino, H., and Hashimoto, T. (2010) Pharmacologically induced thoracic and abdominal aortic aneurysms in mice. *Hypertension* **55**, 1267-1274

44. Gertz, S. D., Kurgan, A., and Eisenberg, D. (1988) Aneurysm of the rabbit common carotid artery induced by periarterial application of calcium chloride in vivo. *J Clin Invest* **81**, 649-656

45. Bhamidipati, C. M., Mehta, G. S., Lu, G., Moehle, C. W., Barbery, C., DiMusto, P. D., Laser, A., Kron, I. L., Upchurch, G. R., Jr., and Ailawadi, G. (2012) Development of a novel murine model of aortic aneurysms using peri-adventitial elastase. *Surgery* **152**, 238-246

46. Huang, T., and Hinck, A. P. (2016) Production, Isolation, and Structural Analysis of Ligands and Receptors of the TGF-beta Superfamily. *Methods Mol Biol* **1344**, 63-92

47. Jung, B., Staudacher, J. J., and Beauchamp, D. (2017) Transforming Growth Factor beta Superfamily Signaling in Development of Colorectal Cancer. *Gastroenterology* **152**, 36-52

48. Nagaraj, N. S., and Datta, P. K. (2010) Targeting the transforming growth factor-beta signaling pathway in human cancer. *Expert Opin Investig Drugs* **19**, 77-91

49. Massague, J., Seoane, J., and Wotton, D. (2005) Smad transcription factors. *Genes Dev* **19**, 2783-2810

50. Massague, J. (2008) TGFbeta in Cancer. *Cell* **134**, 215-230

51. Seoane, J. (2008) The TGFBeta pathway as a therapeutic target in cancer. *Clin*

Transl Oncol **10**, 14-19

52. Dietz, H. C., Loeys, B., Carta, L., and Ramirez, F. (2005) Recent progress towards a molecular understanding of Marfan syndrome. *Am J Med Genet C Semin Med Genet* **139C**, 4-9

53. Chaudhry, S. S., Cain, S. A., Morgan, A., Dallas, S. L., Shuttleworth, C. A., and Kielty, C. M. (2007) Fibrillin-1 regulates the bioavailability of TGFbeta1. *J Cell Biol* **176**, 355-367

54. Franken, R., den Hartog, A. W., de Waard, V., Engele, L., Radonic, T., Lutter, R., Timmermans, J., Scholte, A. J., van den Berg, M. P., Zwinderman, A. H., Groenink, M., and Mulder, B. J. (2013) Circulating transforming growth factor-beta as a prognostic biomarker in Marfan syndrome. *Int J Cardiol* **168**, 2441-2446

55. Habashi, J. P., Judge, D. P., Holm, T. M., Cohn, R. D., Loeys, B. L., Cooper, T. K., Myers, L., Klein, E. C., Liu, G., Calvi, C., Podowski, M., Neptune, E. R., Halushka, M. K., Bedja, D., Gabrielson, K., Rifkin, D. B., Carta, L., Ramirez, F., Huso, D. L., and Dietz, H. C. (2006) Losartan, an AT1 antagonist, prevents aortic aneurysm in a mouse model of Marfan syndrome. *Science* **312**, 117-121

56. Gomez, D., Al Haj Zen, A., Borges, L. F., Philippe, M., Gutierrez, P. S., Jondeau, G., Michel, J. B., and Vranckx, R. (2009) Syndromic and non-syndromic aneurysms of the human ascending aorta share activation of the Smad2 pathway. *J Pathol* **218**, 131-142

57. Mizuguchi, T., Collod-Beroud, G., Akiyama, T., Abifadel, M., Harada, N., Morisaki, T., Allard, D., Varret, M., Claustres, M., Morisaki, H., Ihara, M., Kinoshita, A., Yoshiura, K., Junien, C., Kajii, T., Jondeau, G., Ohta, T., Kishino, T.,

Furukawa, Y., Nakamura, Y., Niikawa, N., Boileau, C., and Matsumoto, N. (2004) Heterozygous TGFBR2 mutations in Marfan syndrome. *Nat Genet* **36**, 855-860

58. Loeys, B. L., Schwarze, U., Holm, T., Callewaert, B. L., Thomas, G. H., Pannu, H., De Backer, J. F., Oswald, G. L., Symoens, S., Manouvrier, S., Roberts, A. E., Faravelli, F., Greco, M. A., Pyeritz, R. E., Milewicz, D. M., Coucke, P. J., Cameron, D. E., Braverman, A. C., Byers, P. H., De Paepe, A. M., and Dietz, H. C. (2006) Aneurysm syndromes caused by mutations in the TGF-beta receptor. *N Engl J Med* **355**, 788-798

59. Loeys, B. L., Chen, J., Neptune, E. R., Judge, D. P., Podowski, M., Holm, T., Meyers, J., Leitch, C. C., Katsanis, N., Sharifi, N., Xu, F. L., Myers, L. A., Spevak, P. J., Cameron, D. E., De Backer, J., Hellemans, J., Chen, Y., Davis, E. C., Webb, C. L., Kress, W., Coucke, P., Rifkin, D. B., De Paepe, A. M., and Dietz, H. C. (2005) A syndrome of altered cardiovascular, craniofacial, neurocognitive and skeletal development caused by mutations in TGFBR1 or TGFBR2. *Nat Genet* **37**, 275-281

60. Morissette, R., Schoenhoff, F., Xu, Z., Shilane, D. A., Griswold, B. F., Chen, W., Yang, J., Zhu, J., Fert-Bober, J., Sloper, L., Lehman, J., Commins, N., Van Eyk, J. E., and McDonnell, N. B. (2014) Transforming growth factor-beta and inflammation in vascular (type IV) Ehlers-Danlos syndrome. *Circ Cardiovasc Genet* **7**, 80-88

61. Pannu, H., Fadulu, V. T., Chang, J., Lafont, A., Hasham, S. N., Sparks, E., Giampietro, P. F., Zaleski, C., Estrera, A. L., Safi, H. J., Shete, S., Willing, M. C., Raman, C. S., and Milewicz, D. M. (2005) Mutations in transforming growth

factor-beta receptor type II cause familial thoracic aortic aneurysms and dissections. *Circulation* **112**, 513-520

62. Nataatmadja, M., West, J., and West, M. (2006) Overexpression of transforming growth factor-beta is associated with increased hyaluronan content and impairment of repair in Marfan syndrome aortic aneurysm. *Circulation* **114**, I371-377

63. Holm, T. M., Habashi, J. P., Doyle, J. J., Bedja, D., Chen, Y., van Erp, C., Lindsay, M. E., Kim, D., Schoenhoff, F., Cohn, R. D., Loeys, B. L., Thomas, C. J., Patnaik, S., Marugan, J. J., Judge, D. P., and Dietz, H. C. (2011) Noncanonical TGFbeta signaling contributes to aortic aneurysm progression in Marfan syndrome mice. *Science* **332**, 358-361

64. Lindsay, M. E., Schepers, D., Bolar, N. A., Doyle, J. J., Gallo, E., Fert-Bober, J., Kempers, M. J., Fishman, E. K., Chen, Y., Myers, L., Bjeda, D., Oswald, G., Elias, A. F., Levy, H. P., Anderlid, B. M., Yang, M. H., Bongers, E. M., Timmermans, J., Braverman, A. C., Canham, N., Mortier, G. R., Brunner, H. G., Byers, P. H., Van Eyk, J., Van Laer, L., Dietz, H. C., and Loeys, B. L. (2012) Loss-of-function mutations in TGFB2 cause a syndromic presentation of thoracic aortic aneurysm. *Nat Genet* **44**, 922-927

65. van de Laar, I. M., Oldenburg, R. A., Pals, G., Roos-Hesselink, J. W., de Graaf, B. M., Verhagen, J. M., Hoedemaekers, Y. M., Willemsen, R., Severijnen, L. A., Venselaar, H., Vriend, G., Pattynama, P. M., Collee, M., Majoor-Krakauer, D., Poldermans, D., Frohn-Mulder, I. M., Micha, D., Timmermans, J., Hilhorst-Hofstee, Y., Bierma-Zeinstra, S. M., Willems, P. J., Kros, J. M., Oei, E. H., Oostra,

B. A., Wessels, M. W., and Bertoli-Avella, A. M. (2011) Mutations in SMAD3 cause a syndromic form of aortic aneurysms and dissections with early-onset osteoarthritis. *Nat Genet* **43**, 121-126

66. Curci, J. A., Liao, S., Huffman, M. D., Shapiro, S. D., and Thompson, R. W. (1998) Expression and localization of macrophage elastase (matrix metalloproteinase-12) in abdominal aortic aneurysms. *J Clin Invest* **102**, 1900-1910

67. LeMaire, S. A., Wang, X., Wilks, J. A., Carter, S. A., Wen, S., Won, T., Leonardelli, D., Anand, G., Conklin, L. D., Wang, X. L., Thompson, R. W., and Coselli, J. S. (2005) Matrix metalloproteinases in ascending aortic aneurysms: bicuspid versus trileaflet aortic valves. *J Surg Res* **123**, 40-48

68. Kim, E. S., Kim, M. S., and Moon, A. (2004) TGF-beta-induced upregulation of MMP-2 and MMP-9 depends on p38 MAPK, but not ERK signaling in MCF10A human breast epithelial cells. *Int J Oncol* **25**, 1375-1382

69. Hijova, E. (2005) Matrix metalloproteinases: their biological functions and clinical implications. *Bratisl Lek Listy* **106**, 127-132

70. Majesky, M. W., Dong, X. R., Regan, J. N., and Hoglund, V. J. (2011) Vascular smooth muscle progenitor cells: building and repairing blood vessels. *Circ Res* **108**, 365-377

71. Wang, Y., Ait-Oufella, H., Herbin, O., Bonnin, P., Ramkhelawon, B., Taleb, S., Huang, J., Offenstadt, G., Combadiere, C., Renia, L., Johnson, J. L., Tharaux, P. L., Tedgui, A., and Mallat, Z. (2010) TGF-beta activity protects against inflammatory aortic aneurysm progression and complications in angiotensin II-

infused mice. *J Clin Invest* **120**, 422-432

72. King, V. L., Lin, A. Y., Kristo, F., Anderson, T. J., Ahluwalia, N., Hardy, G. J., Owens, A. P., 3rd, Howatt, D. A., Shen, D., Tager, A. M., Luster, A. D., Daugherty, A., and Gerszten, R. E. (2009) Interferon-gamma and the interferon-inducible chemokine CXCL10 protect against aneurysm formation and rupture. *Circulation* **119**, 426-435

73. Dai, X., Shen, J., Annam, N. P., Jiang, H., Levi, E., Schworer, C. M., Tromp, G., Arora, A., Higgins, M., Wang, X. F., Yang, M., Li, H. J., Zhang, K., Kuivaniemi, H., and Li, L. (2015) SMAD3 deficiency promotes vessel wall remodeling, collagen fiber reorganization and leukocyte infiltration in an inflammatory abdominal aortic aneurysm mouse model. *Sci Rep* **5**, 10180

74. Gao, F., Chambon, P., Offermanns, S., Tellides, G., Kong, W., Zhang, X., and Li, W. (2014) Disruption of TGF-beta signaling in smooth muscle cell prevents elastase-induced abdominal aortic aneurysm. *Biochem Biophys Res Commun* **454**, 137-143

75. Barnum, S. R., and Jones, J. L. (1994) Transforming growth factor-beta 1 inhibits inflammatory cytokine-induced C3 gene expression in astrocytes. *J Immunol* **152**, 765-773

76. Gamble, J. R., Khew-Goodall, Y., and Vadas, M. A. (1993) Transforming growth factor-beta inhibits E-selectin expression on human endothelial cells. *J Immunol* **150**, 4494-4503

77. Werner, F., Jain, M. K., Feinberg, M. W., Sibinga, N. E., Pellacani, A., Wiesel, P., Chin, M. T., Topper, J. N., Perrella, M. A., and Lee, M. E. (2000) Transforming

growth factor-beta 1 inhibition of macrophage activation is mediated via Smad3. *J Biol Chem* **275**, 36653-36658

78. Shi, X., Guo, L. W., Seedial, S. M., Si, Y., Wang, B., Takayama, T., Suwanabol, P. A., Ghosh, S., DiRenzo, D., Liu, B., and Kent, K. C. (2014) TGF-beta/Smad3 inhibit vascular smooth muscle cell apoptosis through an autocrine signaling mechanism involving VEGF-A. *Cell Death Dis* **5**, e1317

79. Dai, J., Michineau, S., Franck, G., Desgranges, P., Becquemin, J. P., Gervais, M., and Allaire, E. (2011) Long term stabilization of expanding aortic aneurysms by a short course of cyclosporine A through transforming growth factor-beta induction. *PLoS One* **6**, e28903

80. Lederle, F. A., Johnson, G. R., Wilson, S. E., Chute, E. P., Hye, R. J., Makaroun, M. S., Barone, G. W., Bandyk, D., Moneta, G. L., and Makhoul, R. G. (2000) The aneurysm detection and management study screening program: validation cohort and final results. Aneurysm Detection and Management Veterans Affairs Cooperative Study Investigators. *Arch Intern Med* **160**, 1425-1430

81. Kertai, M. D., Boersma, E., Westerhout, C. M., van Domburg, R., Klein, J., Bax, J. J., van Urk, H., and Poldermans, D. (2004) Association between long-term statin use and mortality after successful abdominal aortic aneurysm surgery. *Am J Med* **116**, 96-103

82. Cowan, J. A., Jr., Dimick, J. B., Henke, P. K., Huber, T. S., Stanley, J. C., and Upchurch, G. R., Jr. (2003) Surgical treatment of intact thoracoabdominal aortic aneurysms in the United States: hospital and surgeon volume-related outcomes. *J Vasc Surg* **37**, 1169-1174

83. Lederle, F. A. (2004) Abdominal aortic aneurysm--open versus endovascular repair. *N Engl J Med* **351**, 1677-1679

84. Prault, T. L., Stevens, S. L., Freeman, M. B., Cassada, D., Hardin, R., and Goldman, M. H. (2004) Open versus endo: early experience with endovascular abdominal aortic aneurysm repair beyond the clinical trials. *Heart Surg Forum* **7**, E459-461

85. Hirsch, A. T., Haskal, Z. J., Hertzer, N. R., Bakal, C. W., Creager, M. A., Halperin, J. L., Hiratzka, L. F., Murphy, W. R., Olin, J. W., Puschett, J. B., Rosenfield, K. A., Sacks, D., Stanley, J. C., Taylor, L. M., Jr., White, C. J., White, J., White, R. A., Antman, E. M., Smith, S. C., Jr., Adams, C. D., Anderson, J. L., Faxon, D. P., Fuster, V., Gibbons, R. J., Hunt, S. A., Jacobs, A. K., Nishimura, R., Ornato, J. P., Page, R. L., Riegel, B., American Association for Vascular, S., Society for Vascular, S., Society for Cardiovascular, A., Interventions, Society for Vascular, M., Biology, Society of Interventional, R., Disease, A. A. T. F. o. P. G. W. C. t. D. G. f. t. M. o. P. W. P. A., American Association of, C., Pulmonary, R., National Heart, L., Blood, I., Society for Vascular, N., TransAtlantic Inter-Society, C., and Vascular Disease, F. (2006) ACC/AHA 2005 Practice Guidelines for the management of patients with peripheral arterial disease (lower extremity, renal, mesenteric, and abdominal aortic): a collaborative report from the American Association for Vascular Surgery/Society for Vascular Surgery, Society for Cardiovascular Angiography and Interventions, Society for Vascular Medicine and Biology, Society of Interventional Radiology, and the ACC/AHA Task Force on Practice Guidelines (Writing Committee to Develop Guidelines for the

Management of Patients With Peripheral Arterial Disease): endorsed by the American Association of Cardiovascular and Pulmonary Rehabilitation; National Heart, Lung, and Blood Institute; Society for Vascular Nursing; TransAtlantic Inter-Society Consensus; and Vascular Disease Foundation. *Circulation* **113**, e463-654

86. Shores, J., Berger, K. R., Murphy, E. A., and Pyeritz, R. E. (1994) Progression of aortic dilatation and the benefit of long-term beta-adrenergic blockade in Marfan's syndrome. *N Engl J Med* **330**, 1335-1341

CHAPTER 3

MESENCHYME HOMEOBOX 1, A NOVEL REGULATOR IN TGF-B-INDUCED SMOOTH MUSCLE CELL DIFFERENTIATION[1]

[1] Kun Dong, Xia Guo, Qiang Shao, Amanda Hsu and Shi-You Chen. To be submitted to *Journal of Biological Chemistry*.

Abstract

Smooth muscle cell (SMC) differentiation is an important process during vasculogenesis and angiogenesis. VSMC phenotypic alterations are essential for the progression of several cardiovascular disorders such as atherosclerosis, hypertension, and restenosis after angioplasty, etc. However, molecular mechanisms controlling VSMC differentiation are not completely understood. Mesenchyme homeobox 1 (Meox1) is expressed in the early developing somite and its derivatives during embryogenesis. Somite has been shown to be one of the origins for SMC. In the present study, we identified a novel role of Meox1 in SMC differentiation. Transforming growth factor-β (TGF-β) induces Meox1 expression in the initial phase of SMC differentiation of pluripotent C3H10T1/2 cells. Knockdown of Meox1 by specific shRNA suppresses TGF-β-induced expression of SMC early markers. In vivo, we also found that Meox1 knockdown in mouse embryos exhibited decreased SMC markers expression in descending aorta of neonatal mice. Meox1 overexpression, on the other hand, increases the marker expression. Mechanistically, Meox1 promotes high level Smad3 nuclear retention during the early stage of TGF-β stimulation, which is achieved by inhibiting phosphorylated Smad2/3 phosphatase, Mg^{2+}/Mn^{2+} dependent 1A (PPM1A) expression through increasing its degradation rate, leading to a sustained level of Smad3 phosphorylation and thus allows Smad3 to precisely regulate SMC marker gene transcription. Our results indicate that Meox1 is a novel regulator for TGF-β-induced SMC differentiation.

Keywords: Differentiation, Smooth Muscle, Transforming Growth Factor-β (TGF-β), Mesenchyme Homeobox 1 (Meox1), SMAD Family Member 3 (Smad3)

Introduction

Smooth muscle cell (SMC) is mainly involved in blood vessel contraction, pressure regulation, and blood flow distribution (1). SMCs in different segments of arteries are derived from a number of precursors such as neural crest, proepicardium, mesothelium, somites, mesoangioblast, etc. For example, smooth muscles located in dorsal aorta are originated from somite (2). A number of studies have suggested that several cardiovascular diseases including atherosclerosis are associated with the diversity of SMCs originating from different sources (3). However, the underlying mechanisms remain largely unknown. Several in vitro models are available for exploring mechanisms controlling SMC differentiation from different progenitors. For instance, Monc-1 cells originated from mouse neural crest can be induced into contractile SMC by TGF-β treatment (4), mouse pluripotent embryonal carcinoma derived A404 cells can be induced to express several SMC markers with the treatment of all-*tran* retinoic acid followed by puromycin (5), and the mesoderm-derived C3H/10T1/2 cells can be induced by TGF-β to express SMC markers such as α-SMA, calponin and SM22α (6).

Large amount of previous study have been focused on the receptors and signaling pathways that activated by growth factors and cytokines in the vascular system during normal development and pathologic vasculogenesis (7), however, the molecular mechanism and function of activated downstream transcription factors which are involved in regulating SMC growth and differentiation are rarely known. Among those transcription factors, homeobox genes which cell differentiation, proliferation and migration have been identified as an ideal candidate to study the mechanism of vascular development in embryogenesis, angiogenesis and adult vascular diseases (8,9). For

example, in 2013, Hox gene has been reported to participate in SMC differentiation from adventitia vascular wall-resident multipotent stem cell (10). This finding gives an important clue for vascular diseases therapy such as tumor vascularization and neointima formation. In our previous microarray analysis, thousands of genes have been screened before and after TGF-β treatment in C3H/10T1/2 cells. Among these genes, we found mesenchyme homeobox 1 (Meox1) which belongs to a diverged subfamily of homeobox transcription factors (11) has been up-regulated during SMC differentiation. Previous study has discovered that Meox1 is expressed in the early developing somite and plays an important role in somitogenesis during embryogenesis (12). In adult, Meox1 is expressed in a variety of cells including endothelial cells (13) and vascular SMCs (14). Recent studies show that Meox1 is critical for the specification of endothelial cells in the endotome of the somites, which further give rise to haematopoietic stem cells (15). Because Meox1 was expressed by somite-derived cell in embryo and can be induced by TGF-β during SMC differentiation in 10T1/2 cell according to our microarray analysis, we hypothesize that Meox1, like a lot other homeobox genes, may be involved in SMC differentiation during embryonic development.

In the present study, we found that Meox1 was up-regulated along with SMC early markers in 10T1/2 cells by TGF-β induction. Knockdown or overexpression of Meox1 dramatically altered SMC marker gene expression. In vivo, Meox1 knockdown in mouse embryos exhibited decreased SMC markers expression in descending aorta of neonatal mice. Mechanically, Meox1 impeded nuclear Smad3 shuttling back to cytoplasm during the early stage of TGF-β stimulation. Meox1 appeared to promote Smad3 nuclear retention through inhibiting the expression of the protein phosphatase, Mg^{2+}/Mn^{2+}

dependent 1A (PPM1A) which is reported to be a p-Smad2/3 phosphatase to terminate TGF-β signaling (16) via promoting its degradation rate. Our research finds a novel role of Meox1 in SMC differentiation which is likely important for embryonic vasculature development.

RESULTS

Meox1 Expression Was Up-regulated in TGF-β-induced SMC Differentiation

TGF-β-induced SMC differentiation of 10T1/2 cells is a widely-used model for studying SMC differentiation. We confirmed that TGF-β induced the expression of SMC early differentiation markers α-SMA, Calponin and SM22α in 10T1/2 cells in both mRNA (Figure. 3.1, A-D) and protein levels (Figure. 3.1, E-I). TGF-β induced Meox1 expression along with the SMC marker expression. Importantly, Meox1 expression was induced as early as 2 hours following TGF-β stimulation, suggesting that Meox1 may be involved in TGF-β-induced SMC differentiation.

Meox1 Was Essential for TGF-β-induced SMC differentiation

To test if Meox1 plays a role in TGF-β -induced SMC differentiation, we knocked down Meox1 expression using Meox1 shRNA delivered via adenoviral vector prior to the TGF-β induction. As shown in Figure 2, A, Meox1 and SMC markers were induced simultaneously by TGF-β significantly. Meox1 expression was effectively blocked by its shRNA (Figure 3.2, A-B). Of importance, knockdown of Meox1 blocked TGF-β-induced expression of SMC early markers α-SMA, Calponin and SM22α by 46%, 43% and 48%, respectively. In addition, knockdown Meox1 in cells treated without TGF-β doesn't

change the basal level of SMC markers significantly. These results indicated that Meox1 played a critical role in SMC differentiation.

Meox1 deficiency impeded the embryonic vascular development

To identify Meox1 function during SMC differentiation in vivo, shMeox1 or ctrl adenoviral vector were intraamniotically administrated into C57BL/6J mouse embryo on E12.5. Descending aortas of both shMeox1 and ctrl adenoviral vectors administration groups have been collected after the mice were born on P1. As shown in Figure 3, A-C, Meox1 as well as SMC markers α-SMA and Calponin mRNA levels were detected in descending aorta from both ctrl and shMeox1 adenoviral vector delivery groups. Meox1 was significantly knocked down by shMeox1 adenoviral vector in descending aorta. This result was also confirmed by Meox1 immunofluorescence staining of descending aorta frozen section (Figure 3, D). To further study the effect of Meox1 deficiency in embryonic vascular development, SMC markers α-SMA, Calponin expressions were measured by immunofluorescence staining (Figure 3, E-G). As expected, both SMC markers expression decreased after Meox1 was knocked down in the medium layer of descending aorta. The decreased SMC markers may lead to a less contractile artery. In addition, SMC numbers were analyzed (Figure 3, H) by counting α-SMA positive cells in Figure 3 D. There is no significant difference of SMC numbers in both control and shMeox1 adenoviral injection aorta. These data indicated that Meox1 deficiency in embryo resulted in decreased SMC marker expression in postnatal mouse and may lead to less contractile artery development.

Meox1 is Sufficient for SMC Differentiation of 10T1/2 cells

To further investigate the role of Meox1 in SMC differentiation, we tested if Meox1 alone can induce SMC marker gene expression. Thus, we forcefully expressed Meox1 in 10T1/2 cells via adenoviral transduction of Meox1 cDNA and detected the expression of SMC early differentiation markers. As shown in Figure 3.4, Meox1 was robustly expressed in 10T1/2 cells with a 5-fold increase compared with control group. Importantly, overexpression of Meox1 promoted the protein expression of α-SMA and Calponin, indicating that Meox1 was able to stimulate 10T1/2 cell to differentiate toward SMC lineage.

Meox1 Regulated SMC Marker Gene Transcription and Mediated Smad3 Function

Transcriptional activation of SMC genes is one of the molecular mechanisms controlling SMC differentiation (17-19). Therefore, we sought to test if Meox1 regulates SMC differentiation by mediating SMC marker gene transcription. We first detected if Meox1 affects SMC marker mRNA levels, and found that knockdown of Meox1 by its shRNA dramatically attenuated TGF-β-induced mRNA expression of α-SMA and SM22α genes but not the basal level of SMC markers (Figure 3.5, A-D), suggesting that Meox1 may be involved in SMC marker gene transcription. Indeed, knockdown of Meox1 inhibited TGF-β induction of α-SMA and SM22α promoter activities, as shown by the SMC promoter-reporter luciferase assay (Figure 3.5, E-F). Remarkably, Meox1 shRNA reduced α-SMA and SM22α promoter activities by 58.6% and 43%, respectively, demonstrating that Meox1 is a critical regulator for SMC gene transcription.

We and others have reported previously that Smad3 is the key factor mediating TGF-β function in SMC differentiation of 10T1/2 cells (6,20,21). Smad3 mainly regulates gene transcription of SMC early differentiation markers in the initiation stage of SMC differentiation (20). Therefore, we sought to determine if Meox1 is involved in Smad3-mediated SMC gene transcription. As shown in Figure 3.5, G-H, forced expression of Smad3 markedly up-regulated SMC marker genes α-SMA and SM22α promoter activity. However, knockdown of Meox1 blocked Smad3 function in increasing the promoter activities of both α-SMA and SM22α genes. Of importance, Smad3 expression increased the promoter activities even in the basal state, i.e., without TGF-β treatment, and knockdown of Meox1 completely blocked Smad3-mediated promoter activities, indicating that in addition to TGF-β-induced SMC differentiation, the basal level of Meox1 may also be important for Smad3 activity in the quiescent SMC.

Meox1 Was Essential for Smad3 Nuclear Location

Since Smad3 is continuously shuttling back and forth between cytoplasm and nuclei with or without TGF-β treatment (22), and Smad3 nuclear translocation is required for its transcription activity in SMC differentiation, we tested if Meox1 affects Smad3 nuclear localization. Immunofluorescence staining showed that TGF-β treatment for 30 minutes caused the majority of Smad3 located in the nuclei of 10T1/2 cells (Figure 3.6, A). However, knockdown of Meox1 by its shRNA caused less Smad3 located in the nuclei (Figure 6, A). Since Meox1 is a nuclear protein, these data suggest that Meox1 may be important for Smad3 nuclear retention. To confirm the Meox1 function in Smad3 nuclear location, we detected cytoplasmic and nuclear Smad3 levels in TGF-β-treated cells when

the Meox1 expression was manipulated. As shown in Figure 3.6, *B-C*, TGF-β induction for 2 hours maintained a significantly higher level of nuclear Smad3 compared to the untreated cells along with a reduction of cytoplasmic Smad3. Knockdown of Meox1, however, significantly reduced the nuclear Smad3 level with a 48.7% decrease compared with TGF-β-treated cells with intact Meox1 (Figure 3.6, B-C). These data further demonstrated that Meox1 played an important role in Smad3 nuclear retention.

Meox1 maintained nuclear Smad3 phosphorylation by limiting PPM1A expression

To determine the mechanism underlying Meox1 function in Smad3 nuclear retention, we tested if Meox1 regulates Smad3 phosphorylation status because Smad3 phosphorylation leads to the nuclear location while de-phosphorylation of the protein causes Smad3 export from the nuclei (23). Therefore, the phosphorylated Smad3 reflects the nuclear Smad3 protein level. Time-dependent study showed that Smad3 was phosphorylated 10 min after TGF-β induction, and the phospho-Smad3 reached the highest level at 10-30 min but gradually decreased after 2 hours of TGF-β treatment (Figure 3.7, A-B). However, knockdown of Meox1 by shRNA significantly or completely diminished the phospho-Smad3 level during the course of TGF-β induction. Since Meox1 is not located in the cytoplasm, it is unlikely that Meox1 blocks TGF-β-induced Smad3 phosphorylation process. Instead, we hypothesized that Meox1 may be essential in preserving the phospharylation of nuclear Smad3, which can be removed by PPM1A (16). PPM1A is a phosphatase belongs to protein serine/threonine phosphates (PS/TPs) family which targets to remove phosphates upon serine/threonine residues (24,25). In 2006, Feng et al has identified PPM1A as the only phosphatase which may dephosphorylate

pSmad2/3 on C-terminal and terminate TGF-β signaling among all 49 PS/TPs they screened (26,27). PPM1A-mediated Smad3 dephosphorylation is known to reduce Smad3 phosphorylation and facilitate Smad3 nuclear export. Indeed, knockdown of Meox1 significantly enhanced the expression of PPM1A in both vehicle and TGF-β-treated cells (Figure 3.7, C-D). To investigate the mechanism how Meox1 inhibits PPM1A expression, degradation level of PPM1A was detected by treating both Ctrl and Meox1 knocked down cells with cycloheximide (CHX) in a time course method. When Meox1 was knocked down, PPM1A degradation is slower than that in control group with higher steady-state level and half-life of PPM1A (Figure 3.7, E-F). This result suggests that Meox1 inhibits PPM1A expression by increasing its degradation rate. Because knocking down Meox1 dramatically increased PPM1A expression in 10T1/2 cells (Figure 3.7, C-D), we also overexpressed Meox1 to detect PPM1A expression in 10T1/2 cells. Compared with control, PPM1A expression decreased in cells transfected with Meox1 overexpression adenoviral vectors (Figure 3.6, G-H). Nevertheless, these data suggest that Meox1 facilitated Smad3 nuclear location by inhibiting PPM1A expression through increasing its degradation rate, and thus preserving the phosphorylation of Smad3 in the nuclei of the cells.

DISCUSSION

The present studies have demonstrated that Meox1 plays an important role in regulating TGF-β-induced SMC differentiation. Meox1 is induced along with the expression of early SMC markers, suggesting that Meox1 may be important for the initiation of SMC differentiation program. Indeed, knockdown of Meox1 inhibits SMC marker genes

expression while forced expression of Meox1 enhances the marker expression. The essential roles of Meox1 in TGF-β-induced SMC marker gene mRNA expression and promoter activities suggest that Meox1 regulates SMC differentiation by controlling SMC gene transcription. It appears that Meox1 is involved in Smad3 regulation of SMC genes because knockdown of Meox1 diminishes Smad3-mediated SMC gene promoter activities. Mechanistically, Meox1 blocks PPM1A expression, which permits Smad3 to preserve its phosphorylation status in the nuclei of 10T1/2 cells upon TGF-β treatment, and thus allows Smad3 to activate SMC gene transcription, leading to the initiation of SMC differentiation.

TGF-β/Smad signaling plays a critical role in SMC differentiation (28-31). In fact, Smad proteins are involved in progenitor-specific regulation of SMC differentiation, i.e., Smad2 is important for neural crest cell differentiation to SMC while Smad3 is essential for the SMC differentiation from mesenchymal progenitors (32). Although PPM1A dephosphorylates and promotes nuclear export of both the TGFβ-activated Smad2 and Smad3 (16), we only focus on the effect of PPM1A on Smad3 phosphorylation because Smad2 appears not to be involved in TGF-β-induced SMC differentiation from mesenchymal progenitors (33,34). Smad3 activity may be regulated in multiple levels such as expression, phosphorylation, nuclear translocation, and interactions with other transcription factor or Smad binding elements on the target gene promoters. Our results suggest that Meox1 regulates Smad3 phosphorylation status in the nuclei rather than participating in the TGF-β receptor-mediated Smad3 phosphorylation in the cytoplasm, largely due to the natural nuclear location of Meox1. Meox1 appears to be a novel suppressor for PPM1A expression because knockdown of Meox1 promotes the

expression of PPM1A, even in the basal state prior to TGF-β stimulation. By PPM1A degradation detection, the mechanism that Meox1 knockdown accelerates PPM1A expression is due to decreased PPM1A degradation rate.

In addition to serve as a PPM1A inhibitor, Meox1 is likely to also function as a transcription factor directly regulating SMC gene promoter. This notion is supported by the fact that Meox1 alone is sufficient to up-regulate the exogenously-introduced SMC promoters in quiescent SMCs where Smad3 is mainly located in the cytoplasm. These results are consistent with a previous report showing that Meox1 may be involved in gene transcription because it can specifically bind the DNA sequences recognized by Hoxa2 on its functional target genes (35). A future identification of the Meox1 binding element and in vivo function may provide more detailed insights into the regulatory mechanism governing Meox1 function in SMC differentiation.

Taken together, our studies have identified Meox1 as a novel regulator for TGF-β-induced SMC differentiation from mesenchymal progenitors. Meox1 regulates SMC marker gene expression by preserving Smad3 phosphorylation in cell nuclei through blocking the PPM1A expression via maintaining certain PPM1A degradation rate and thus preventing Smad3 dephosphorylation. Meox1 may also serve as a transcription factor directly regulating SMC gene promoter activation. Since Meox1 is involved in early somite development, and somite is one of the progenitors for vascular SMCs, Meox1-mediated SMC differentiation is likely to be important for embryonic vasculature development.

EXPERIMENAL PROCEDURES

Cell Culture and Transfection

C3H10T1/2 (10T1/2) cells were cultured in Dulbecco's modified Eagle's medium containing 10% fetal bovine serum and 5% L-glutamine. Cells were starved in serum-free medium for 48 h followed by incubating with TGF-β (5 ng/ml) for various times as needed. For transfection of plasmid DNA, cells were plating on 12-well plates or 6-cm dishes with 70-80% confluence. 24 h later, transfection was carried out using Lipofectamine LTX reagents (Life Technologies) according to the manufacturer's instruction.

Construction of Adenoviral Vectors

Mouse Meox1 cDNA was inserted into the XhoI site of pShuttle- IREShrGFP-1 (Agilent Technologies) and was confirmed by sequencing. For Meox1 shRNA adenoviral vector, double-stranded DNAs coding Meox1 shRNAs were cloned into pRNAT-H1.1/Adeno shuttle vector (Genscript). Recombinant adenoviral vector was produced in AD-1 competent cells (Agilent Technologies) according to the manufacturer's instruction (36). Short hairpin RNA (shRNA) target sequences for mouse Meox1 were: 5'-GGA CTG AGC GAA TCT TCA ACG AGC AGC AT-3' (top strand) and 5'-ATG CTG CTC GTT GAA GAT TCG CTC AGT CC-3' (bottom strand).

Viral Inoculation of Mouse Embryo

For timed pregnant mating, noon of the day after mating was considered embryonic day 0.5 (E0.5). Pregnant C57BL/6J mice with E12.5 e*mb*ryos were intraamniotic administrated 3 ul 5.3 x 10^5 TCID50/ml shMeox1 adenovirus into E12.5 embryo, shScramble adenovirus served as control. To improve retention of the pregnancy, we

avoided viral injection of the two embryos next to the ovaries and the two embryos next to the upper vagina. Injected embryos were placed back to pregnant dams and allowed to develop after surgery. Postnatal mice descending aorta was collected after the mice were born on P1.

Quantitative Reverse Transcription-PCR (qPCR)

Total RNA was extracted from cells using Trizol Reagent (Life Technologies) followed by a reverse transcription using iScript cDNA Synthesis Kit (Bio-Rad) according to the manufacturer's instructions. qPCR was performed using Mx3005P qPCR machine with SYBR Green mater mix (Agilent Technologies). Mouse Meox1 primers used were: 5'-GGA AGG AGA GGA CAG CCT TC-3' (forward) and 5'-CCC TTC ACA CGT TTC CAC TT-3' (reverse). Smooth muscle marker primers were described previously (29,33).

Immunocytofluorescent Staining

10T1/2 cells were seeded on sterile coverslips and transfected with Meox1 or Ctrl shRNA in complete medium for 1 day and then starved for 2 days before TGF-β treatment for 30 min and 2 hours. Cells were washed with PBS for 3 times before fixing in 4% paraformaldehyde (PFA) for 5 min. The fixed cells were washed by PBS for 3 times followed by incubation with PBS containing 0.1% Triton X-100 for 10 min. After washing with PBS for 3 times, 5% goat serum in PBS was used to block cells for 30 min. Anti-Meox1 (Abcam, ab105349) and anti-Smad3 (Cell Signaling Technology, 9523s) primary antibodies were diluted at 1:50 and 1:100 separately and incubated the cells overnight. Cells were then incubated with FITC- or TRITC-conjugated secondary antibodies (1:150 and 1:50 respectively) for 30 min followed by PBS washing for 3 times. Cells were observed and imaged with Nikon Eclipse 90i microscope, and images were

captured with Nikon 12.7MP digital Sight DS-Ri1 color camera as previously described (37). For tissue immunofluorescent staining, 10μm fresh frozen sections were air dried for 30 minutes at room temperature followed by 10 minutes fixation with 4% paraformaldehyde. After 3 times washing with phosphate-buffered saline, the section is permeabilized with 0.01% Triton X-100 in phosphate-buffered saline for 10 minutes, blocked with 5% goat serum for 30 minutes, and incubated with anti-Meox1, anti-α-SMA and anti-Calponin antibody overnight at 4℃, followed by incubation with FITC-conjugated or TRITC-conjugated secondary antibodies. Cell nuclei were stained with DAPI (Molecular Probes). Stained tissue sections were imaged using a Nikon 12.7MP digital Sight DS-Ri1 color camera as previously described

Western Blotting

10T1/2 cells were cultured in DMEM and treated with or without TGF-β or other factors as needed. Total proteins were extracted as previous described (38). Nuclear and cytoplasmic proteins were extracted using nuclear extraction kit (Millipore) according to the instruction of manufacturer. Protein concentration was measured using BCA Protein Assay reagent (Thermo Scientific). Protein lysates were resolved by SDS-PAGE and transferred to PVDF membrane (Bio-Rad) or nitrocellulose membrane (Bio-Rad) that were blocked with 5% nonfat dry milk or 5% BSA separately. Membranes were then incubated with the following primary antibodies in blocking buffers in room temperature for 2-3 hours or in 4℃ overnight: anti-Phospho-Smad3 (Cell Signaling Technology, 9520s), anti-PPM1A (Thermo Scientific, PA5-29275), anti-αSMA (Sigma-Aldrich, A2547), anti-SM22α (Abcam, ab10135), anti-calponin (Abcam, ab46794), anti-α-Tubulin (Sigma-Aldrich, T9026), anti-GAPDH (Sigma-Aldrich, G8795). Then, HRP-conjugated

or immunofluorescent secondary antibodies were incubated with the membranes for 1 h. The protein expression levels were detected with enhanced chemiluminescence (Millipore) or scanned by Odyssey fluorescence scanner (LI-COR) (39).

Promoter-reporter Luciferase Assay—α-SMA or SM22α luciferase promoter constructs were transfected into 10T1/2 cells with or without other plasmids using Lipofectamine LTX (Life Technologies) as described previously (40). 24 h after the transfection, 10T1/2 cells were starved for 2 days before TGF-β treatment for 8 hours. Luciferase activity was measured using the Dual-Luciferase Reporter Assay System (Promega).

Statistical Analysis

All values are expressed as mean ± S.E. Data were evaluated with a 2-tailed, unpaired Student t test or compared by one-way ANOVA followed by Fisher t test. A p value <0.05 was considered statistically significant.

REFERENCES

1. Owens, G. K., Kumar, M. S., and Wamhoff, B. R. (2004) Molecular regulation of vascular smooth muscle cell differentiation in development and disease. *Physiol Rev* **84**, 767-801
2. Majesky, M. W. (2007) Developmental basis of vascular smooth muscle diversity. *Arteriosclerosis, thrombosis, and vascular biology* **27**, 1248-1258
3. Majesky, M. W., Dong, X. R., Regan, J. N., and Hoglund, V. J. (2011) Vascular smooth muscle progenitor cells: building and repairing blood vessels. *Circ Res* **108**, 365-377
4. Ferreira, L. S., Gerecht, S., Shieh, H. F., Watson, N., Rupnick, M. A., Dallabrida,

S. M., Vunjak-Novakovic, G., and Langer, R. (2007) Vascular progenitor cells isolated from human embryonic stem cells give rise to endothelial and smooth muscle like cells and form vascular networks in vivo. *Circulation research* **101**, 286-294

5. Manabe, I., and Owens, G. K. (2001) Recruitment of serum response factor and hyperacetylation of histones at smooth muscle-specific regulatory regions during differentiation of a novel P19-derived in vitro smooth muscle differentiation system. *Circulation research* **88**, 1127-1134
6. Hirschi, K. K., Rohovsky, S. A., and D'Amore, P. A. (1998) PDGF, TGF-beta, and heterotypic cell-cell interactions mediate endothelial cell-induced recruitment of 10T1/2 cells and their differentiation to a smooth muscle fate. *J Cell Biol* **141**, 805-814
7. Mack, C. P. (2011) Signaling mechanisms that regulate smooth muscle cell differentiation. *Arterioscler Thromb Vasc Biol* **31**, 1495-1505
8. Gorski, D. H., and Walsh, K. (2003) Control of vascular cell differentiation by homeobox transcription factors. *Trends in cardiovascular medicine* **13**, 213-220
9. Oyama, Y., Kawai-Kowase, K., Sekiguchi, K., Sato, M., Sato, H., Yamazaki, M., Ohyama, Y., Aihara, Y., Iso, T., Okamaoto, E., Nagai, R., and Kurabayashi, M. (2004) Homeobox protein Hex facilitates serum responsive factor-mediated activation of the SM22alpha gene transcription in embryonic fibroblasts. *Arteriosclerosis, thrombosis, and vascular biology* **24**, 1602-1607
10. Klein, D., Benchellal, M., Kleff, V., Jakob, H. G., and Ergun, S. (2013) Hox genes are involved in vascular wall-resident multipotent stem cell differentiation into

smooth muscle cells. *Scientific reports* **3**, 2178

11. Candia, A. F., Hu, J., Crosby, J., Lalley, P. A., Noden, D., Nadeau, J. H., and Wright, C. V. (1992) Mox-1 and Mox-2 define a novel homeobox gene subfamily and are differentially expressed during early mesodermal patterning in mouse embryos. *Development* **116**, 1123-1136
12. Mankoo, B. S., Skuntz, S., Harrigan, I., Grigorieva, E., Candia, A., Wright, C. V., Arnheiter, H., and Pachnis, V. (2003) The concerted action of Meox homeobox genes is required upstream of genetic pathways essential for the formation, patterning and differentiation of somites. *Development* **130**, 4655-4664
13. Douville, J. M., Cheung, D. Y., Herbert, K. L., Moffatt, T., and Wigle, J. T. (2011) Mechanisms of MEOX1 and MEOX2 regulation of the cyclin dependent kinase inhibitors p21 and p16 in vascular endothelial cells. *PloS one* **6**, e29099
14. Wasteson, P., Johansson, B. R., Jukkola, T., Breuer, S., Akyurek, L. M., Partanen, J., and Lindahl, P. (2008) Developmental origin of smooth muscle cells in the descending aorta in mice. *Development* **135**, 1823-1832
15. Nguyen, P. D., Hollway, G. E., Sonntag, C., Miles, L. B., Hall, T. E., Berger, S., Fernandez, K. J., Gurevich, D. B., Cole, N. J., Alaei, S., Ramialison, M., Sutherland, R. L., Polo, J. M., Lieschke, G. J., and Currie, P. D. (2014) Haematopoietic stem cell induction by somite-derived endothelial cells controlled by meox1. *Nature* **512**, 314-318
16. Lin, X., Duan, X., Liang, Y. Y., Su, Y., Wrighton, K. H., Long, J., Hu, M., Davis, C. M., Wang, J., Brunicardi, F. C., Shi, Y., Chen, Y. G., Meng, A., and Feng, X. H. (2006) PPM1A functions as a Smad phosphatase to terminate TGFbeta signaling.

Cell **125**, 915-928

17. Mack, C. P., Somlyo, A. V., Hautmann, M., Somlyo, A. P., and Owens, G. K. (2001) Smooth muscle differentiation marker gene expression is regulated by RhoA-mediated actin polymerization. *J Biol Chem* **276**, 341-347
18. Miano, J. M. (2003) Serum response factor: toggling between disparate programs of gene expression. *J Mol Cell Cardiol* **35**, 577-593
19. Mack, C. P., and Hinson, J. S. (2005) Regulation of smooth muscle differentiation by the myocardin family of serum response factor co-factors. *J Thromb Haemost* **3**, 1976-1984
20. Xie, W. B., Li, Z., Miano, J. M., Long, X., and Chen, S. Y. (2011) Smad3-mediated myocardin silencing: a novel mechanism governing the initiation of smooth muscle differentiation. *The Journal of biological chemistry* **286**, 15050-15057
21. Shi, X., DiRenzo, D., Guo, L. W., Franco, S. R., Wang, B., Seedial, S., and Kent, K. C. (2014) TGF-beta/Smad3 stimulates stem cell/developmental gene expression and vascular smooth muscle cell de-differentiation. *PLoS One* **9**, e93995
22. Hill, C. S. (2009) Nucleocytoplasmic shuttling of Smad proteins. *Cell Res* **19**, 36-46
23. Massague, J., and Wotton, D. (2000) Transcriptional control by the TGF-beta/Smad signaling system. *The EMBO journal* **19**, 1745-1754
24. Mumby, M. C., and Walter, G. (1993) Protein serine/threonine phosphatases: structure, regulation, and functions in cell growth. *Physiol Rev* **73**, 673-699

25. Shi, Y. (2009) Serine/threonine phosphatases: mechanism through structure. *Cell* **139**, 468-484

26. Schmierer, B., and Hill, C. S. (2005) Kinetic analysis of Smad nucleocytoplasmic shuttling reveals a mechanism for transforming growth factor beta-dependent nuclear accumulation of Smads. *Molecular and cellular biology* **25**, 9845-9858

27. Gallego, M., and Virshup, D. M. (2005) Protein serine/threonine phosphatases: life, death, and sleeping. *Current opinion in cell biology* **17**, 197-202

28. Chen, S., Crawford, M., Day, R. M., Briones, V. R., Leader, J. E., Jose, P. A., and Lechleider, R. J. (2006) RhoA modulates Smad signaling during transforming growth factor-beta-induced smooth muscle differentiation. *J Biol Chem* **281**, 1765-1770

29. Chen, S., and Lechleider, R. J. (2004) Transforming growth factor-beta-induced differentiation of smooth muscle from a neural crest stem cell line. *Circ Res* **94**, 1195-1202

30. Kurpinski, K., Lam, H., Chu, J., Wang, A., Kim, A., Tsay, E., Agrawal, S., Schaffer, D. V., and Li, S. (2010) Transforming growth factor-beta and notch signaling mediate stem cell differentiation into smooth muscle cells. *Stem Cells* **28**, 734-742

31. Sinha, S., Hoofnagle, M. H., Kingston, P. A., McCanna, M. E., and Owens, G. K. (2004) Transforming growth factor-beta1 signaling contributes to development of smooth muscle cells from embryonic stem cells. *Am J Physiol Cell Physiol* **287**, C1560-1568

32. Xie, W. B., Li, Z., Shi, N., Guo, X., Tang, J., Ju, W., Han, J., Liu, T., Bottinger, E.

P., Chai, Y., Jose, P. A., and Chen, S. Y. (2013) Smad2 and myocardin-related transcription factor B cooperatively regulate vascular smooth muscle differentiation from neural crest cells. *Circulation research* **113**, e76-86

33. Chen, S., Kulik, M., and Lechleider, R. J. (2003) Smad proteins regulate transcriptional induction of the SM22alpha gene by TGF-beta. *Nucleic Acids Res* **31**, 1302-1310

34. Li, L., Miano, J. M., Cserjesi, P., and Olson, E. N. (1996) SM22 alpha, a marker of adult smooth muscle, is expressed in multiple myogenic lineages during embryogenesis. *Circ Res* **78**, 188-195

35. Kirilenko, P., He, G., Mankoo, B. S., Mallo, M., Jones, R., and Bobola, N. (2011) Transient activation of meox1 is an early component of the gene regulatory network downstream of hoxa2. *Mol Cell Biol* **31**, 1301-1308

36. Luo, J., Deng, Z. L., Luo, X., Tang, N., Song, W. X., Chen, J., Sharff, K. A., Luu, H. H., Haydon, R. C., Kinzler, K. W., Vogelstein, B., and He, T. C. (2007) A protocol for rapid generation of recombinant adenoviruses using the AdEasy system. *Nature protocols* **2**, 1236-1247

37. Shi, N., Xie, W. B., and Chen, S. Y. (2012) Cell division cycle 7 is a novel regulator of transforming growth factor-beta-induced smooth muscle cell differentiation. *The Journal of biological chemistry* **287**, 6860-6867

38. Shi, N., and Chen, S. Y. (2013) Cell division cycle 7 mediates transforming growth factor-beta-induced smooth muscle maturation through activation of myocardin gene transcription. *J Biol Chem* **288**, 34336-34342

39. Shirai, T., Nazarewicz, R. R., Wallis, B. B., Yanes, R. E., Watanabe, R., Hilhorst,

M., Tian, L., Harrison, D. G., Giacomini, J. C., Assimes, T. L., Goronzy, J. J., and Weyand, C. M. (2016) The glycolytic enzyme PKM2 bridges metabolic and inflammatory dysfunction in coronary artery disease. *The Journal of experimental medicine* **213**, 337-354

40. Li, F., Luo, Z., Huang, W., Lu, Q., Wilcox, C. S., Jose, P. A., and Chen, S. (2007) Response gene to complement 32, a novel regulator for transforming growth factor-beta-induced smooth muscle differentiation of neural crest cells. *The Journal of biological chemistry* **282**, 10133-10137

Figure legends

Fig 3.1: TGF-β induced Meox1 expression along with SMC early differentiation markers. *A-D*, TGF-β induced Meox1 and SMC marker mRNA expression in 10T1/2 cells. Serum-starved 10T1/2 cells were treated with vehicle (-) or TGF-β (5 ng/ml) for the times indicated. mRNA expression levels were detected by qPCR. **P* < 0.01 compared with the vehicle-treated group (0 h), n=3. *E*, Meox1 protein expression was induced in the initial stage of TGF-β stimulation in 10T1/2 cells. 10T1/2 cells were starved 48 hours followed by vehicle (-) or TGF-β (5 ng/ml) induction for the times indicated. Meox1 and SMC marker protein expression levels were detected by Western blot. *F-I*, Quantification of Meox1 and SMC marker expression shown in E. The protein expression was normalized to the α-Tubulin level. **P* < 0.01 compared with the vehicle-treated group (0 h), n=3. (Ctrl, set as 1)

Figure 3.2: Meox1 was essential for TGF-β-induced SMC differentiation. *A*, Meox1 knockdown decreased TGF-β-induced SMC marker protein expression in 10T1/2 cells. 10T1/2 cells were transduced with control (shCtrl) or Meox1 shRNA (shMeox1) adenoviral vector. Following starvation for 48 hours, 10T1/2 cells were treated with TGF-β for 24 hours. Western Blot were performed to detect Meox1 and SMC marker protein expression. *B-E*, Quantification of the protein expression shown in panel A. Meox1 and SMC marker protein levels were normalized to α-Tubulin. $*P < 0.01$ compared with the vehicle-treated group (0 h), n=3. $^{\#}P < 0.01$ compared with the TGF-β-treated cells transduced with Ctrl adenoviral vector, n=3. $^{\&}P < 0.05$ compared to the shCtrl group without TGF-β treatment, $n = 3$. $^{\$}P>0.05$ compared to the shCtrl group without TGF-β treatment, $n = 3$.

Figure 3.3: Knockdown of Meox1 attenuated SMC differentiation during mouse embryonic development. A, Intraamniotic administration of shMeox1 via adenoviral delivery into mouse E12.5 embryo attenuated Meox1 expression while inhibiting the mRNA expression of SMC markers in descending aortas of postnatal day 1 mice as measured by qPCR. B. Knockdown of Meox1 attenuated SMC marker expression in aorta of new born mice. Meox1 (green), SMC marker α-SMA (red) and Calponin (red) protein expression were detected by immunofluorescent staining. 4,6-diamidino-phenylidole (DAPI) stains the nuclei (200×). Scale: 50 μm. C-E, Quantification of the relative Meox1, α-SMA and calponin levels shown in B by calibrating the positive staining intensity to the mean signal in aorta and by setting the control shRNA group (Ctrl) as 1. *P < 0.01 compared with the Ctrl group. F, Quantification of the relative

smooth muscle cell numbers in aorta by counting α-SMA positive cells and by setting the control shRNA group (Ctrl) set as 1. N.S. indicates no significant difference.

Figure 3.4. Meox1 alone was able to induce SMC early differentiation marker expression. *A*, Meox1 increased SMC marker expression. 10T1/2 cells were transduced with Control (Ctrl, GFP adenoviral vector) or Meox1 adenoviral vectors for 48 hours. Meox1 and SMC marker protein expression were analyzed by Western Blot. *B-D*, Quantitative analysis of Meox1 and SMC marker protein expression shown in A by normalizing to the α-Tubulin level. **P*<0.05 compared with the Ctrl group (*n* = 3).

Figure 3.5. Meox1 was required for the activation of SMC marker promoters by TGF-β/Smad3. *A-D*, knockdown of Meox1 diminished SMC marker mRNA expression in 10T1/2 cells. 10T1/2 cells were transduced with scramble (shCtrl) or Meox1 shRNA adenoviral vector (shMeox1). 24 hours later, the cells were serum-starved for 48 hours followed by vehicle (-) or TGF-β (5 ng/ml) treatment for 8 hours. Meox1 (A), α-SMA (B) and Calponin (C) and SM22α (D) mRNA expression was detected by qPCR. **P*<0.05 compared with the shCtrl group without TGF-β treatment (*n* = 3). $^{\#}$*P*<0.01 compared with the TGF-β-treated group transfected with shCtrl, n=3. $^{\$}$*P*<0.05 compared to the shCtrl group without TGF-β treatment, *n* = 3. *E* and *F*, Knockdown of Meox1 blocked TGF-β-induced promoter activities of SMC marker genes. 10T1/2 cells were co-transfected with α-SMA (*E*) or SM22α (*F*) promoter construct with shCtrl or shMeox1 followed by TGF-β treatment for 8 hours. Luciferase assays were performed. **P*<0.01 compared with the shCtrl group (*n*=3). *G-H*, knockdown of Meox1 blocked Smad3 function in enhancing

TGF-β-induced SMC marker promoter activities. 10T1/2 cells were transduced with shCtrl or shMeox1 adenoviral vector followed by co-transfection of pcDNA or Smad3 plasmids with α-SMA (*G*) or SM22α (*H*) promoter construct. Following 24 hours starvation, cells were treated with vehicle (Ctrl) or TGF-β for 8 hours followed by luciferase assays. **P*<0.01 compared to the pcDNA/shCtrl groups (*n* = 3). $^{\#}$*P*<0.01 compared to the Smad3/shCtrl groups (*n* = 3).

Figure 3.6. Meox1 was critical for TGF-β-induced Smad3 nuclear localization. *A*, Knockdown of Meox1 reduced Smad3 nuclear location. 10T1/2 cells were transduced with scramble (Ctrl) or Meox1 shRNA (shMeox1) adenoviral vectors for 1 day followed by 2-day starvation. The cells were then treated with TGF-β (5 ng/ml) for 0h or 30 min. Immunostaining was performed to detect Smad3 cellular location. DAPI stains nuclei (600×). Scale: 20 μm. *B-C*, Knockdown of Meox1 blocked TGF-β-induced Smad3 nuclear accumulation.10T1/2 cells were transduced with Ctrl or shMeox1 similarly as in A followed by treatment with vehicle (-) or TGF-β (5 ng/ml) for 1 h. Nuclear and cytoplasmic proteins were extracted to perform Western blot using antibodies as indicated. *C*, Quantification of Smad3 levels by normalized to α-Tubulin (cytoplasmic portion) or Lamin B (nuclear portion). **P*<0.05 compared to shCtrl with TGF-β treatment; $^{\#}$*P*>0.05 compared to shMeox1 with vehicle treatment for cytoplasmic Smad3; $^{\$}$*P*<0.05 compared to all other groups. *n* = 3 .

Figure 3.7. Meox1 preserved Smad3 phosphorylation by inhibiting PPM1A expression through increasing its degradation. *A,* knockdown of Meox1 decreased p-Smad3 level. 10T1/2 cells were transduced with scramble (shCtrl) or Meox1 shRNA (shMeox1) adenoviral vectors for 1 day followed by 2-day starvation. The cells were then treated with TGF-β (5 ng/ml) for the times indicated. Total Smad3 and phosphorylated Smad3 (p-Smad3) levels in total cell lysates were analyzed by Western blot. *B,* phospho-Smad3 was quantified by normalizing the p-Smad3 shown in A to GAPDH level in each time points. **P*<0.05 compared with shMeox1-treated group in each time point (*n* = 3). *C,* knockdown of Meox1 increased PPM1A expression. 10T1/2 cells were transduced with shCtrl or shMeox1 for 1 day followed by 2 day serum starvation. The cells were then treated with TGF-β (5 ng/ml) for the times indicated. PPM1A expression level was measured by Western blot. *D,* Quantification of PPM1A protein levels shown in C by normalized to the α-Tubulin level at each time point, respectively. **P*<0.05 compared with shCtrl group for each time point, respectively (n = 3). E, knockdown of Meox1 slowed down the degradation of PPM1A. 10T1/2 cells were transduced with shCtrl or shMeox1 adenoviral vectors for 3 days followed by 30 μg/ml cycloheximide (CHX) treatment for the indicated time. PPM1A expression level was measured by Western blot. F, Remaining PPM1A percentage was quantified by normalizing the PPM1A to α-Tubulin level in each time point. *P<0.05 compared with shMeox1-treated group in each time point (n = 3). G, Overexpression of Meox1 decreased PPM1A expression. 10T1/2 cells were transduced with Control (Ctrl, GFP adenoviral vector) or Meox1 adenoviral vectors for 48 hours. PPM1A expression was analyzed by Western Blot. H, PPM1A was quantified by normalizing the PPM1A to α-Tubulin level in each time points. *P<0.05

compared with AdMeox1-treated group in each time point (n = 3).

Figure 3.8. A schematic mechanism by which Meox1 regulates SMC differentiation. After TGF-β stimulation, Smad3 is phosphorylated and shuttled into nucleus where Smad3 binds to SBE in SMC marker genes to initiate SMC marker genes transcription and SMC differentiation. As a mild activator for SMC genes, Smad3 facilitates SMC differentiation in early stage of TGF-β treatment through a temperate and precise regulation. In late stage, nuclear Smad3 is exported to cytoplasm after dephosphorylating by PPM1A. In initiation stage of SMC differentiation, Meox1 plays a novel role in inhibiting PPM1A expression through maintaining certain PPM1A degradation rate which enhances nuclear Smad3 retention and guarantees SMC marker genes to transcript and SMC to differentiate properly.

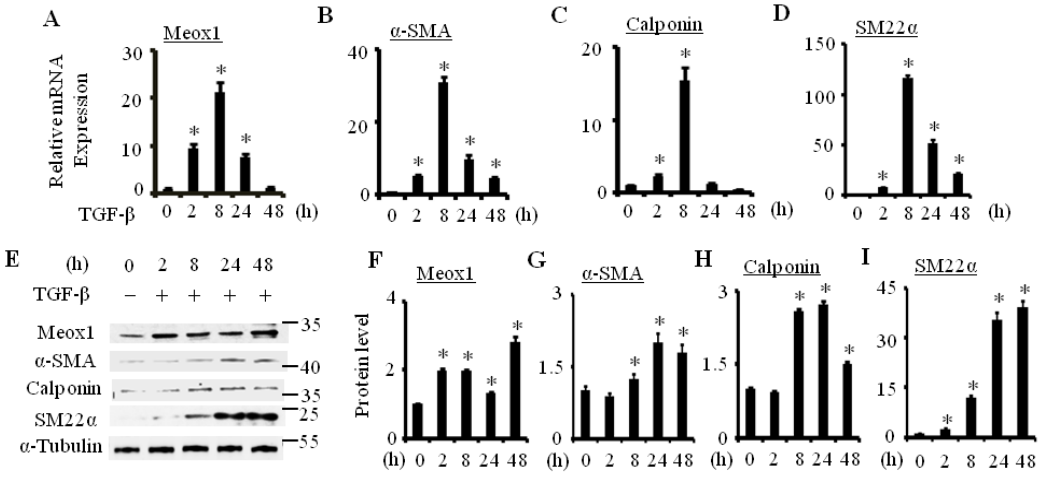

Fig 3.1: TGF-β induced Meox1 expression along with SMC early differentiation markers.

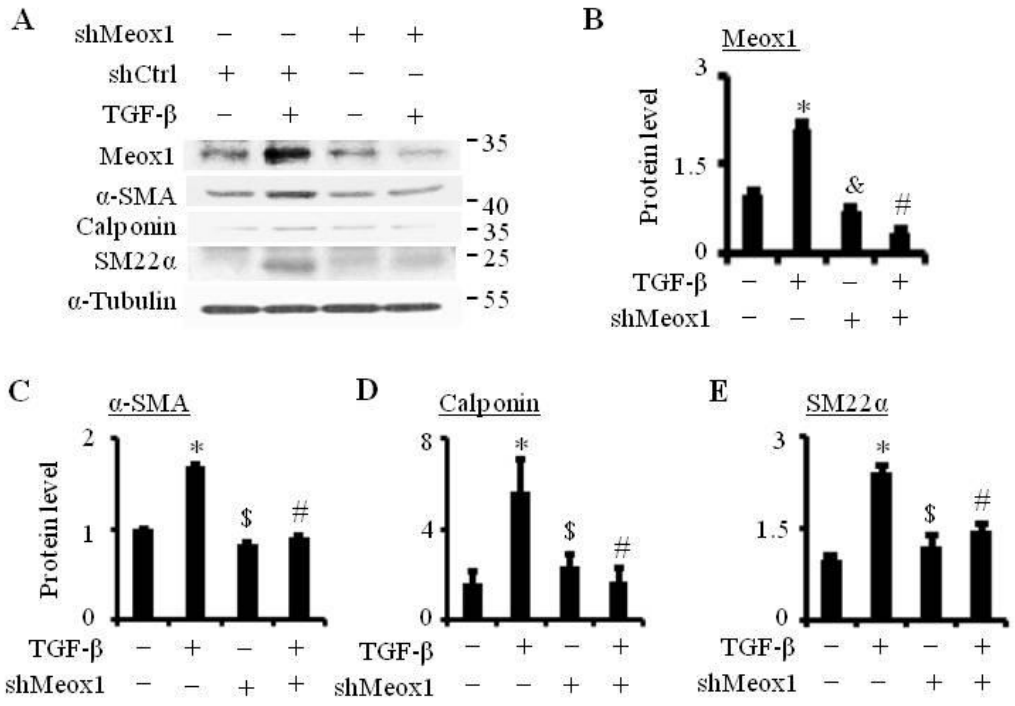

Figure 3.2: Meox1 was essential for TGF-β-induced SMC differentiation

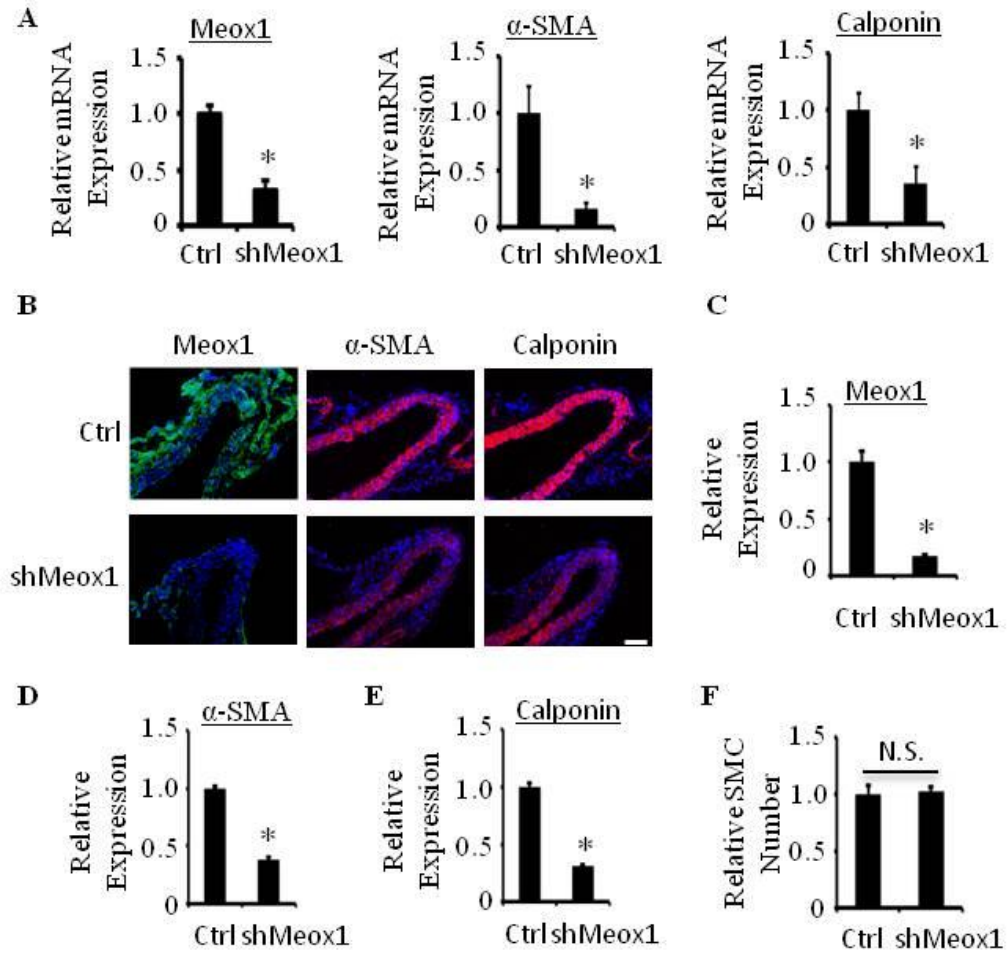

Figure 3.3: Knockdown of Meox1 attenuated SMC differentiation during mouse embryonic development.

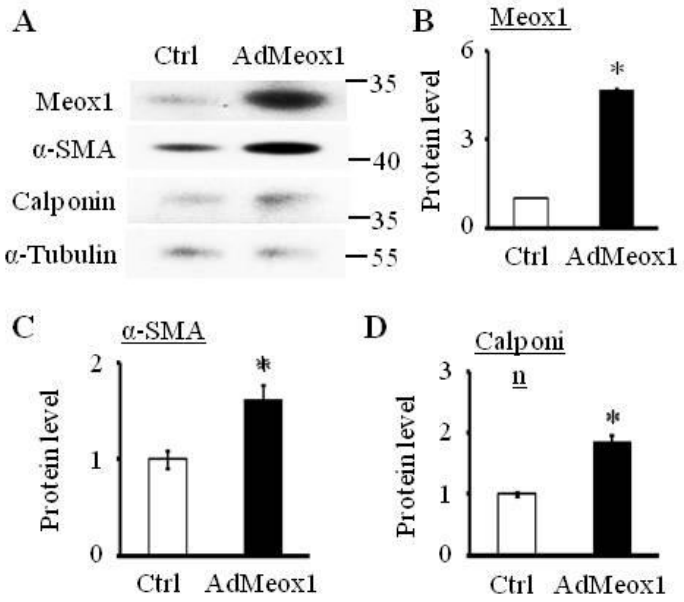

Figure 3.4. Meox1 alone was able to induce SMC early differentiation marker expression.

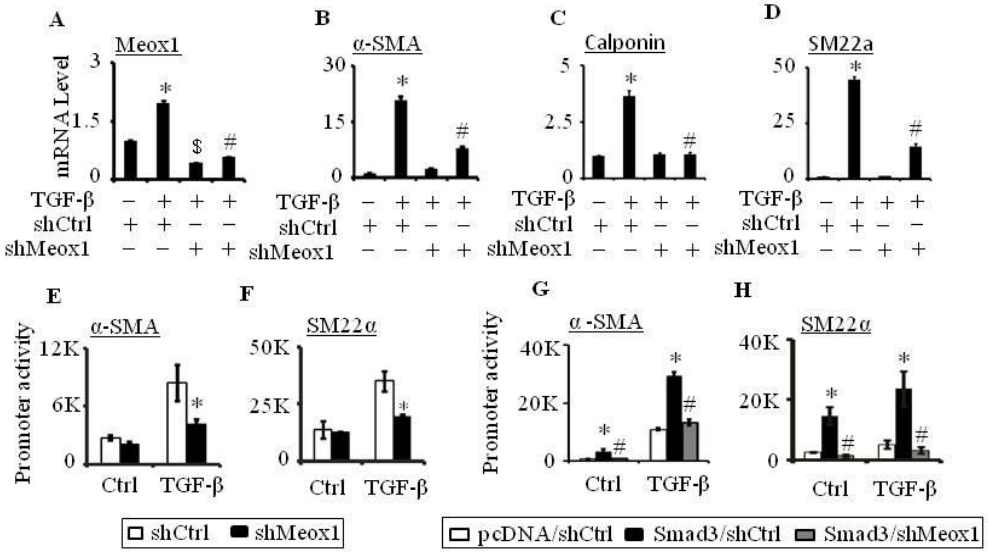

Figure 3.5. Meox1 was required for the activation of SMC marker promoters by TGF-β/Smad3.

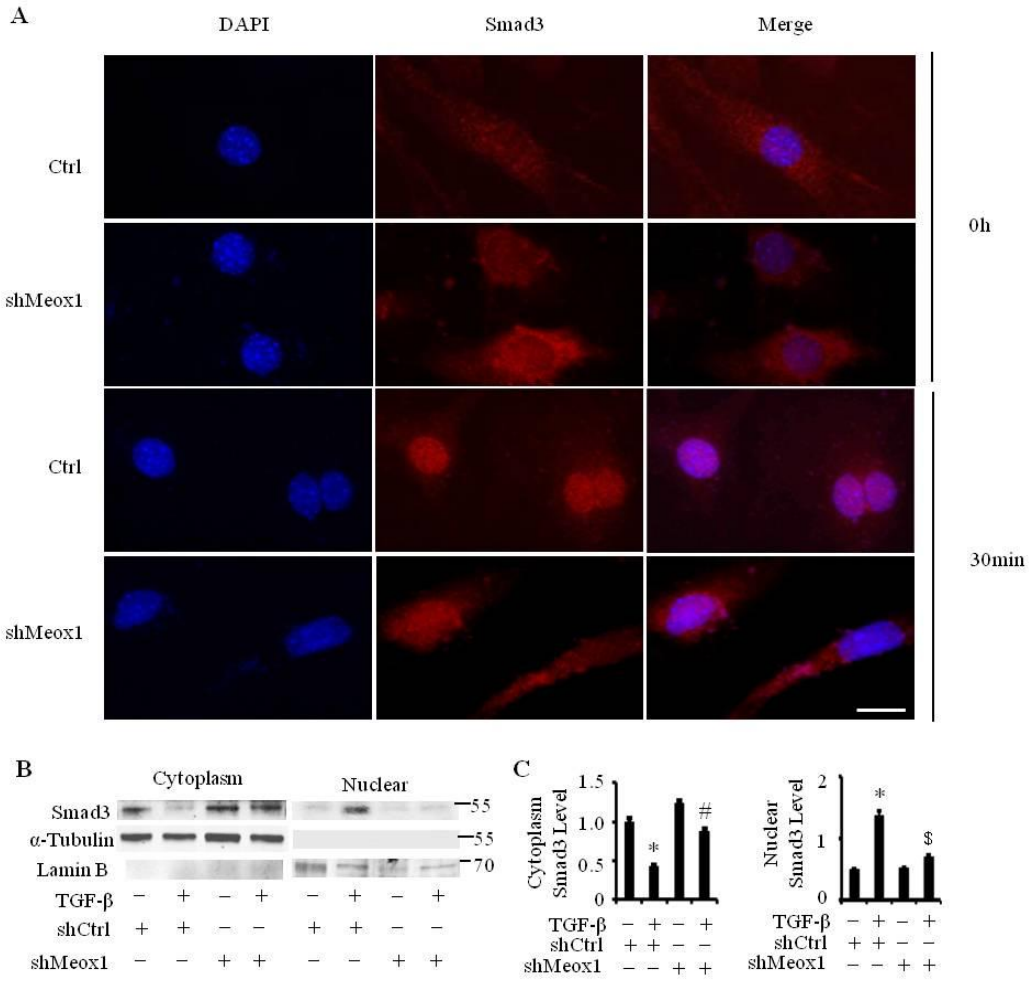

Figure 3.6. Meox1 was critical for TGF-β-induced Smad3 nuclear localization.

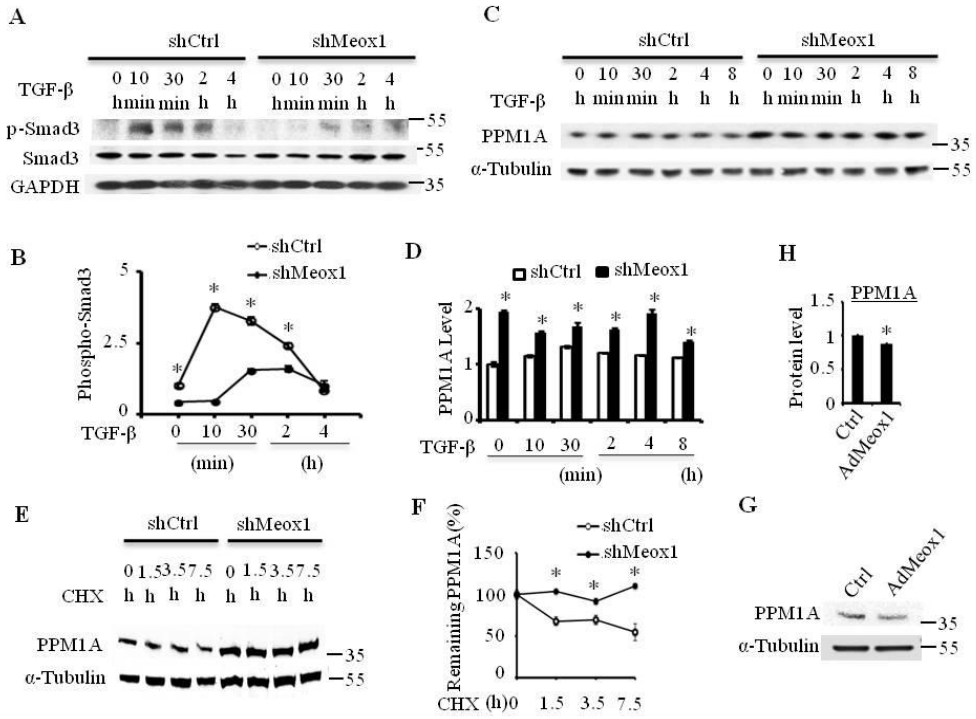

Figure 3.7. Meox1 preserved Smad3 phosphorylation by inhibiting PPM1A expression through increasing its degradation

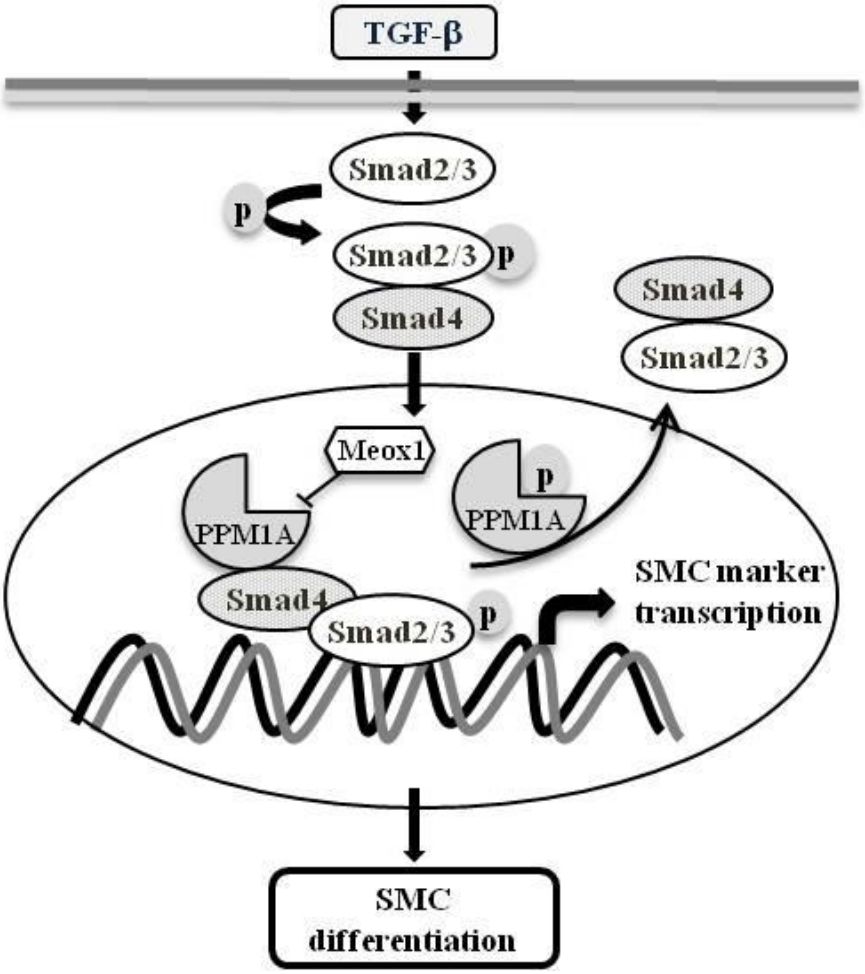

Figure 3.8. A schematic mechanism by which Meox1 regulates SMC differentiation.

CHAPTER 4

SMAD2 DEFICIENCY PROMOTES ATHEROSCLEROSIS DEVELOPMENT[2]

[2] Kun Dong, Li Li, Xiaobing Cui, Xiaohan Mei, Gui Zhang and Shi-You Chen. To be submitted to *Arteriosclerosis, Thrombosis and Vascular Biology*.

Abstract

Vascular smooth muscle cell (VSMC) is the main component of the fibrous cap that is critical for plaque stabilization in advanced atherosclerotic lesion. Elucidating mechanisms controlling VSMC function during the development of atherosclerosis is critical for the understanding of this cardiovascular disease. By using Smad2 SMC-specific knockout $LDLR^{-/-}$ mouse model, we found that Smad2 deficiency in SMC caused a larger atherosclerotic plaque area in the whole aorta but not in the aortic root. It also caused an unstable plaque formation due to the increased MMP2/9 expression and activity. Mechanistically, Smad2 impeded SMC transdifferentiation to macrophage-like cells.

Keywords: Smooth Muscle Transdifferentiation, Transforming Growth Factor-β (TGF-β), SMAD Family Member 2 (Smad2), Atherosclerosis, Plaque Stability

Introduction

According to World health organization (WHO) statistics updated in 2017, cardiovascular diseases (CVDs) is the number 1 cause of death, which represents about 31% mortality globally. Among all deaths from CVD, atherosclerosis-related diseases, such as myocardial infarction, angina, and stroke are one of the major causes (1,2). Atherosclerosis is a chronic inflammatory disease characterized by narrowing of blood vessels due to the formation of atherosclerotic plaque (3). At the late stage of atherosclerosis, the fibrous cap covering the plaque ruptures, which releases the plaque into the vessel causing thrombosis in the coronary or cerebral artery, leading to heart attack and stroke. Plaque instability is one of the major issues in atherosclerosis because it determines the disease outcome. A stable plaque has several characters such as the thick fibrous cap with high collagen content, high VSMC content, small lipid pool and few inflammatory cells (4-7). SMC is the major component in the fibrous cap, which is critical for plaque stability. Recent studies indicated that SMC participates in necrotic core formation through differentiation to foam cell. Also, phenotype modulated SMC may contribute to the weakened atherosclerotic plaque (8,9). In 2014, Owen et al. used lineage tracing approach found that more than 33% of macrophages in advance plaque are derived from SMC (10). As a result, SMCs play very important roles in the development of atherosclerosis.

Smad2 (SMAD Family Member 2) belongs to Smad family in which the proteins are similar to the gene products of the Drosophila gene 'mothers against decapentaplegic' (Mad) (11). The main function of Smad2 is a signal transducer and transcriptional modulator in TGF-β signaling. TGF-β signaling has multiple functions in SMC

differentiation, fibroblast activation, endothelial to mesenchymal transition and extracellular matrix synthesis in endothelial cells and vascular smooth muscle cells. In TGF-β signaling pathways, Smad signaling is the major pathway controlling cell-fate determination, cell-cycle arrest and apoptosis. Previous studies have demonstrated that TGF-β signaling is involved in the development of a number of cardiovascular diseases (12-14). Our previous studies show that Smad2 plays a critical role in SMC differentiation from neural crest cells and the blood vessel formation during embryonic development (15). However, it is unknown if Smad2 is involved in the development of adult vascular diseases, such as atherosclerosis.

To investigate the potential role of Smad2 during the atherosclerosis development, Smad2-SMC knockout mice in $LDLR^{-/-}$ background were used. In our study, we found that $Smad2^{-/-}$ in SMCs promoted atherosclerosis development and caused instable plaques. The decreased plaque stability was due to the increased MMP2/9 expression and activity. $Smad2^{-/-}$ SMCs can become macrophage-like cells, which caused the formation of larger necrotic core and unstable fibrous cap.

Results

Smad2 deficiency in SMC increased aorta atherosclerotic plaque formation.

Our previous studies showed that Smad2 plays a critical role in SMC differentiation from neural crest cells and the blood vessel formation during embryonic development (15). We sought to determine if Smad2 is involved in the development of adult vascular diseases such as atherosclerosis. To study the role of SMC Smad2 in atherosclerosis, we generated SMC-specific Smad2 knockout mouse in $LDLR^{-/-}$ background ($LDLR^{-/-}$ SM22α-

Cre;Smad2$^{fl/fl}$) and fed mice with high-fat diet for 12 weeks. As shown in Fig 4.1 A-B, Smad2 deficiency in SMC resulted in the formation of more atherosclerotic plaques as compared to the control mice.

The aortic root is a common place reflecting the overall plaque formation in animal models, and it is therefore the most interested area to characterize the atherosclerosis development. Interestingly, there was no significant difference in plaque area between Smad2 SMC specific knockout and Ctrl mice (Fig. 4.1, C-D).

SMC Smad2 deficiency contributed to unstable plaque formation

Although there was no difference in plaque area between the aortic root, necrotic core area was increased in Smad2sm-/- aortic root (Fig 4.2, A). We sought to determine if Smad2 deficiency in SMCs affects plaque stability. Thus, we performed H&E staining to detect the cap thickness. As shown in Fig 4.2, B, Smad2 deficiency in SMC decreased the thickness of the fibrous cap. Masson's Trichrome staining showed that Smad2 deficiency in SMC also reduced the collagen content (Fig 4.2, C). Since SMCs content is one of the important characters for plaque stability (33), we used immunohistochemical (IHC) staining of SMC marker α--SMA to detect SMC content in the fibrous cap. As shown in Fig 4.2, D, Smad2 deficiency in SMC caused a decreased SMC content in the lesion area, especially the fibrous cap area. Together, these results suggest that Smad2 knockout in SMC led to increased plaque vulnerability due to the larger necrotic core area, decreased fibrous cap thickness, less collagen content and SMC content.

Smad2 deficiency in SMC increased the expression and activities of Matrix metalloproteinase MMP2 and MMP9.

MMPs are calcium-dependent zinc-containing endopeptidases participating in the progression of atherosclerosis and plaque rupture. In MMPs family, MMP-2 and MMP-9 have been identified in the pathogenesis of atherosclerosis and aneurysm formation causing collagen degradation, SMC migration from the medium layer and less stable fibrous cap. MMP2/9 can be secreted by macrophage and SMCs (34-36). Since Smad2 deficiency in SMC caused decrease in collagen content, we detected if Smad2 affect MMP2/9 expression /activity. IHC staining of MMP2 and MMP9 was performed respectively to detect their expression in lesions of aortic root. A shown in Fig 4.5, A-B, Smad2 deletion in SMC increased MMP2/9 expression in the lesion area. In situ zymography (30-32) showed that Smad2 deletion in SMC also increased MMP2 and MMP9 activity in the lesion (Fig 4.3, C). The elevated MMP2/9 expression and activity in Smad2-SMC knockout mice indicated that Smad2 may directly or indirectly regulate MMP2/9 expression and activity during atherosclerosis development.

Smad2 deficiency in SMC increased macrophage content in the lesion.

In atherosclerotic plaque, macrophages are major contributors to the inflammatory response by secreting pro-inflammatory mediator and MMPs and thus lead to necrotic core formation and fibrous cap rupture (37,38). Thus, we detected the macrophage content in in lesions of aortic roots by co-immunostaining of the macrophage maker CD68 and SMC maker α-SMA. As shown in Fig 4.4, A-B, Smad2 deficiency in SMC

increased the macrophage content, which may result in more vulnerable atherosclerotic plaques.

Smad2 played an important role in SMC transdifferentiation to macrophage-like cells.

Recent studies have reported the contribution of SMC to cholesterol accumulation and macrophage-like cells in lesion. Since necrotic core formation is due to the foam cell formation and macrophage-like cell function (9), we detected if Smad2 contributes to the macrophage or foam cell transition from SMC. Primary cultured rat VSMCs were treated with water-soluble cholesterol (Chol:MβCD complex) (Chol) in a dose-dependent manner from 0-40 ug/ml as previously described (39). After 72 hours treatment, cells were harvested to detect protein expression of Smad2, phosphor-Smad2, SMC and macrophage markers. As shown in Fig 4.5, A-D, Phospho-Smad2 level decreased by cholesterol treatment along with a decrease of SMC marker SM22a and an increase of macrophage marker Mac2, suggesting that Smad2 may inhibit the SMC-macrophage transition. To test if Smad2 impedes the SMC to macrophage transition, primary cultured $Smad2^{-/-}$ SMCs from Smad2 SMC specific knockout mice were transduced with Ad- GFP (Ctrl) or Ad-Smad2 overexpression adenovirus for 2 days followed by Cholesterol (30ug/ml) or Ctrl BSA treatment. Quantitative PCR (qPCR) was performed to detect macrophage marker expression during SMC macrophage-like cell transition. In Ad-GFP-treated cells, cholesterol successfully induced the expression of macrophage maker. However, overexpression of Smad2 inhibited the cholesterol-induced macrophage marker

expression in Smad2$^{-/-}$ SMCs (Fig. 4.5 E), suggesting that Smad2 blocks the SMC trans-differentiation to macrophage.

Smad2 deficiency promoted SMC foam cell formation.

To test if Smad2 affects the functional property of macrophage-like cells derived from SMC, we performed cholesterol loading experiments and used oil red O staining to observe the lipid uptake by macrophage-like cells converted from SMC. WT SMCs were transduced with Ad-GFP (Ctrl) or Smad2 shRNA adenovirus (Ad-shSmad2), while Smad2-/- SMCs were transduced with Ad-GFP or Smad2 overexpression adenovirus (Ad-Smad2) for 2 days followed by culturing the cells with DMEM medium containing Cholesterol (30 ug/ml) or BSA (Ctrl) for 72 hours. WT SMC slightly uptook cholesterol. When Smad2 was knocked down or knockout, cholesterol uptake was significantly increased. However, if Smad2 was restored in smad2-/- SMCs, the cholesterol uptake was inhibited. These data demonstrated that Smad2 deficiency promoted SMC differentiation to foam cells.

Discussion

SMCs are a group of cells with a wide range of different phenotypes at different stages of development, and even in the adult organism, the cells are capable of major changes in their phenotype in response to changes in their local environment (40,41). During atherosclerosis progression, VSMC is the main component of the fibrous cap, plays a role in plaque stabilization, and may participate in the necrotic core formation through

differentiation to foam cell. Here we have demonstrated a critical role of Smad2 in the development of atherosclerosis.

Smad2 SMC knockout increased plaque area in the whole aorta (Fig 1 A-B). In addition, $Smad2^{-/-}$ in SMC caused the formation of unstable plaques due to the larger necrotic core area, increased fibrous cap thickness, less SMC and collagen content (Fig 4.2). Smad2 knockout in SMC also led to the increased expression and activity of MMP2 and MMP9, which in turn caused degradation of extracellular matrix and atherosclerotic plaque instability (Fig 4.3). Another vulnerable plaque factor, macrophage accumulation was also increased in the lesions with Smad2 deletion in SMC (Fig 4.4).

Previous studies have shown that TGF-β promotes monocytes-derived macrophages transdifferentiation into SMC-like cells. During this process, p-Smad2 expression is up-regulated (42). Our in vitro study showed that phospho-Smad2 level was decreased during SMC-macrophage transition with water-soluble cholesterol treatment. Importantly, overexpression of Smad2 in $Smad2^{-/-}$ SMCs inhibited the macrophage marker expression induced by cholesterol, suggesting that Smad2 inhibited SMC transdifferentiation to macrophages. Although there is no study showing if Smad2 regulates the macrophage to SMC-like cell transition, our findings suggest that Smad2 may play an important role in both SMC-macrophage and macrophage-SMC transitions.

Functional study of macrophage-like cells derived from SMCs revealed that Smad2 knockdown or knockout in SMCs increased the cholesterol uptake. However, when Smad2 was over-expressed to restore Smad2 expression in Smad2 deficient SMCs, the cholesterol uptake was blocked (Fig. 4.6). Previous studies suggest that Smad2 is a major player in inhibiting macrophages uptake of modified LDL in human atherosclerosis (43).

Our finding indicates that besides the monocyte-derived macrophages, Smad2 also prevents the lipid uptake of macrophages-like cells derived from SMCs.

Collectively, our results suggest that maintaining or increasing Smad2 level may represent a promising approach to prevent atherosclerosis.

Materials and Methods

Cell Culture

SMCs were cultured by enzyme digestion method from rat or mouse thoracic aorta as described previously (8,16,17). The primary cultured SMCs was confirmed by the expression of smooth muscle α-SMA and SM22α. SMCs were cultured in Dulbecco's modified Eagle's medium containing 10% fetal bovine serum and 5% L-glutamine. SMCs less than 6 passages with 70-80% of confluence were used in the experiments. Rat VSMC or mouse VSMC were treated with water-soluble cholesterol (Sigma-Aldrich C4951) (20μg/ml) for 48-72 hours as described (8).

Animal Procedures

Smad2-floxed ($Smad2^{fl/fl}$) and SM22α-Cre mice were previously described (15,18,19). To generate Smad2 deletion in SMCs, SM22α-Cre male mice were crossbred with $Smad2^{fl/fl}$ mice to produce SM22α-Cre;$Smad2^{fl/+}$ mice. The male and female SM22α-Cre;$Smad2^{fl/+}$ mice were then crossbred to produce SM22α-Cre;$Smad2^{fl/fl}$ mice. SM22α-Cre;$Smad2^{+/+}$ littermates serve as controls. SM22α-Cre;$Smad2^{fl/fl}$ mice were crossed with LDLR-deficient mice, also on the SM22α-Cre;$Smad2^{+/+}$ littermates, to generate mice heterozygous at both loci. These $LDLR^{+/-}$ SM22α-Cre;$Smad2^{fl/+}$ mice were then intercrossed to produce $LDLR^{-/-}$ SM22α-Cre;$Smad2^{fl/fl}$ and $LDLR^{-/-}$ SM22α-

Cre;Smad2$^{+/+}$ littermates that were used as controls for studies. Atherosclerosis was induced by feeding the mice from 12 weeks of age for 12 weeks with a high-fat western-type diet containing 1.25% cholesterol (ResearchDiets, D12108). All animal protocols were approved by the Institutional Animal Care Use Committee of the University of Georgia.

Construction of Adenovirus

Adenoviral vectors expressing scramble or Smad2 short hairpin RNA (shRNA) (shSmad2) were constructed, and the viruses were purified as described previously (15,20,21).

Western Blot

SMC cells were cultured in DMEM and treated with or without water-soluble cholesterol or other factors as needed. Total proteins were extracted as previous described (21,22). Protein concentration was measured using BCA Protein Assay reagent (Thermo Scientific). Protein lysates were resolved by SDS-PAGE and transferred to PVDF membrane (Bio-Rad) or nitrocellulose membrane (Bio-Rad) that were blocked with 5% nonfat dry milk or 5% BSA separately. Membranes were then incubated with the following primary antibodies in blocking buffers in room temperature for 2-3 hours or in 4℃ overnight: anti-Phospho-Smad2 (Cell Signaling Technology, 3108), anti-MMP2 (Abcam, ab37150), anti-CD68 (Bio-Rad, MCA1957), anti-MMP9 (Proteintech, 10375-2-AP), anti-Mac2 (Abcam, ab2785), anti-αSMA (Sigma-Aldrich, A2547), anti-SM22α (Abcam, ab10135), anti-calponin (Abcam, ab46794), anti-α-Tubulin (Sigma-Aldrich, T9026), anti-GAPDH (Sigma-Aldrich, G8795). Then, HRP-conjugated or immunofluorescent secondary antibodies were incubated with the membranes for 1 h.

The protein expression levels were detected with enhanced chemiluminescence (Millipore) or scanned by Odyssey fluorescence scanner (LI-COR) (23).

Quantitative Reverse Transcription-PCR (qPCR)

Total RNA was extracted from cells using Trizol Reagent (Life Technologies) followed by a reverse transcription using iScript cDNA Synthesis Kit (Bio-Rad) according to the manufacturer's instructions. qPCR was performed using the Mx3005P qPCR machine with SYBR Green mater mix (Agilent Technologies). Mouse Smad2 primers used were: 5′-CCG GCT GAA CTG TCT CCT AC -3′ (forward) and 5′-GCA GAA CCT CTC CGA GTT TG-3′ (reverse). Smooth muscle marker primers were described previously (24,25).

Atherosclerosis quantification, Histology, Immunohistochemistry and Immunofluorescent staining

Mouse aortas were fixed with 4% paraformaldehyde, and paraffin-embedded and aortic roots were fixed with either 4% paraformaldehyde and paraffin-embedded for 5 μm thick cross section or fresh frozen and embedded in OCT for 10 μm thick cross section. Atherosclerosis was quantified on both en face surface area of oil red O-positive lesions of whole aortas and the plaque area on aortic root cross-sections as previously described (26). The sections were stained with hematoxylin and eosin staining (H&E staining) for structural observation, Elastica van Gieson for elastin and Masson's trichrome for Collagen and captured using a Nikon microscope. For immunohistochemistry, sections were rehydrated, blocked with 5% goat serum, permeabilized with 0.01% Triton X-100 in phosphate-buffered saline, and incubated with rabbit anti-pSmad2, α-SMA, MMP2, MMP9 antibody overnight at 4℃, followed by incubation with horseradish peroxidase (HRP)–conjugated secondary antibody. Smad2 staining was visualized using Vectastain

ABC-AP kit by following the manufacturer's protocol (Vector Laboratories). The vessel sections were counterstained with hematoxylin. For fluorescent staining, 10μm fresh frozen sections were air dried for 30 minutes at room temperature followed by 10 minutes fixation with 4% paraformaldehyde. After 3 times washing with phosphate-buffered saline, the section is permeabilized with 0.01% Triton X-100 in phosphate-buffered saline for 10 minutes, blocked with 5% goat serum for 30 minutes, and incubated with rat anti-CD68, mouse anti-α-SMA antibody overnight at 4℃, followed by incubation with FITC-conjugated or TRITC-conjugated secondary antibodies. Cell nuclei were stained with DAPI (Molecular Probes). Stained tissue sections were imaged using a Nikon 12.7MP digital Sight DS-Ri1 color camera as previously described (21,27,28).

In situ zymography

MMP activity was determined by in situ zymography, as previously described (29-32). 10μm thick frozen cross sections were incubated overnight (37℃) with a fluorogenic gelatin substrate (Molecular Probes) dissolved in 25 μg/mL in zymography buffer (50 mmol/L Tris-HCl, 10 mmol/L CaCl2, and protease inhibitor cocktail, pH 7.4). The gelatin with a fluorescent tag remains caged until the gelatin is cleaved by gelatinase activity. In situ gelatinolysis was revealed by the appearance of fluorescence. In negative control experiments, sections were incubated with MMP inhibitors (1,10-phenanthroline and EDTA). MMP2 and MMP9 activity were observed and imaged with Nikon Eclipse 90i microscope and analyzed by Image J software.

Statistical Analysis

All values are expressed as mean ± S.E. Data were evaluated with a 2-tailed, unpaired Student t test or compared by one-way ANOVA followed by Fisher t-test. A *p*-value <0.05 was considered statistically significant.

Reference

1. Heusch, G., and Gersh, B. J. (2017) The pathophysiology of acute myocardial infarction and strategies of protection beyond reperfusion: a continual challenge. *European heart journal* **38**, 774-784
2. Burke, A. P., and Virmani, R. (2007) Pathophysiology of acute myocardial infarction. *The Medical clinics of North America* **91**, 553-572; ix
3. Lusis, A. J. (2000) Atherosclerosis. *Nature* **407**, 233-241
4. Chen, X., Qian, S., Hoggatt, A., Tang, H., Hacker, T. A., Obukhov, A. G., Herring, P. B., and Seye, C. I. (2017) Endothelial Cell-Specific Deletion of P2Y2 Receptor Promotes Plaque Stability in Atherosclerosis-Susceptible ApoE-Null Mice. *Arterioscler Thromb Vasc Biol* **37**, 75-83
5. Grootaert, M. O., Schrijvers, D. M., Hermans, M., Van Hoof, V. O., De Meyer, G. R., and Martinet, W. (2016) Caspase-3 Deletion Promotes Necrosis in Atherosclerotic Plaques of ApoE Knockout Mice. *Oxid Med Cell Longev* **2016**, 3087469
6. Krohn, J. B., Hutcheson, J. D., Martinez-Martinez, E., Irvin, W. S., Bouten, C. V., Bertazzo, S., Bendeck, M. P., and Aikawa, E. (2016) Discoidin Domain Receptor-1 Regulates Calcific Extracellular Vesicle Release in Vascular Smooth Muscle

Cell Fibrocalcific Response via Transforming Growth Factor-beta Signaling. *Arterioscler Thromb Vasc Biol* **36**, 525-533

7. Zhang, K., Liu, X., Yu, Y., Luo, T., Wang, L., Ge, C., Liu, X., Song, J., Jiang, X., Zhang, Y., Qin, S., and Zhang, M. (2014) Phospholipid transfer protein destabilizes mouse atherosclerotic plaque. *Arterioscler Thromb Vasc Biol* **34**, 2537-2544
8. Rong, J. X., Shapiro, M., Trogan, E., and Fisher, E. A. (2003) Transdifferentiation of mouse aortic smooth muscle cells to a macrophage-like state after cholesterol loading. *Proc Natl Acad Sci U S A* **100**, 13531-13536
9. Allahverdian, S., Chehroudi, A. C., McManus, B. M., Abraham, T., and Francis, G. A. (2014) Contribution of intimal smooth muscle cells to cholesterol accumulation and macrophage-like cells in human atherosclerosis. *Circulation* **129**, 1551-1559
10. Shankman, L. S., Gomez, D., Cherepanova, O. A., Salmon, M., Alencar, G. F., Haskins, R. M., Swiatlowska, P., Newman, A. A., Greene, E. S., Straub, A. C., Isakson, B., Randolph, G. J., and Owens, G. K. (2015) KLF4-dependent phenotypic modulation of smooth muscle cells has a key role in atherosclerotic plaque pathogenesis. *Nat Med* **21**, 628-637
11. Riggins, G. J., Thiagalingam, S., Rozenblum, E., Weinstein, C. L., Kern, S. E., Hamilton, S. R., Willson, J. K., Markowitz, S. D., Kinzler, K. W., and Vogelstein, B. (1996) Mad-related genes in the human. *Nat Genet* **13**, 347-349
12. Kretschmer, A., Moepert, K., Dames, S., Sternberger, M., Kaufmann, J., and Klippel, A. (2003) Differential regulation of TGF-beta signaling through Smad2,

Smad3 and Smad4. *Oncogene* **22**, 6748-6763

13. Lu, Z., Murray, J. T., Luo, W., Li, H., Wu, X., Xu, H., Backer, J. M., and Chen, Y. G. (2002) Transforming growth factor beta activates Smad2 in the absence of receptor endocytosis. *J Biol Chem* **277**, 29363-29368

14. Nakao, A., Imamura, T., Souchelnytskyi, S., Kawabata, M., Ishisaki, A., Oeda, E., Tamaki, K., Hanai, J., Heldin, C. H., Miyazono, K., and ten Dijke, P. (1997) TGF-beta receptor-mediated signalling through Smad2, Smad3 and Smad4. *EMBO J* **16**, 5353-5362

15. Xie, W. B., Li, Z., Shi, N., Guo, X., Tang, J., Ju, W., Han, J., Liu, T., Bottinger, E. P., Chai, Y., Jose, P. A., and Chen, S. Y. (2013) Smad2 and myocardin-related transcription factor B cooperatively regulate vascular smooth muscle differentiation from neural crest cells. *Circulation research* **113**, e76-86

16. Guo, X., Shi, N., Cui, X. B., Wang, J. N., Fukui, Y., and Chen, S. Y. (2015) Dedicator of cytokinesis 2, a novel regulator for smooth muscle phenotypic modulation and vascular remodeling. *Circulation research* **116**, e71-80

17. Golovina, V. A., and Blaustein, M. P. (2006) Preparation of primary cultured mesenteric artery smooth muscle cells for fluorescent imaging and physiological studies. *Nature protocols* **1**, 2681-2687

18. Ju, W., Ogawa, A., Heyer, J., Nierhof, D., Yu, L., Kucherlapati, R., Shafritz, D. A., and Bottinger, E. P. (2006) Deletion of Smad2 in mouse liver reveals novel functions in hepatocyte growth and differentiation. *Molecular and cellular biology* **26**, 654-667

19. Holtwick, R., Gotthardt, M., Skryabin, B., Steinmetz, M., Potthast, R., Zetsche, B.,

Hammer, R. E., Herz, J., and Kuhn, M. (2002) Smooth muscle-selective deletion of guanylyl cyclase-A prevents the acute but not chronic effects of ANP on blood pressure. *Proceedings of the National Academy of Sciences of the United States of America* **99**, 7142-7147

20. Wang, J. N., Shi, N., Xie, W. B., Guo, X., and Chen, S. Y. (2011) Response gene to complement 32 promotes vascular lesion formation through stimulation of smooth muscle cell proliferation and migration. *Arteriosclerosis, thrombosis, and vascular biology* **31**, e19-26
21. Shi, N., Xie, W. B., and Chen, S. Y. (2012) Cell division cycle 7 is a novel regulator of transforming growth factor-beta-induced smooth muscle cell differentiation. *The Journal of biological chemistry* **287**, 6860-6867
22. Shi, N., and Chen, S. Y. (2013) Cell division cycle 7 mediates transforming growth factor-beta-induced smooth muscle maturation through activation of myocardin gene transcription. *J Biol Chem* **288**, 34336-34342
23. Shirai, T., Nazarewicz, R. R., Wallis, B. B., Yanes, R. E., Watanabe, R., Hilhorst, M., Tian, L., Harrison, D. G., Giacomini, J. C., Assimes, T. L., Goronzy, J. J., and Weyand, C. M. (2016) The glycolytic enzyme PKM2 bridges metabolic and inflammatory dysfunction in coronary artery disease. *The Journal of experimental medicine* **213**, 337-354
24. Chen, S., and Lechleider, R. J. (2004) Transforming growth factor-beta-induced differentiation of smooth muscle from a neural crest stem cell line. *Circ Res* **94**, 1195-1202
25. Chen, S., Kulik, M., and Lechleider, R. J. (2003) Smad proteins regulate

transcriptional induction of the SM22alpha gene by TGF-beta. *Nucleic Acids Res* **31**, 1302-1310

26. Sukhanov, S., Higashi, Y., Shai, S. Y., Vaughn, C., Mohler, J., Li, Y., Song, Y. H., Titterington, J., and Delafontaine, P. (2007) IGF-1 reduces inflammatory responses, suppresses oxidative stress, and decreases atherosclerosis progression in ApoE-deficient mice. *Arterioscler Thromb Vasc Biol* **27**, 2684-2690
27. Shi, N., Guo, X., and Chen, S. Y. (2014) Olfactomedin 2, a novel regulator for transforming growth factor-beta-induced smooth muscle differentiation of human embryonic stem cell-derived mesenchymal cells. *Mol Biol Cell* **25**, 4106-4114
28. Qiu, Y., Yang, J., Wang, W., Zhao, W., Peng, F., Xiang, Y., Chen, G., Chen, T., Chai, C., Zheng, S., Watkins, D. J., and Feng, J. (2014) HMGB1-promoted and TLR2/4-dependent NK cell maturation and activation take part in rotavirus-induced murine biliary atresia. *PLoS pathogens* **10**, e1004011
29. Dumont, O., Loufrani, L., and Henrion, D. (2007) Key role of the NO-pathway and matrix metalloprotease-9 in high blood flow-induced remodeling of rat resistance arteries. *Arteriosclerosis, thrombosis, and vascular biology* **27**, 317-324
30. George, S. J., and Johnson, J. L. (2010) In situ zymography. *Methods Mol Biol* **622**, 271-277
31. Hadler-Olsen, E., Kanapathippillai, P., Berg, E., Svineng, G., Winberg, J. O., and Uhlin-Hansen, L. (2010) Gelatin in situ zymography on fixed, paraffin-embedded tissue: zinc and ethanol fixation preserve enzyme activity. *J Histochem Cytochem* **58**, 29-39
32. Porto, I. M., Rocha, L. B., Rossi, M. A., and Gerlach, R. F. (2009) In situ

zymography and immunolabeling in fixed and decalcified craniofacial tissues. *J Histochem Cytochem* **57**, 615-622

33. Borissoff, J. I., Otten, J. J., Heeneman, S., Leenders, P., van Oerle, R., Soehnlein, O., Loubele, S. T., Hamulyak, K., Hackeng, T. M., Daemen, M. J., Degen, J. L., Weiler, H., Esmon, C. T., van Ryn, J., Biessen, E. A., Spronk, H. M., and ten Cate, H. (2013) Genetic and pharmacological modifications of thrombin formation in apolipoprotein e-deficient mice determine atherosclerosis severity and atherothrombosis onset in a neutrophil-dependent manner. *PloS one* **8**, e55784

34. Caird, J., Napoli, C., Taggart, C., Farrell, M., and Bouchier-Hayes, D. (2006) Matrix metalloproteinases 2 and 9 in human atherosclerotic and non-atherosclerotic cerebral aneurysms. *Eur J Neurol* **13**, 1098-1105

35. Vacek, T. P., Rehman, S., Neamtu, D., Yu, S., Givimani, S., and Tyagi, S. C. (2015) Matrix metalloproteinases in atherosclerosis: role of nitric oxide, hydrogen sulfide, homocysteine, and polymorphisms. *Vasc Health Risk Manag* **11**, 173-183

36. Wagsater, D., Zhu, C., Bjorkegren, J., Skogsberg, J., and Eriksson, P. (2011) MMP-2 and MMP-9 are prominent matrix metalloproteinases during atherosclerosis development in the Ldlr(-/-)Apob(100/100) mouse. *Int J Mol Med* **28**, 247-253

37. Moore, K. J., Sheedy, F. J., and Fisher, E. A. (2013) Macrophages in atherosclerosis: a dynamic balance. *Nat Rev Immunol* **13**, 709-721

38. Randolph, G. J. (2014) Mechanisms that regulate macrophage burden in atherosclerosis. *Circ Res* **114**, 1757-1771

39. Qin, L., Yang, Y. B., Yang, Y. X., Zhu, N., Gong, Y. Z., Zhang, C. P., Li, S. X., and

Liao, D. F. (2014) Ezetimibe suppresses cholesterol accumulation in lipid-loaded vascular smooth muscle cells in vitro via MAPK signaling. *Acta Pharmacol Sin* **35**, 1129-1136

40. Sata, M., Saiura, A., Kunisato, A., Tojo, A., Okada, S., Tokuhisa, T., Hirai, H., Makuuchi, M., Hirata, Y., and Nagai, R. (2002) Hematopoietic stem cells differentiate into vascular cells that participate in the pathogenesis of atherosclerosis. *Nat Med* **8**, 403-409
41. Oh, J., Richardson, J. A., and Olson, E. N. (2005) Requirement of myocardin-related transcription factor-B for remodeling of branchial arch arteries and smooth muscle differentiation. *Proc Natl Acad Sci U S A* **102**, 15122-15127
42. Ninomiya, K., Takahashi, A., Fujioka, Y., Ishikawa, Y., and Yokoyama, M. (2006) Transforming growth factor-beta signaling enhances transdifferentiation of macrophages into smooth muscle-like cells. *Hypertens Res* **29**, 269-276
43. Michael, D. R., Salter, R. C., and Ramji, D. P. (2012) TGF-beta inhibits the uptake of modified low density lipoprotein by human macrophages through a Smad-dependent pathway: a dominant role for Smad-2. *Biochim Biophys Acta* **1822**, 1608-1616
44. Back, M., and Hansson, G. K. (2015) Anti-inflammatory therapies for atherosclerosis. *Nat Rev Cardiol* **12**, 199-211
45. Jamkhande, P. G., Chandak, P. G., Dhawale, S. C., Barde, S. R., Tidke, P. S., and Sakhare, R. S. (2014) Therapeutic approaches to drug targets in atherosclerosis. *Saudi Pharm J* **22**, 179-190
46. Khan, R., Spagnoli, V., Tardif, J. C., and L'Allier, P. L. (2015) Novel anti-

inflammatory therapies for the treatment of atherosclerosis. *Atherosclerosis* **240**, 497-509

Figure legends

Fig 4.1: Smad2 deficiency in SMC caused more atherosclerosis plaque formation. $LDLR^{-/-}$, Smad2sm-/-$LDLR^{-/-}$ mice fed HFD for 3 months. **(A)** Representative En face oil red O staining of the aorta. **(B)** Quantification of plaque area as a percentage of the total aorta surface area as analyzed with Image J software. *P < 0.05 compared with the $LDLR^{-/-}$ (Ctrl) group, n=5. **(C)** Oil red O staining of plaques in aortic roots. Representative pictures of each genotype are shown (40×). Scale: 400 μm. **(D)** Quantification of plaque cross-sectional area as a percentage of total aortic root surface area. *P < 0.05 compared with the Ctrl group, n=5.

Fig 4.2: Smad2 deficiency caused unstable plaques. (A) Necrotic core area was shown by Masson's Trichrome staining and normalized to the $LDLR^{-/-}$ (Ctrl) group (set as 1) (40×). Scale: 400 μm. The necrotic area was circled by the yellow line. The total necrotic core area in each aortic root was analyzed by Image J software. *P < 0.05 compared with the Ctrl group, n=5. **(B)** Fibrous cap area was shown by HE staining and normalized to the $LDLR^{-/-}$ (Ctrl) group (set as 1) (100×). Scale: 200 μm. *P < 0.05 compared with the Ctrl group, n=5. **(C)** Collagen content was measured by Masson's Trichrome staining and quantified as the percentage of the total lesion area (100×). Scale: 200 μm. Total collagen content in each aortic root was analyzed by Image J software, *P < 0.05 compared with the Ctrl group, n=5. **(D)** SMC content was measured by IHC staining of α-SMA and

quantified as the percentage of the total lesion area (100×). Scale: 200 μm. *P < 0.05 compared with the Ctrl group, n=5.

Fig 4.3: Smad2 deficiency increased MMP2/9 expression and activity in the lesion. (A-B) MMP2 and MMP9 expression as the percentage of the lesion area were determined by IHC. *P < 0.05 compared with the Ctrl group, n=5. **(C)** MMP2 and MMP9 activity were detected by in situ zymography and observed with Nikon Eclipse 90i microscope, and images were captured with Nikon 12.7MP digital Sight DS-Ri1 color camera (100×). MMP2/9 activity was quantified as fluorescent signal intensity relative to the total lesion area using Image J software. *P < 0.05 compared with the Ctrl group, n=5. Scale: 200 μm

Fig 4.4: Smad2 deficiency increased macrophage content. (A) Macrophage content was measured by CD68 Immunofluorescent staining (green), and α-SMA staining (red) shows the cap area (100×). Scale: 200 μm. **(B)** Quantification of macrophage content as the percentage of the lesion area. *P < 0.05 compared with the Ctrl group, n=5.

Fig 4.5: Smad2 played a role in SMC trans-differentiation to macrophage-like cells. (A) Smad2 phosphorylation was inhibited during SMC transdifferentiation to macrophage-like cells. SMC treated with various dosage of cholesterol for 72 hours as indicated, and phospho-Smad2, total Smad2 and SM22 α levels were detected. **(B-D)** Quantification of the protein shown in A by normalized to GAPDH. *P < 0.01 compared with the vehicle-treated group, n=3. **(E)** Smad2 impeded SMC transition to macrophage-like cells. Primary cultured SMCs from Smad2 SMC specific knockout mice were

transduced with Ad-GFP (Ctrl) or Ad-Smad2 (S2) overexpression adenoviral vector for 2 days followed by treatment with BSA(Ctrl) or Cholesterol (30 ug/ml, Chol) for 72 hours. Cells were harvested, and mRNA was extracted. Quantitative PCR (qPCR) was performed to detect Mac2 expression in the Mx3005P qPCR machine using SYBR Green master mix (Agilent Technologies) *P < 0.05 compared with the Ad-GFP-transduced and BSA-treated group, n=3. #P < 0.05 compared with the Ad-GFP-transduced and Chol-treated group, n=3.

Fig 4.6: Smad2 deficiency promoted the cholesterol uptake of macrophage-like cells.

A-H, SMCs isolated from wild type (WT) were transduced with adenovirus expressing control or Smad2 shRNA (Ad-shSmad2),while SMCs isolated from Smad2sm-/- mice were transduced with adenovirus expressing control or Smad2 cDNA (Ad-Ad-Smad2) for 2 days followed by treatment with vehicle (Ctrl) or cholesterol (30ug/ml, Chol) for 72 hrs**.** Chol uptake was detected by Oil red O staining (100×). Scale: 200 μm. **I**, Oil red O staining was quantified by measuring the lipid density in cells. *P < 0.05 compared with the WT with Chol treatment (E) group, n=3. #P < 0.05 compared with the AdshSmad2 (F) and Smad2-/- (G) with Chol treatment, n=3.

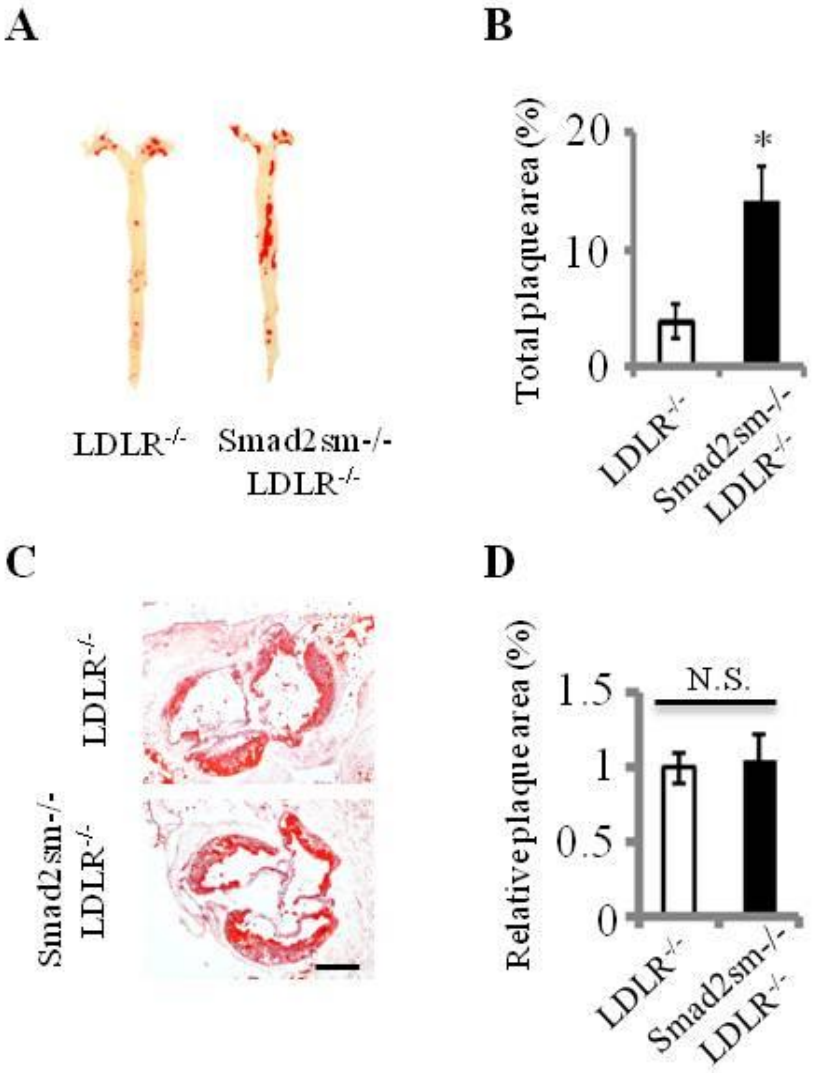

Fig 4.1: Smad2 deficiency in SMC caused more atherosclerosis Plaque formation.

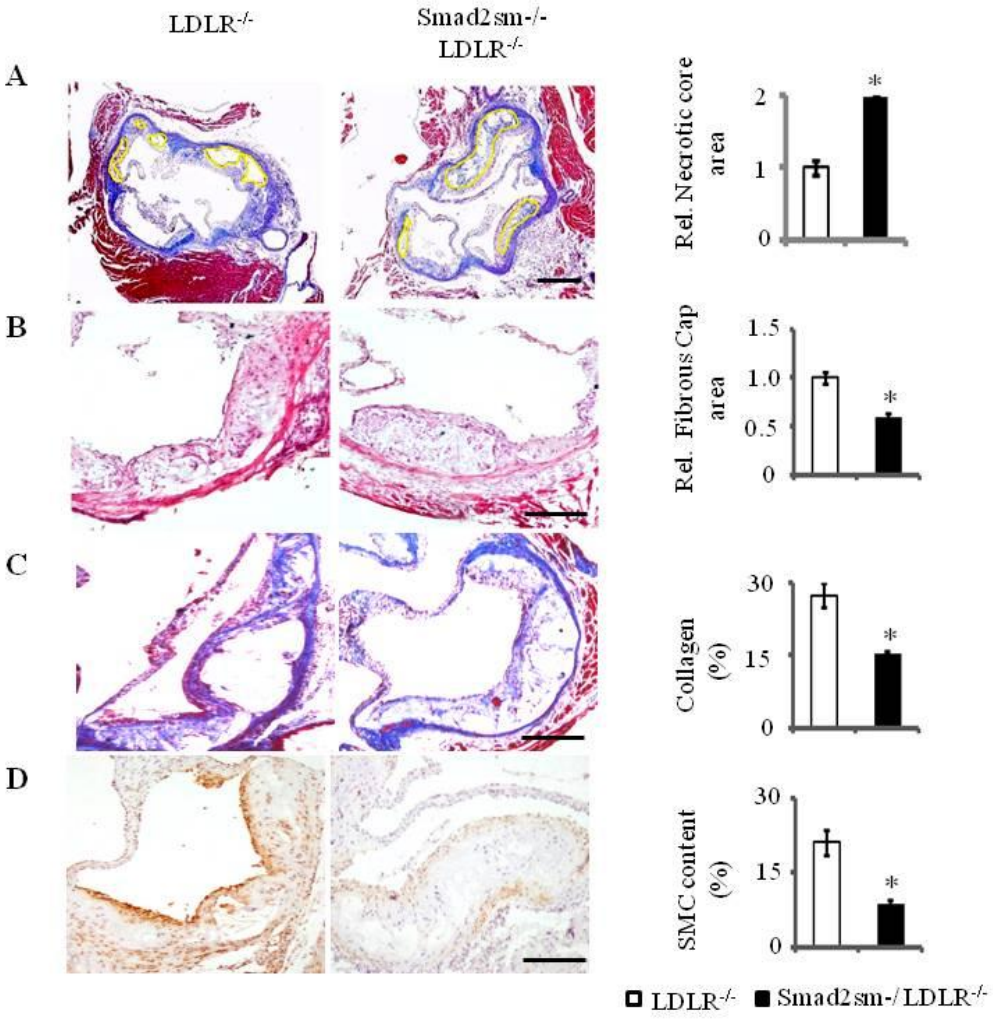

Fig 4.2: Smad2 deficiency caused the formation of unstable plaques.

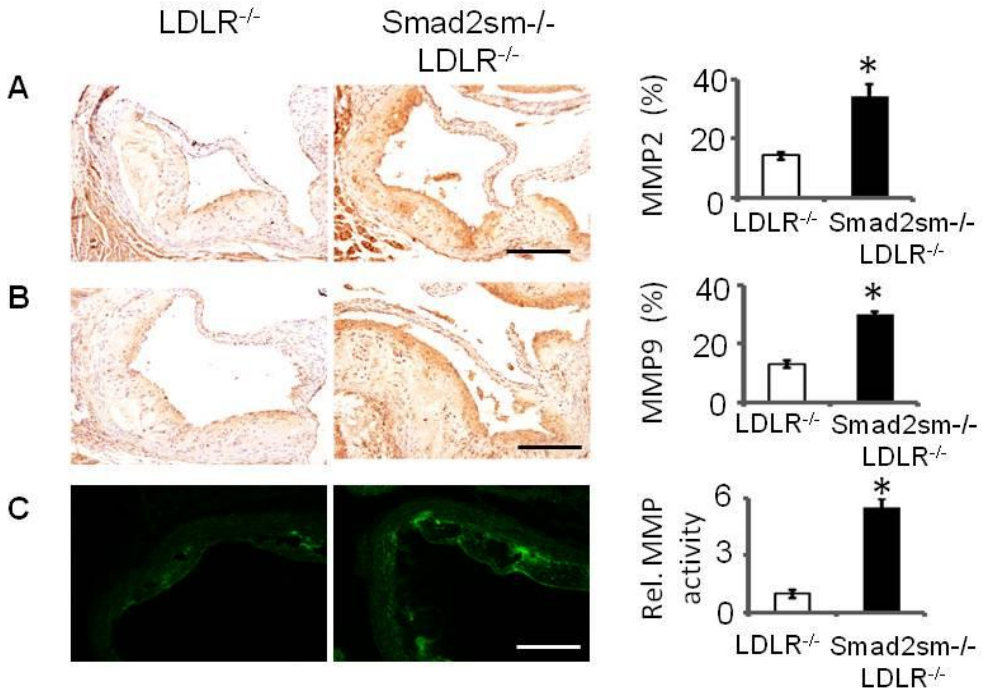

Fig 4.3: Smad2 deficiency in SMC increased MMP2/9 expression and activity in lesions.

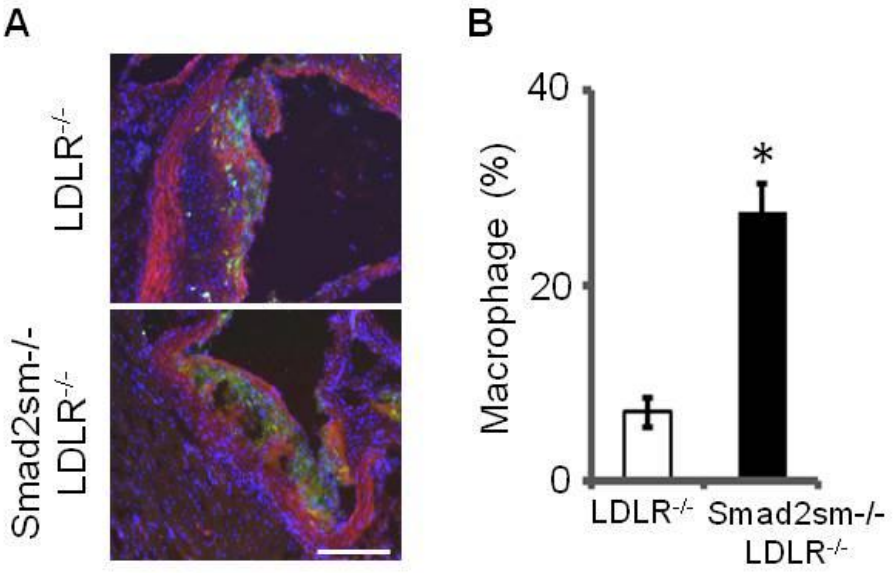

Fig 4.4: Smad2 deficiency caused the increased macrophage content.

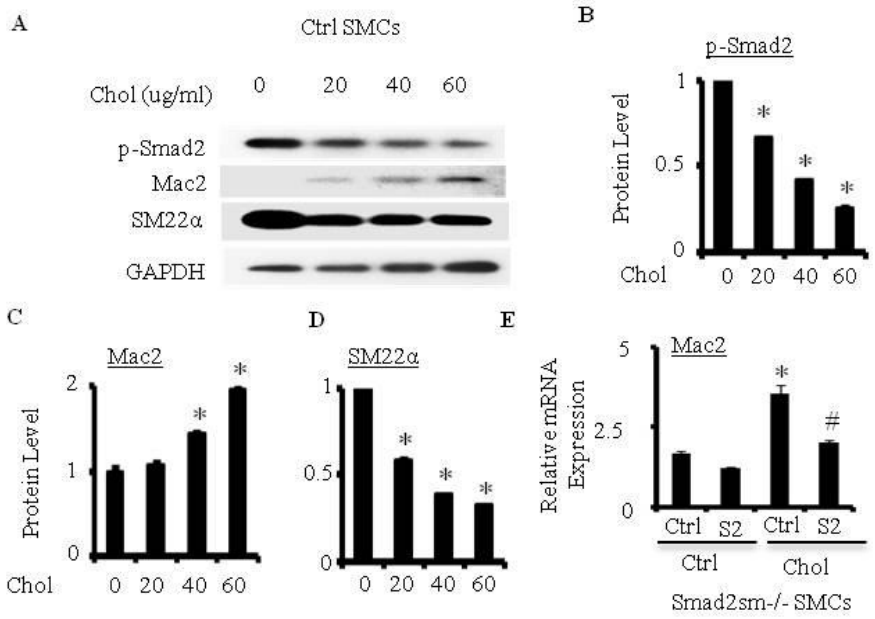

Fig 4.5: Smad2 negatively regulated the cholesterol-induced SMC trans-differentiation to macrophage-like cells.

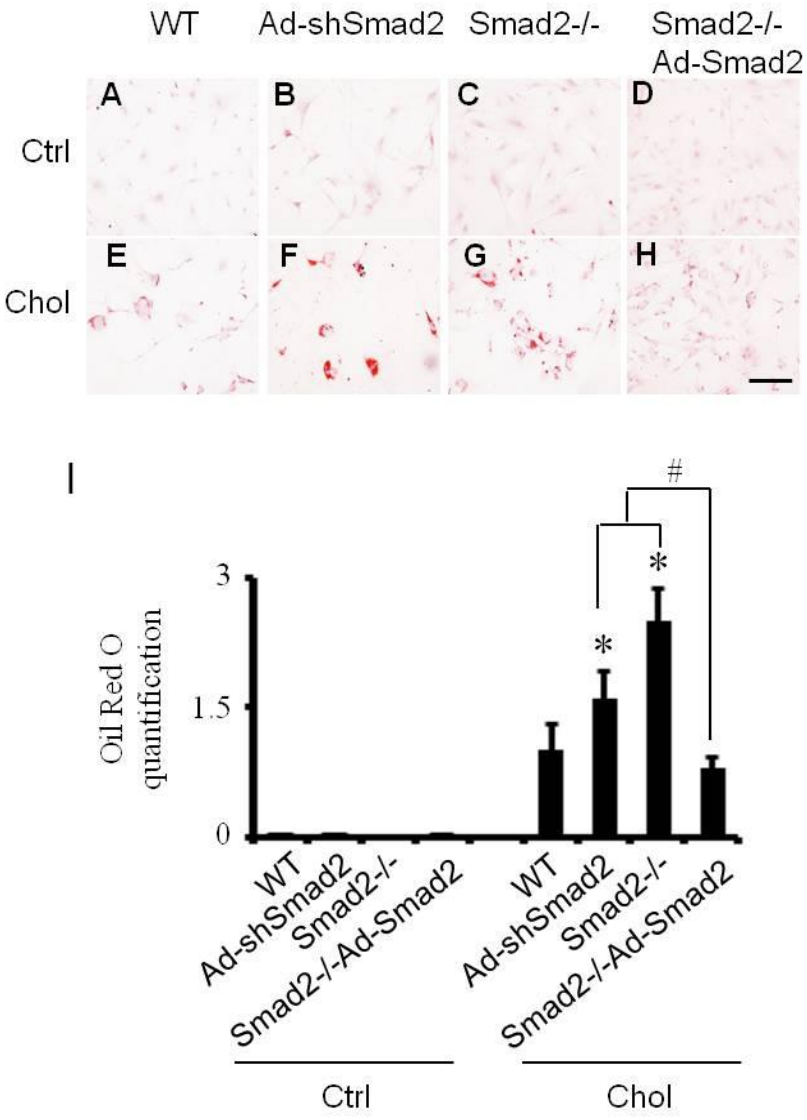

Fig 4.6: Smad2 deficiency promoted the cholesterol uptake of the macrophage-like cells.

CHAPTER 5

SMAD2 DEFICIENCY PROMOTES ABDOMINAL AORTIC ANEURYSM FORMATION[3]

[3] Kun Dong, Li Li, Xiaobing Cui, Xia Guo, Gui Zhang and Shi-You Chen. To be submitted to *Arteriosclerosis, Thrombosis and Vascular Biology*.

Abstract

Abdominal aortic aneurysm (AAA) is a localized dilation in infra-renal segment of abdominal aorta characterized by increased inflammatory cell infiltration, extracellular matrix (ECM) degradation, loss of media smooth muscle cells (SMC), and adventitia proliferation. SMCs have multiple functions during AAA formation. However, the role of SMC Smad2 during AAA development remains unknown. By using SMC-specific Smad2 knockout mice and topical elastase AAA model, we found that Smad2 deficiency in SMC (Smad2sm-/-) caused a larger vessel dilation, higher AAA incidence, increased ECM degradation, and more loss of media SMCs as compared to the wild type control arteries. The more severe elastin degradation was also observed in AAA tissues of $APOE^{-/-}$ Smad2sm-/- mice treated with Angiotensin II (Ang II), another well-established AAA model. Moreover, matrix metalloproteinase MMP-2 and MMP-9 expression in aorta media was increased in Smad2sm-/- mice. Interestingly, there was a less fibroblast proliferation in the adventitia layer of the aneurysm tissues when Smad2 was deleted in SMC, leading to a smaller tissue mass surrounding the dilated arteries. Additional studies suggested that SMC-derived factor, but not the fibroblast-intrinsic factors, had caused the decreased fibroblast proliferation._RNA-seq analysis revealed that thrombosponding-1 (TSP1), a secreting protein, was increased in Smad2-/- SMC. Since TSP1 has been shown to promote MMPs level and inhibits FGF2 function, Smad2 may impede AAA formation by inhibiting TSP1 expression. Taken together, our results indicate that Smad2 protects mice from the aneurysm formation by modulating SMC function.

Keywords: Abdominal Aortic Aneurysm (AAA), SMAD Family Member 2 (Smad2), Fibroblasts Proliferation, MMP

Introduction

AAA is a localized dilatation of the abdominal aorta which is 1.5-fold larger than normal, for patients, the diameters are 3.0 cm or greater (1). Every year, 200,000 people in the U.S. are diagnosed with an abdominal aortic aneurysm (AAA). A ruptured AAA is the 15th leading cause of death in the US, and the 10th leading cause of death in men older than 55. AAA usually develops in the infra-renal segment characterized by increased inflammation, extracellular matrix (ECM) degradation includes elastin and collagen, and media SMC apoptosis (2). Currently, the therapy for AAA mainly relies on surgery such as endovascular stent graft repair according to the dilation size (3). For the patients with smaller AAA which doesn't reach the size of surgery requirement, β-blocker medication therapy is commonly used (4). Considering the side effect of β-blocker such as bradycardia (5), a better drug treatment is definitely in need. In order to develop the novel management procedures and therapeutic strategies, a better understanding of AAA formation mechanism is essential.

SMCs are the major cells in the aorta media layer, and are essential in maintaining aortic structure and functions through controlling cell proliferation and by secreting and maintaining a dynamic extracellular matrix (ECM). More importantly, SMC-derived factors can be involved in AAA formation. For example, *Patel et. al.* discovered that medial SMCs isolated from AAA tissue produce significantly higher levels of matrix metalloproteinases (MMPs) including MMP-2 and MMP-9 which may degrade the ECM such as elastin and collagen and lead to media SMCs loss and vessel wall dilation (6).

Smad2 (SMAD Family Member 2) is a signal transducer and transcriptional modulator in TGF-β signaling. In TGF-β signaling pathways, Smad signaling is the major pathway

controlling cell-fate determination, cell-cycle arrest and apoptosis. Large amount of studies have been focused on TGF-β, however, the view on that if TGF-β promotes or inhibits AAA formation is still contradictory (7,8). Another important TGF-β downstream transcriptional modulator, Smad3 deficiency has been demonstrated to increases wall thickening, inflammatory cell infiltration and result in AAA formation (9). However, as an essential TGF-β signaling transducer, it is still unknown whether Smad2 is involved in the development of AAA formation.

Because our previous study shows that Smad2 plays a critical role in SMC differentiation from neural crest cells and the blood vessel formation during embryonic development (10), in addition, SMCs have multiple functions during AAA development; we are interested in if SMC Smad2 participates in AAA formation.

Results

Smad2 deficiency in SMCs attenuated elastase-induced abdominal aortic aneurysm

To investigate the role of SMC Smad2 in AAA development, Wild type (Ctrl) and SMC-specific Smad2 knockout mice (SM22α-Cre;Smad2$^{fl/fl}$, Smad2sm-/-) were used in topical elastase induced AAA model. The abdominal aorta diameters were measured prior to elastase (PPE) or inactive PPE (IE) treatment and 7 days after PPE or IE treatment. After PPE treatment, both Ctrl and Smad2sm-/- mice showed an increased artery dilation with lumen sizes 1.5 times larger than the initial lumen. Importantly, the dilation of Smad2sm-/- arteries was statistically more than the Ctrl arteries (Fig 5.1, A-B). In addition, the AAA incidence of Smad2sm-/- mice was 30% higher than the Ctrl mice (Fig 5.1, C), indicating Smad2 deficiency in SMCs promoted AAA development. Interestingly,

Smad2 expression was not decreased, rather elevated by approximately 12- and 1.8-fold in human and mouse AAA tissues, respectively (Fig 5.1 D-F), indicating that a protective response was activated in the AAA tissues. The increased expression of Smad2 is mainly found in medial SMC layer adjacent to the adventitia layer suggest that SMC Smad2 may influence the activity of adventitia.

Smad2 deletion increased extracellular matrix degradation and loss of medial SMCs in topical elastase AAA model.

AAA is characterized with increased elastin and collagen degradation as well as medial SMC loss. To detect if Smad2 deficiency in SMC causes structural defects in arteries, Masson's staining was used for detecting collagen deposition (Fig 5.2, A); VG staining was performed to detect elastin fragmentation (Fig 5.2, C); and IHC staining of SMC marker SMMHC was used for observe SMC content (Fig 5.2, E). As shown in Fig 5.2, B, D, and F, abdominal aorta from Smad2sm-/- mice exhibited an increased collagen deposition and elastin degradation as well as more SMC loss after 7 day of the PPE treatment as compare with the WT Ctrl group. These results were in agreement with our findings that Smad2 deletion in SMC promotes larger vessel dilation and higher AAA incidence.

Smad2 deficiency in SMC caused more elastin degradation in Ang II-induced AAA.

To validate the finding in topical elastase model, we used Ang II-induced AAA model to observe the elastin degradation. In order to observe the elastin fragmentation in early stage of AAA, Ctrl ($APOE^{-/-}$;SM22α-Cre) and $APOE^{-/-}$;Smad2sm-/- ($APOE^{-/-}$;SM22α-

Cre;Smad2 $^{fl/fl}$) mice were treated by Ang II for one week using osmotic minipump. At this early stage, elastin degradation was not obvious in abdominal aorta of Ctrl mice. However, Smad2 deficiency in SMC caused elastin breakage (Figure 5.3 A-B). These results confirmed that Smad2 deficiency in SMC indeed causes elastin degradation in artery media.

Smad2 deficiency in SMC elevated MMP2 and MMP9 level in artery media

MMPs are proteinases responsible for degrading elastin and collagen network of the aorta. Previous studies have demonstrated that MMP9, one of the prominently expressed MMPs in aortic aneurysms, works in concert with MMP2 to promote aneurysm progression (22). To determine whether MMPs contribute to the more severe defects in artery wall in Smad2sm-/-mice, we detected MMP2 and MM9 expression by IHC using antibodies against MMP-2 and MMP-9, respectively. Smad2 deletion in SMC increased the expression of both MMP-2 and MMP-9 (Figure 5.4, A-B). These results indicate that Smad2 deficiency in SMC promoted MMP-2/9 levels, which in turn caused more degradation of elastin lamina.

Smad2 deficiency in SMC increased cell proliferation in adventitial layer.

To detect the vessel wall remodeling in elastase-induced AAA, H&E staining was performed in abdominal aorta from Ctrl (SM22α-Cre) and (SM22α-Cre;Smad2$^{fl/fl}$) mice after 7 day of PPE treatment. Aorta from Smad2sm-/- mice exhibited a thinner but more defects in vessel wall compared with the WT Ctrl vessel (Fig 5.5A). More importantly, the adventitia layer was significantly thinner in Smad2sm-/- mice based on the analysis of

adventitia area (Fig 5.5 B). In addition to SMCs, SM22α is also expressed in the adventitia in balloon injured vessel, suggesting the existence of a stem cell-like reservoir in the adventitia (23). To determine whether or not the increased adventitia in Smad2sm-/- aorta was caused by Smad2 deficiency in adventitia cells due to the adventitia SM22α expression, we generated Myh-Cre;Smad2$^{fl/fl}$ mice. Since Myosin Heavy Chain 11 (Myh) also known as SMMHC only expresses in SMCs (24). Myh-Cre mice crossbred with Smad2 $^{fl/fl}$ mouse will delete Smad2 only in SMCs. After 7 days of PPE treatment, we found that Myh-Cre;Smad2$^{fl/fl}$ mouse abdominal aorta also exhibited an decreased adventitial mass compared with the WT Ctrl mice (Fig 5.5 C-D), indicating Smad2 deficiency in SMCs, but not in adventitial cells, caused the less adventitial growth. Since fibroblasts are the major cell population in adventitia, we further detected the effect of Smad2 on fibroblast proliferation. Thus, fibroblast proliferation was measured in both Scramble (Ctrl) or Smad2 shRNA adenoviral vector transduced 10T1/2 cells. As shown in Fig 5.5 E, Smad2 knockdown didn't affect the proliferation of fibroblasts because the fibroblasts proliferated at the same rates with or without Smad2 deficiency. These results led us to hypothesize that medial SMC-derived factors affect the fibroblast proliferation in adventitia. To test this, conditioned medium from primary cultured SMCs isolated from Ctrl (SM22α-Cre) and Smad2sm-/- (SM22α-Cre;Smad2$^{fl/fl}$) mouse abdominal aorta was used to culture fibroblasts. Interestingly, we found that Smad2sm-/-conditioned SMC medium inhibited the fibroblast proliferation (Fig 5.5, F). Taken together, our data suggest that the thinner adventitia in Smad2sm-/- aneurysm tissues was due to the inhibitory effect of factors secreted from medial SMCs.

Thrombospondin-1 (TSP1) may be involved in Smad2 deficiency-caused AAA.

To screen the potential SMC-derived factors that induced the fibroblast proliferation, mRNA profiles of abdominal aortic SMCs isolated from SM22α-Cre (Ctrl) vs SM22α-Cre;Smad2$^{fl/fl}$ and Myh-Cre vs Myh-Cre;Smad2$^{+/+}$ mice were analyzed by RNAseq. Among the genes altered due to Smad2 deficiency, TSP1 was up-regulated in both Smad2sm-/- mice. TSP1 is an extracellular protein that integrates into the structural extracellular matrix (25). Previous study has shown that TSP1 induces vascular inflammation during AAA development. In addition, TSP1 up-regulates MMP2 and MMP9 levels (26,27). Based on these functional properties, we hypothesized that TSP1 might be a key SMC-secreted factor that regulated fibroblast proliferation in adventitia of AAA tissues. Thus, we detected TSP1 expression in AAA by immunofluorescent taining. As shown in Fig 5.6, A-B, TSP1 was expressed in WT Ctrl AAA tissue. However, Smad2sm-/- caused a much higher TSP1 expression in abdominal aortic aneurysm tissues. These results confirmed the RNA-seq data that TSP1 was increased in Smad2-deficient SMC. Moreover, the increased TSP1 expression correlated with the increased MMP-2/9 levels in the medial SMCs.

Discussion

Despite decades of intensive studies in TGF-β pathway, there are paradoxical discoveries on the role of TGF-β signaling in the development of aneurysm. As an important TGF-β signaling transducer, the role of Smad2 is also unclear. Our study explored, for the first time, the role of Smad2 in aneurysm pathophysiology using two murine AAA models. Dai *et. al.* has found that Smad3 expression is decreased in both human and mouse AAA

and Smad2 level is increased when Smad3 is knocked down in mouse $CaCl_2$ AAA model. In addition, Smad3 disruption promotes AAA formation (9). In the present study, we observed an increased smad2 expression in both human and mouse AAA sample (Fig 5.1 D-F) particularly in the media SMCs adjacent to the adventitia layer. This might be a protective response compensatory for the loss of Smad3. However, Smad2 deletion in SMC disrupted this compensatory mechanism and caused more severe AAA formation. Histological and morphological observation of abdominal artery from Smad2sm-/- mice exhibited an increased artery dilation, higher incidence of AAA induced by elastase, and more collagen and elastin degradation and loss of medial SMCs.

In addition, the increased MMP-2 and MMP-9 expression was observed in medial layer when Smad2 was deleted in SMC. Since MMP-2/9 function as proteinases degrading EMC, the elevated MMP2/9 level was responsible for the increased elastin fragmentation as well as collagen degradation in Smad2sm-/- mice, which was confirmed by using the AngII-induced AAA model.

By using two different Smad2sm-/- models (SM22α-Cre;$Smad2^{fl/fl}$ and Myh-Cre;$Smad2^{fl/fl}$), we proved that the Smad2 deficiency-caused fibroblast proliferation was because of Smad2 function in SMCs, but not in fibroblasts. Unbiased RNAseq analyses suggest TSP1 as the most promising factors mediating the SMC function in regulating adventitia proliferation. TSP1 is known to be produced by SMC and secreted out of the cells (28). Importantly, TSP1 participates in MMP2/9 induction (26,29), which is consistent with our observation that increased TSP1 in Smad2-/- SMC promoted MMP2/9 levels and caused ECM degradation. In addition, TSP1 appeared to inhibit fibroblast proliferation by blocking FGF2 activity. TSP1 has been shown to inhibit

fibroblast growth factor (FGF) function (30), while FGF has been reported to promote adventitial cell proliferation and fibroblast differentiation to myofibroblasts (31). Consistent with the RNA-seq data, TSP1 expression was increased in AAA tissues when Smad2 was deleted in SMC. Future studies are required to prove that TSP1 is the essential secreted factor responsible for the less adventitia mass.

Since there is currently no effective drug to treat AAA, understanding the mechanism of AAA development and progression is essential for therapeutic invention. Smad2 deficiency promoted AAA formation likely due to the increased TSP-1 levels because increased TSP1 might be responsible for both the increased MM-2/9 level and thinner vessel wall. Therefore, enhancing Smad2 expression might be a promising therapeutic strategy for treating AAA.

Method

Cell Culture

SMCs were cultured by enzyme digestion method from mouse abdominal aorta as described previously (11-13). The primary cultured SMCs were confirmed by the expression of smooth muscle α-SMA and SM22α. SMCs were cultured in Dulbecco's modified Eagle's medium (DMEM) containing 10% fetal bovine serum (FBS) and 5% L-glutamine. SMCs less than 6 passages with 70-80% of confluence were used in the experiments. A total of 10^6 mouse primary cultured cells were plated in a 10-cm dish and incubated overnight. Remove the culture medium and wash the attached cells gently with PBS for 3 times. Add 10 ml DMEM starving medium (without FBS) to incubate the cells for 24 hours. The supernatant was transferred to a 15-ml centrifuge tube and centrifuged

at 1,000 × g for 15 min to remove particles. This conditioned medium was then diluted with starving medium at 1:1 ratio.

Proliferation Assay

Cells were incubated with a modified thymidine analog, EdU (Millipore, EdU-647), throughout the treatment period. EdU incorporation and detection were performed as described by the manufacturer's protocol.

Animal Procedures

Smad2-floxed ($Smad2^{fl/fl}$) and SM22α-Cre mice were previously described (10,14,15). To generate Smad2 deletion in SMCs, SM22α-Cre male mice were crossbred with $Smad2^{fl/fl}$ mice to produce SM22α-Cre;$Smad2^{fl/fl}$ mice. SM22α-Cre;$Smad2^{+/+}$ littermates serve as controls. SM22α-Cre;$Smad2^{fl/fl}$ mice were crossed with ApoE-deficient mice, to produce $ApoE^{-/-}$ SM22α-Cre;$Smad2^{fl/fl}$ and $ApoE^{-/-}$ SM22α-Cre;$Smad2^{+/+}$ littermates that were used as controls for studies. Myh-CreERT mice was from the Jackson laboratory (Bar Harbor, ME, USA) and crossbred with $Smad2^{fl/fl}$ mice to produce Myh-CreERT;$Smad2^{fl/fl}$ mice. The Myh-CreERT;$Smad2^{fl/fl}$ mice were administered with Tamoxifen (Sigma–Aldrich, T5648) at 8-weeks-old for 5 times consecutively to induce Smad2 SMC deletion. Myh-CreERT;$Smad2^{fl/fl}$ injected with corn oil (Sigma–Aldrich, 47112-U) serve as control. All animal protocols were approved by the Institutional Animal Care Use Committee of University of Gerogia.

The mouse model of elastase-induced aortic aneurysm.

The mouse model of elastase-induced AAA has been previously described (16). After anesthesia, a laparotomy was performed, and the abdominal aorta was isolated in situ. Then the infrarenal aorta (from just below the left renal vein to the iliac bifurcation) was

bathed in either 10 μL of 100% elastase (Sigma–Aldrich) or heat-inactivated elastase (control) for 10 min. After elastase exposure, the wound was closed with 6–0 prolene. The maximal aortic diameters were measured in situ before elastase application and at harvest. The standard of AAA was defined as a 100% increase in maximal aortic diameter compared to baseline diameter before elastase treatment [20]. The abdominal aortas were harvested at 7 or 14 days after elastase treatment (n = 20 per treatment group per day) for analysis by histology, immunohistochemistry, and quantitative RT-PCR.

The mouse model of Angiotensin II–induced aortic aneurysm

The mouse model of Ang II–induced aneurysm formation has been previously described (17). Ang II was infused via subcutaneous osmotic pumps at 1,000 ng/kg/min for a maximum of 28 days.

Construction of Adenovirus

Adenoviral vectors expressing scramble or Smad2 short hairpin RNA (shRNA) (shSmad2) were constructed, and the viruses were purified as described previously (10,18,19).

Histology, Immunohistochemistry and Immunofuorescent staining

Mouse abdominal aortas were fixed with 4% paraformaldehyde and paraffin-embedded for 5 μm thick cross section. The sections were stained with hematoxylin and eosin staining (H&E staining) for structural observation, Van Gieson for elastin and Massons trichrome for Collagen and captured using a Nikon microscope. For immunohistochemistry, sections were rehydrated, permeabilized with 0.01% Triton X-100 in phosphate-buffered saline, blocked with 5% goat serum, and incubated with rabbit anti-pSmad2 (Cell Signaling Technology, 3108), SMMHC, MMP2 (Abcam, ab37150), MMP9 (Proteintech, 10375-2-AP) antibody overnight at 4℃, followed by incubation

with horseradish peroxidase (HRP)–conjugated secondary antibody. The staining was visualized using Vectastain ABC-AP kit by following the manufacturer's protocol (Vector Laboratories). The vessel sections were counterstained with hematoxylin. For fluorescent staining, sections were firstly rehydrated. After 3 times washing with phosphate-buffered saline, the section is permeabilized with 0.01% triton X-100 in phosphate-buffered saline for 10 minutes, blocked with 5% goat serum for 30 minutes, and incubated with mouse anti-TSP1, mouse anti-TSP1 antibody (ThermoFisher, MA5-13377) overnight at 4℃, followed by incubation with FITC-conjugated secondary antibodies. Cell nuclei were stained with DAPI (Molecular Probe). Stained tissue sections were imaged using a Nikon 12.7MP digital Sight DS-Ri1 color camera as previously described (19-21).

Statistical Analysis

All values are expressed as mean ± S.E. Data were evaluated with a 2-tailed, unpaired Student t test or compared by one-way ANOVA followed by Fisher t test. A p value <0.05 was considered statistically significant.

Reference

1. Legg, J. S., and Legg, L. M. (2016) Abdominal Aortic Aneurysms. *Radiol Technol* **88**, 145-163
2. Lopez-Candales, A., Holmes, D. R., Liao, S., Scott, M. J., Wickline, S. A., and Thompson, R. W. (1997) Decreased vascular smooth muscle cell density in medial degeneration of human abdominal aortic aneurysms. *Am J Pathol* **150**, 993-1007

3. Aggarwal, S., Qamar, A., Sharma, V., and Sharma, A. (2011) Abdominal aortic aneurysm: A comprehensive review. *Exp Clin Cardiol* **16**, 11-15

4. Gadowski, G. R., Pilcher, D. B., and Ricci, M. A. (1994) Abdominal aortic aneurysm expansion rate: effect of size and beta-adrenergic blockade. *J Vasc Surg* **19**, 727-731

5. Ishikura, F., Takano, Y., and Ueyama, T. (2012) Acute effects of beta-blocker with intrinsic sympathomimetic activity on stress-induced cardiac dysfunction in rats. *J Cardiol* **60**, 470-474

6. Patel, M. I., Melrose, J., Ghosh, P., and Appleberg, M. (1996) Increased synthesis of matrix metalloproteinases by aortic smooth muscle cells is implicated in the etiopathogenesis of abdominal aortic aneurysms. *J Vasc Surg* **24**, 82-92

7. Gao, F., Chambon, P., Offermanns, S., Tellides, G., Kong, W., Zhang, X., and Li, W. (2014) Disruption of TGF-beta signaling in smooth muscle cell prevents elastase-induced abdominal aortic aneurysm. *Biochem Biophys Res Commun* **454**, 137-143

8. Wang, Y., Ait-Oufella, H., Herbin, O., Bonnin, P., Ramkhelawon, B., Taleb, S., Huang, J., Offenstadt, G., Combadiere, C., Renia, L., Johnson, J. L., Tharaux, P. L., Tedgui, A., and Mallat, Z. (2010) TGF-beta activity protects against inflammatory aortic aneurysm progression and complications in angiotensin II-infused mice. *J Clin Invest* **120**, 422-432

9. Dai, X., Shen, J., Annam, N. P., Jiang, H., Levi, E., Schworer, C. M., Tromp, G., Arora, A., Higgins, M., Wang, X. F., Yang, M., Li, H. J., Zhang, K., Kuivaniemi, H., and Li, L. (2015) SMAD3 deficiency promotes vessel wall remodeling,

collagen fiber reorganization and leukocyte infiltration in an inflammatory abdominal aortic aneurysm mouse model. *Sci Rep* **5**, 10180

10. Xie, W. B., Li, Z., Shi, N., Guo, X., Tang, J., Ju, W., Han, J., Liu, T., Bottinger, E. P., Chai, Y., Jose, P. A., and Chen, S. Y. (2013) Smad2 and myocardin-related transcription factor B cooperatively regulate vascular smooth muscle differentiation from neural crest cells. *Circulation research* **113**, e76-86
11. Guo, X., Shi, N., Cui, X. B., Wang, J. N., Fukui, Y., and Chen, S. Y. (2015) Dedicator of cytokinesis 2, a novel regulator for smooth muscle phenotypic modulation and vascular remodeling. *Circulation research* **116**, e71-80
12. Golovina, V. A., and Blaustein, M. P. (2006) Preparation of primary cultured mesenteric artery smooth muscle cells for fluorescent imaging and physiological studies. *Nature protocols* **1**, 2681-2687
13. Rong, J. X., Shapiro, M., Trogan, E., and Fisher, E. A. (2003) Transdifferentiation of mouse aortic smooth muscle cells to a macrophage-like state after cholesterol loading. *Proc Natl Acad Sci U S A* **100**, 13531-13536
14. Ju, W., Ogawa, A., Heyer, J., Nierhof, D., Yu, L., Kucherlapati, R., Shafritz, D. A., and Bottinger, E. P. (2006) Deletion of Smad2 in mouse liver reveals novel functions in hepatocyte growth and differentiation. *Molecular and cellular biology* **26**, 654-667
15. Holtwick, R., Gotthardt, M., Skryabin, B., Steinmetz, M., Potthast, R., Zetsche, B., Hammer, R. E., Herz, J., and Kuhn, M. (2002) Smooth muscle-selective deletion of guanylyl cyclase-A prevents the acute but not chronic effects of ANP on blood pressure. *Proceedings of the National Academy of Sciences of the United States of*

America **99**, 7142-7147

16. Bhamidipati, C. M., Mehta, G. S., Lu, G., Moehle, C. W., Barbery, C., DiMusto, P. D., Laser, A., Kron, I. L., Upchurch, G. R., Jr., and Ailawadi, G. (2012) Development of a novel murine model of aortic aneurysms using peri-adventitial elastase. *Surgery* **152**, 238-246
17. Cao, R. Y., Adams, M. A., Habenicht, A. J., and Funk, C. D. (2007) Angiotensin II-induced abdominal aortic aneurysm occurs independently of the 5-lipoxygenase pathway in apolipoprotein E-deficient mice. *Prostaglandins Other Lipid Mediat* **84**, 34-42
18. Wang, J. N., Shi, N., Xie, W. B., Guo, X., and Chen, S. Y. (2011) Response gene to complement 32 promotes vascular lesion formation through stimulation of smooth muscle cell proliferation and migration. *Arteriosclerosis, thrombosis, and vascular biology* **31**, e19-26
19. Shi, N., Xie, W. B., and Chen, S. Y. (2012) Cell division cycle 7 is a novel regulator of transforming growth factor-beta-induced smooth muscle cell differentiation. *The Journal of biological chemistry* **287**, 6860-6867
20. Shi, N., Guo, X., and Chen, S. Y. (2014) Olfactomedin 2, a novel regulator for transforming growth factor-beta-induced smooth muscle differentiation of human embryonic stem cell-derived mesenchymal cells. *Mol Biol Cell* **25**, 4106-4114
21. Qiu, Y., Yang, J., Wang, W., Zhao, W., Peng, F., Xiang, Y., Chen, G., Chen, T., Chai, C., Zheng, S., Watkins, D. J., and Feng, J. (2014) HMGB1-promoted and TLR2/4-dependent NK cell maturation and activation take part in rotavirus-induced murine biliary atresia. *PLoS pathogens* **10**, e1004011

22. Longo, G. M., Xiong, W., Greiner, T. C., Zhao, Y., Fiotti, N., and Baxter, B. T. (2002) Matrix metalloproteinases 2 and 9 work in concert to produce aortic aneurysms. *J Clin Invest* **110**, 625-632

23. Faggin, E., Puato, M., Zardo, L., Franch, R., Millino, C., Sarinella, F., Pauletto, P., Sartore, S., and Chiavegato, A. (1999) Smooth muscle-specific SM22 protein is expressed in the adventitial cells of balloon-injured rabbit carotid artery. *Arterioscler Thromb Vasc Biol* **19**, 1393-1404

24. Owens, G. K., Kumar, M. S., and Wamhoff, B. R. (2004) Molecular regulation of vascular smooth muscle cell differentiation in development and disease. *Physiol Rev* **84**, 767-801

25. Liu, Z., Morgan, S., Ren, J., Wang, Q., Annis, D. S., Mosher, D. F., Zhang, J., Sorenson, C. M., Sheibani, N., and Liu, B. (2015) Thrombospondin-1 (TSP1) contributes to the development of vascular inflammation by regulating monocytic cell motility in mouse models of abdominal aortic aneurysm. *Circ Res* **117**, 129-141

26. Albo, D., Shinohara, T., and Tuszynski, G. P. (2002) Up-regulation of matrix metalloproteinase 9 by thrombospondin 1 in gastric cancer. *J Surg Res* **108**, 51-60

27. Bornstein, P., Agah, A., and Kyriakides, T. R. (2004) The role of thrombospondins 1 and 2 in the regulation of cell-matrix interactions, collagen fibril formation, and the response to injury. *Int J Biochem Cell Biol* **36**, 1115-1125

28. Ichii, T., Koyama, H., Tanaka, S., Shioi, A., Okuno, Y., Otani, S., and Nishizawa, Y. (2002) Thrombospondin-1 mediates smooth muscle cell proliferation induced by interaction with human platelets. *Arterioscler Thromb Vasc Biol* **22**, 1286-1292

29. Lee, T., Esemuede, N., Sumpio, B. E., and Gahtan, V. (2003) Thrombospondin-1 induces matrix metalloproteinase-2 activation in vascular smooth muscle cells. *J Vasc Surg* **38**, 147-154

30. Taraboletti, G., Belotti, D., Borsotti, P., Vergani, V., Rusnati, M., Presta, M., and Giavazzi, R. (1997) The 140-kilodalton antiangiogenic fragment of thrombospondin-1 binds to basic fibroblast growth factor. *Cell Growth Differ* **8**, 471-479

31. Zhang, L., Chen, Y., Li, G., Chen, M., Huang, W., Liu, Y., and Li, Y. (2016) TGF-beta1/FGF-2 signaling mediates the 15-HETE-induced differentiation of adventitial fibroblasts into myofibroblasts. *Lipids Health Dis* **15**, 2

Figure legends

Figure 5.1. Deletion of Smad2 in smooth muscle cell promoted elastase-induced AAA formation. (A) Representative images of SM22α-Cre (Ctrl) and SM22α-Cre;Smad2$^{fl/fl}$ (Smad2sm-/-) arteries with 7 days of treatment with inactive elastase (IE) or elastase (PPE). **(B)** Maximal aortic diameter was shown for Ctrl and Smad2sm-/- arteries 7 days after the treatments. *P < 0.05 compared with the Ctrl with IE group, n=5. $^{\#}$P < 0.05 compared with the Smad2sm$^{-/-}$ with IE treatment group, n=5. $^{\$}$P < 0.05 compared with the Ctrl and Smad2sm-/- with PPE-7 days-treatment group, n=5. **(C)** Percentage of AAA incidence of Ctrl and Smad2sm-/- at day 7 after elastase treatment. *P < 0.05 compared with the Ctrl with elastase treatment group, n=5. **(D)** Smad2 IHC staining of human abdominal aorta from normal and AAA patient, and WT mouse

abdominal aorta treated with inactive elastase (normal) or PPE (AAA) (200×). Scale: 50 μm. **(E)** Quantification of Smad2 in human normal and AAA samples. *P < 0.05 compared with the normal group (200×), n=5. Scale: 50 μm. **(F)** Quantification of Smad2 in mouse normal and AAA samples. *P < 0.05 compared with the normal group, n=5.

Figure5.2. Smad2 deficiency in SMC increased medial extracellular matrix degradation and the loss of SMC in artery media of elastase-induced AAA. Representative images of abdominal aortic segments of SM22α-Cre (Ctrl) and SM22α-Cre;Smad2$^{fl/fl}$ (Smad2sm-/-) mice treated with elastase or inactivated elastase (IE) for 7 days. (A) Collagen content was determined by Masson's Trichrome staining (100×). Scale: 200 μm. (B) Quantitative analysis of collagen content. *P < 0.05 compared with the Ctrl with elastase treatment group, n=5. (C) Van Gieson's staining for elastin (200×). Scale: 50 μm. (D) Semiquantitative analysis of elastin fragmentation grade. *P < 0.05 compared with the Ctrl with elastase treatment group, n=5. (E) SMMHC staining for SMCs. Brown staining showed SMMHC expression, and sections are counterstained with hematoxylin (blue) (200×). Scale: 50 μm. (F) SMC content was calculated as the percentage of the SMMH-positive cell relative to total cells. *P < 0.05 compared with the Ctrl with elastase treatment group, n=5.

Figure 5.3. Deletion of Smad2 in SMCs promoted elastin degradation in Ang II-induced AAA. Ang II was infused via subcutaneous osmotic pumps in APOE$^{-/-}$ SM22α-Cre (Ctrl) and APOE$^{-/-}$ SM22α-Cre;Smad2 $^{fl/fl}$ (APOE$^{-/-}$;Smad2sm-/-) mice for 1 week. (A) Van Gieson's staining for elastin (200×). Scale: 50 μm. (B) Semiquantitative

analysis of elastin fragmentation grade. *P < 0.05 compared with the Ctrl with Ang II treatment group, n=5.

Figure 5.4. SM-specific deletion of Smad2 elevated MMP2 and MMP9 levels. Representative images of abdominal aortic segments of SM22α-Cre (Ctrl) and SM22α-Cre;Smad2$^{fl/fl}$ (Smad2sm-/-) mice treated with elastase for 7 days. (A) MMP2 and MMP9 IHC staining of Ctrl and Smad2sm-/- (200×). Scale: 50 μm. (B) Quantification of MMP2 and MMP9 levels. *P < 0.05 compared with the Ctrl mice with elastase treatment group, n=5.

Figure 5.5. Smad2 deficiency in SMC caused increased adventitial fibroblast proliferation. (A-B) Representative images of abdominal aortic segments of SM22α-Cre (Ctrl) and SM22α-Cre;Smad2$^{fl/fl}$ (Smad2sm-/-) mice treated with elastase for 7 days. The cross section was stained with H&E (100×). Scale: 200 μm. The total adventitia area was measured by image J software. *P < 0.05 compared with the Ctrl mice with elastase treatment, n=5. (C-D) Representative images of abdominal aortic segments from tamoxifen pre-treated Myh-CreERT (Ctrl) and Myh-CreERT;Smad2$^{fl/fl}$ (Smad2 sm-/-) mice with 7 days of elastase treatment. The cross section was stained with H&E. The relative adventitia area was measured as the ratio of total adventitia area (100×). Scale: 200 μm. *P < 0.05 compared with the Ctrl mice with elastase treatment, n=5. **(E)** 10T1/2 cells transduced with Ad-scramble (Ctrl) or Ad-shSmad2 (shSmad2) adenovirus for 2 days and split into 60 mm dish with a density of 5×10^4 cell/ml medium. GFP and EdU-positive cells were accounted and quantified to the total cell numbers of each microscopic

field (10x) from 10 different microscopic fields. N.S. > 0.05 compared with the Ctrl group, n=3. **(F)** Conditioned medium of primary cultured SMCs of SM22α-Cre (Ctrl) and SM22α-Cre;Smad2$^{fl/fl}$ (Smad2sm-/-) mice was diluted with starving medium (DMEM without serum) at 1:1. 10T1/2 cells were seeded at a density of 5×10^4 cell/ml in Ctrl or Smad2sm-/- diluted conditioned medium followed by culture for – days. EdU-positive cells were accounted and quantified to the total cell numbers of each microscopic field (10x) from 10 different microscopic fields. *P < 0.05 compared with the Ctrl group, n=3.

Figure 5.6. Smad2 deletion in SMC exaggerated Thrombospondin-1 expression in elastase-induced AAA tissues. Representative images of abdominal aortic segments from SM22α-Cre (Ctrl) and SM22α-Cre;Smad2$^{fl/fl}$ (Smad2sm-/-) mice treated with elastase (PPE) or inactivated elastase (IE) for 7 days. (A) Immunofluorescence staining of TSP1 (200×). Scale: 50 μm. (B) Quantification of TSP1 by measuring positive staining area to the total media area. *P < 0.05 compared with the Ctrl with IE group, n=5. $^{\#}$P < 0.05 compared with the Smad2sm$^{-/-}$ artery with IE treatment, n=5. $^{\$}$P < 0.05 compared with the Ctrl and Smad2sm-/- artery with PPE treatment for 7 days, n=5.

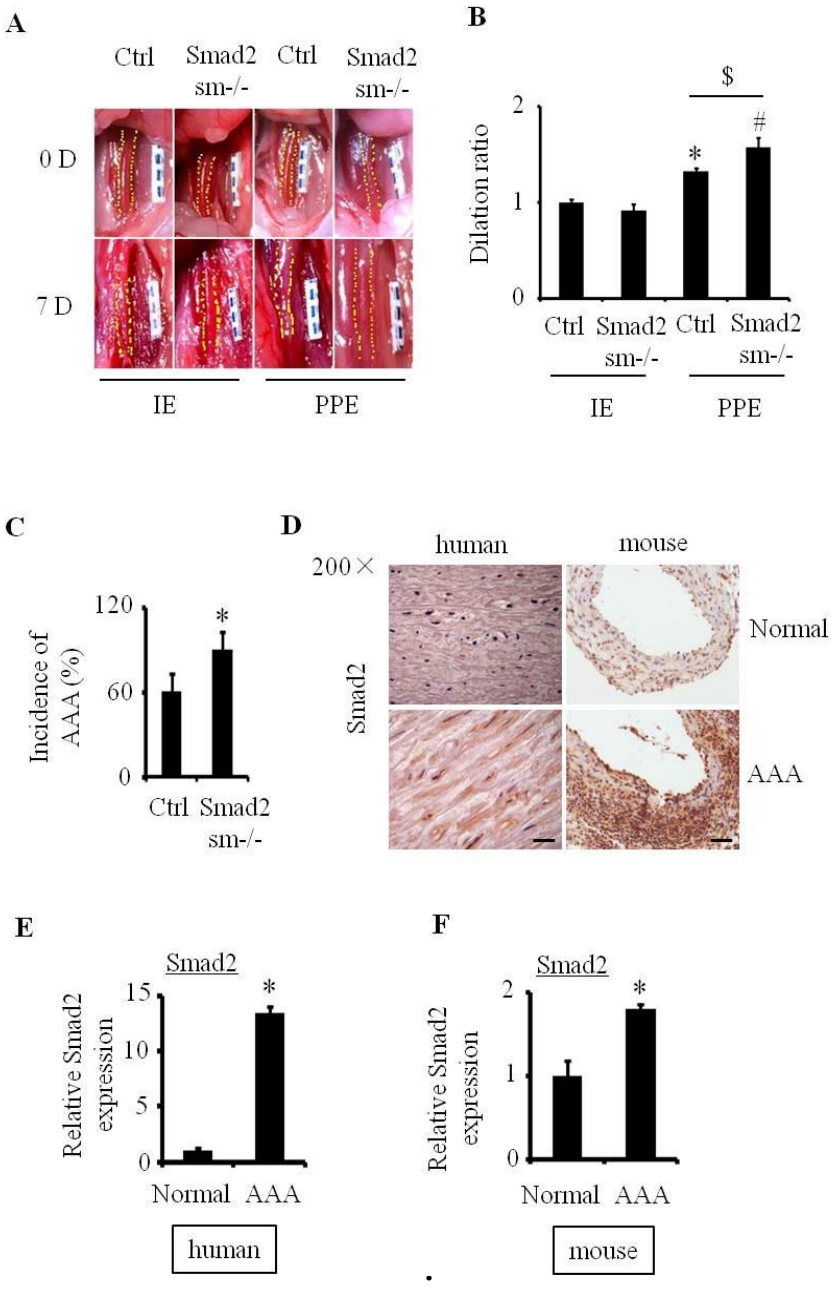

Figure 5.1. Smad2 deficiency in SMCs promoted elastase-induced AAA formation

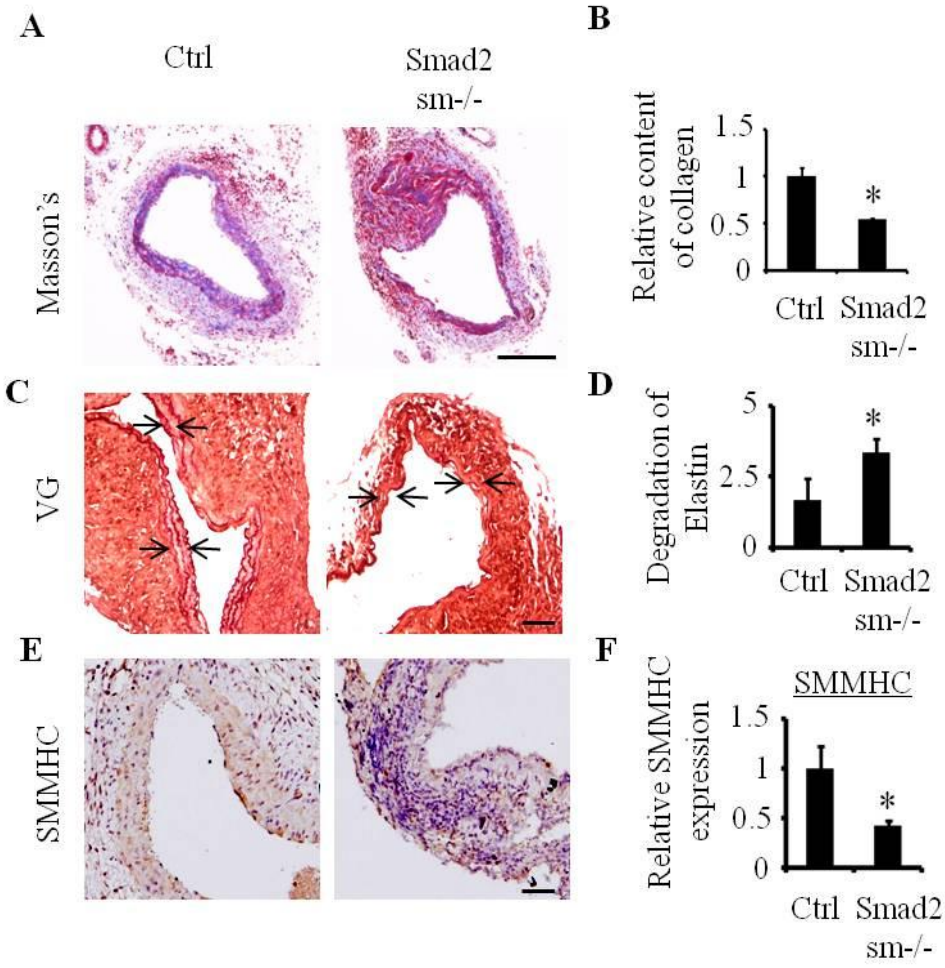

Figure 5.2. Smad2 deficiency in SMC increased medial extracellular matrix degradation and SMC loss in elastase-induced AAA tissues.

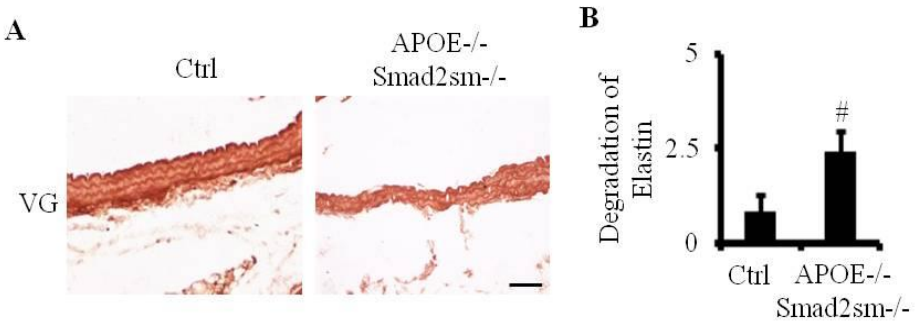

Figure 5.3. Smad2 deficiency in SMCS promoted elastin degradation in Ang II-induced AAA.

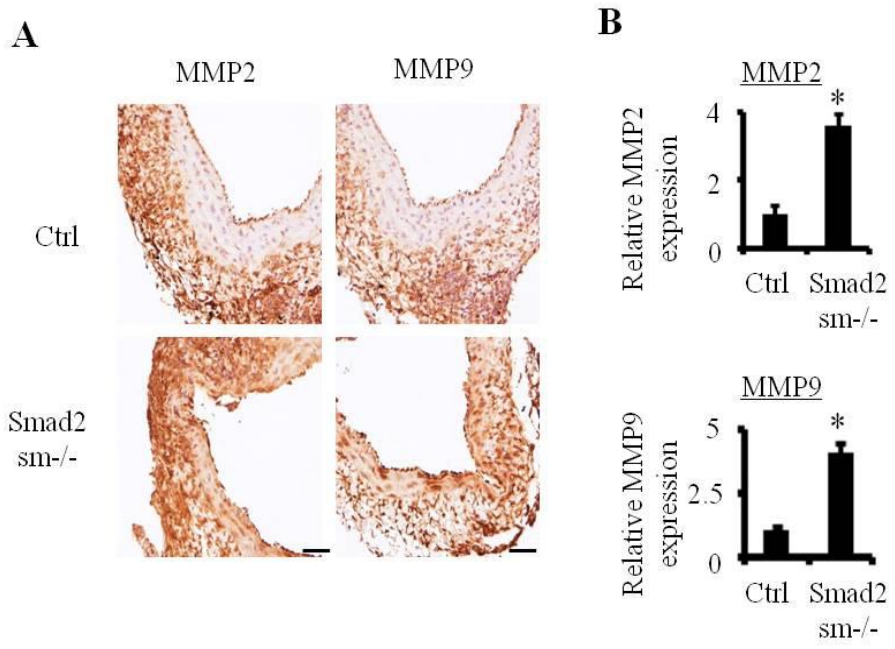

Figure 5.4. SM-specific deletion of Smad2 elevated MMP2 and MMP9 expression in AAA tissues.

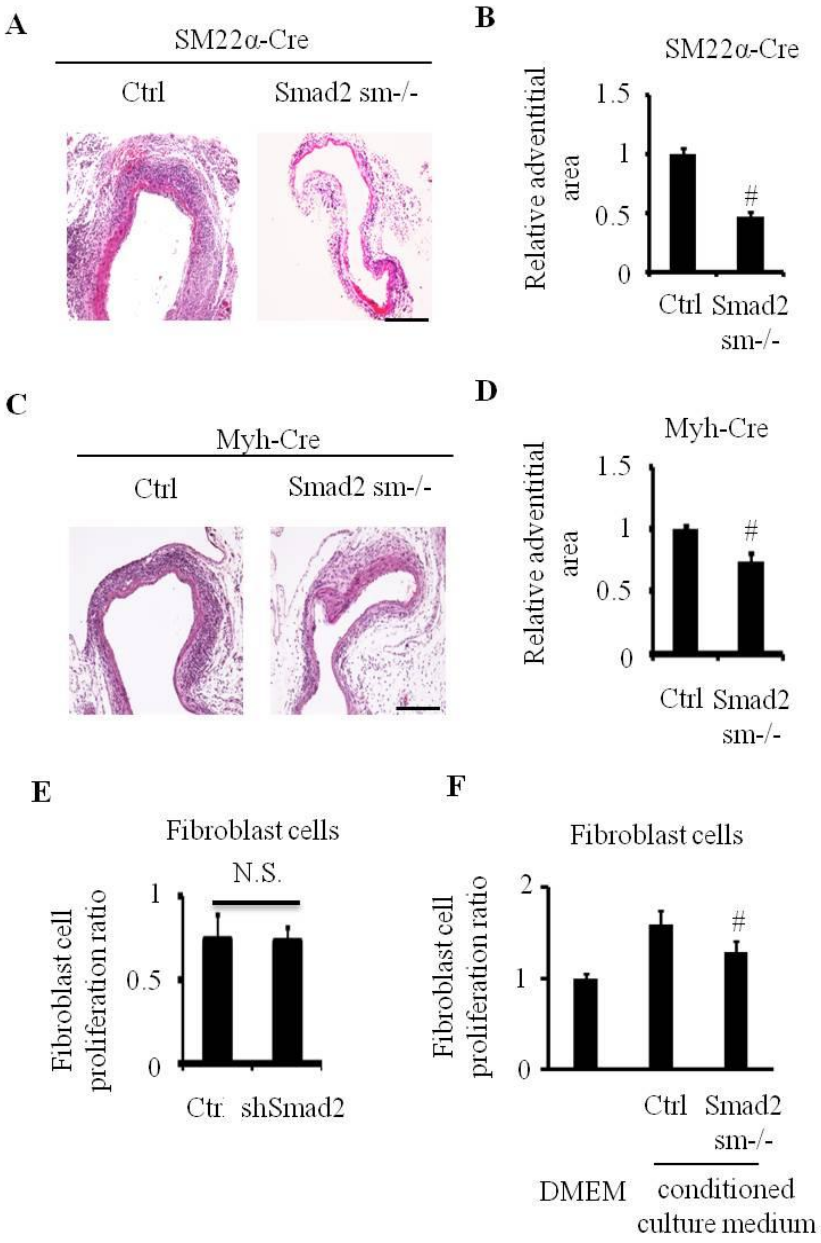

Figure 5.5. Smad2 deficiency in SMC increased adventitial mass and fibroblast proliferation.

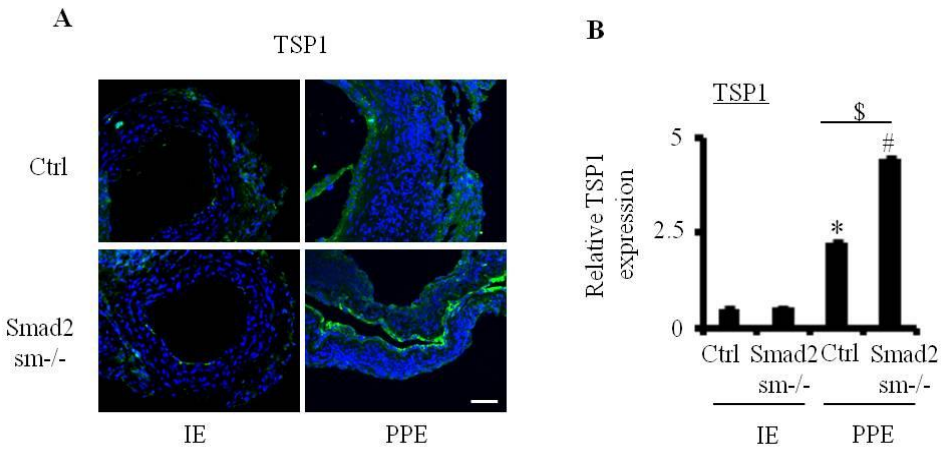

Figure 5.6. Smad2 deletion in SMC exaggerated Thrombospondin-1 expression in elastase-induced AAA.

Chapter 6

CONCLUSION

This dissertation work was dedicated to develop novel mechanisms underlying smooth muscle differentiation and vascular diseases including atherosclerosis and abdominal aortic aneurysm. We majorly focused on molecular mechanisms that regulated TGF-β induced SMC differentiation (Chapter 3), atherosclerosis development (Chapter 4) and abdominal aortic aneurysm (Chapter 5).

In Chapter 3, we hypothesized that Meox1 is a potential regulator in TGF-β induced SMC differentiation because of its highly up-regulated expression from our microarray analysis. In function study, we found that knockdown of Meox1 caused down-regulation of SMC marker genes in both TGF-β induced SMC differentiation in vitro and neonatal mice that were injected with shMeox1 adenovirus on E12.5. Additionally, overexpression of Meox1 induced SMC marker gene expression in pluripotent 10T1/2 cells. These findings confirmed our hypothesis and demonstrated that Meox1 is sufficient and necessary in regulating TGF-β induced SMC differentiation. To further investigate the mechanism how Meox1 regulates SMC differentiation, we found Meox1 deficiency increased PPM1A expression which functions as a phosphatase to dephosphorylate p-Smad3 level, indicating that Meox1 helped retain p-Smad3 level to allow Smad3 to precisely regulate SMC marker gene transcription.

Based on our current findings in Chapter 3, there are still some questions need to be answered. First, how does Meox1 regulate PPM1A degradation? Meox1 may be involved in PPM1A ubiquitination. Previous study has shown the presence of nuclear ubiquitin-proteasome system (1). Since Meox1 is a nuclear protein, Meox1 may impact PPM1A degradation through nuclear ubiquitin-proteasome system. Second, does Meox1 affect PPM1A transcription? Figure 3.7 C showed that knockdown of Meox1 increased PPM1A expression even without TGF-β treatment. Because 10T1/2 cells were transfected with shMeox1 adenoviral vectors for 2 days before TGF-β stimulation, this time is long enough for Meox1 to regulate PPM1A transcription and thus impact the protein expression. Further study may be needed to detect if PPM1A transcription is regulated by Meox1.

In chapter 4, we found Smad2 deficiency in SMC promotes atherosclerosis development and decreases plaque stability. The decreased plaque stability is due to the increased MMP2/9 activity. Smad2-/- SMCs can become macrophage-like cells, which may contribute to the formation of larger necrotic core and unstable fibrous cap.

There are several limitations in the study of chapter 4. Oil Red O staining (Figure 4.1) showed that the plaque area in whole aorta increased mainly in abdominal aorta rather than aortic root. Further study may be needed to investigate why Smad2 deficiency in SMC promotes more plaque formation in abdominal aorta. Second, MMP2/9 expression and activity increased when Smad2 was deficient. However, the mechanism underlying this process is unclear. Since TIMP-1 is the primary inhibitor for MMP9 while TIMP-2 mainly inhibits MMP2, whether or not TIMP-1 and TIMP-2 expression is altered by Smad2 deficiency can be studied. Additionally, other factors such as hydrogen sulfide,

peroxisome proliferator activated receptor-γ and nitric oxide also contribute to MMP activity. An extensive detection of other factors may provide significant novel information. Third, since Cre may degenerate gradually when SM22α expression decreased during SMC transdifferentiation, a better lineage-tracing model such as Myh11-CreER^{T2} ROSA floxed STOP eYFP mice may be used to address this potential issue.

In chapter 5, we discovered that Smad2 knockout in SMC promotes abdominal aortic aneurysm formation. Smad2 deficiency causes more severe AAA by increasing MMP-2/9 level and decreasing adventitia compensation. SMC Smad2 deficiency may inhibit adventitial cell proliferation through paracrine effect of thrombospondin-1 (TSP1).

Based on the findings in chapter 5, it may be necessary to determine if TSP1 is critical for fibroblasts proliferation in adventitia. Additional experiments are needed to test if TSP1 inhibits fibroblast proliferation through blocking fibroblast grow factor (FGF). Moreover, since TSP1 has been demonstrated to promote MMP2/9 level, it would be interesting to study if the increased MMP2/9 level in media layer is due to the elevated TSP1 expression in Smad2-/- SMCs..

Reference

1. von Mikecz, A., Chen, M., Rockel, T., and Scharf, A. (2008) The nuclear ubiquitin-proteasome system: visualization of proteasomes, protein aggregates, and proteolysis in the cell nucleus. Methods Mol Biol 463, 191-202